earthsciences.nz

Stage 1 of Piopiotahi / Milford Sound Tsunami Risk Assessment

WL Power
MAT Clive
GS Leonard
SC Cox
DH Charlton
SJ de Vilder
EV Bretherton

GNS Science Consultancy Report 2026/11
July 2026

Earth Sciences
New Zealand

DISCLAIMER

PURPOSE

This report covers:

- The potential hazard from landslide tsunami at Piopiotahi / Milford Sound.
- An international and national review of events, experience, modelling approaches and risk-management approaches.
- A critical review of hazard and risk modelling work on Piopiotahi / Milford Sound to date.

The report has been written for circulation among stakeholders with interests in managing landslide tsunami risk at Piopiotahi / Milford Sound and is intended to inform the direction for future work.

The report has been prepared with two audiences in mind: technical specialists working to improve understanding of hazard and risk at Piopiotahi / Milford Sound and stakeholders principally concerned with risk management. Sections containing technical science detail (Sections 3.3 and 3.4) include high-level summaries for non-specialists. A glossary of technical terms and acronyms is provided in Appendix 1.

USE OF DATA

Date that Earth Sciences New Zealand can use associated data:
July 2026

BIBLIOGRAPHIC REFERENCE

Power WL, Cox SC, de Vilder SJ, Clive MAT, Charlton DH, Bretherton EV, Leonard GS. 2026. Stage 1 of Piopiotahi / Milford Sound tsunami risk assessment. Lower Hutt (NZ): Earth Sciences New Zealand. 103 p. GNS Science Consultancy Report 2026/11. Prepared for Emergency Management Southland.

CONTENTS

FIGURES

TABLES

APPENDICES

ATTACHMENTS

(Attached to PDF)

Civil Defence – Southland Piopiotahi Milford Sound Collective Hazard Risk Communications Strategy.pdf

EXECUTIVE SUMMARY

The discovery of large rock-avalanche debris deposits on the floor of Piopiotahi / Milford Sound has led to consideration of the tsunami that would have accompanied these events and that might accompany similar events in future. The physical process is that when a rockslide, considered most likely to be triggered by a large earthquake, falls into the Sound, the impact and displacement of water generates tsunami waves that can travel down the Sound at high speed and cause inundation of surrounding areas. Given the large number of tourists that visit Piopiotahi / Milford Sound daily and the longer-term presence of staff at the site, this could pose a substantial casualty risk.

Piopiotahi / Milford Sound is far from alone in facing such risks, as fiord environments are present in many parts of the world, and it is useful to study and understand how these risks have been identified and managed in other countries. Of particular note are Norway and Alaska, which have long histories of tsunami in their fjords and have given extensive consideration to the management of associated risks. Greenland has a shorter historical record (this is partly thought to be due to the sparse population, leaving earlier events unrecorded, and partly due to rapid climate change accelerating the triggering of landslides), but it is of interest for the recent work to mitigate the risks that have taken place there.

Most of the recent work to understand tsunami risk in the countries mentioned above has taken place using numerical modelling approaches, which simulate the physics of the landslide, the interaction between landslide and water and the propagation and inundation of the subsequent waves. This is in contrast to the studies conducted so far at Piopiotahi / Milford Sound, which have relied upon empirical approaches based on curve-fitting to the impacts of historical events elsewhere and/or scaling of generic wave-tank experiments. Adopting a numerical modelling approach for Piopiotahi / Milford Sound would greatly improve accuracy by using the actual detailed bathymetry and high-resolution lidar topography now available, rather than single, simplified values of slope, as well as allowing for multiple waves and their interference. It would also allow for more specific modelling of landslide geometry and rock properties.

With a more accurate understanding of the tsunami hazard, a better-adapted approach to risk management becomes possible. Options include assisting people to leave high-risk locations before a tsunami arrives, reducing the amount of time spent in high-risk locations and reducing the danger to people by strengthening the built environment in ways to make a tsunami more survivable. It is again useful here to learn from overseas experience with, for example, slope monitoring, tsunami-warning systems, evacuation planning and mapping, community re-location and risk communication.

In April 2026, three workshops were held to present the findings of this report to stakeholders in Queenstown, Piopiotahi / Milford Sound and Te Anau. At all venues, engaged discussion took place covering the evidence for past events, comparisons with overseas locations facing similar challenges, proposed hazard-modelling approaches and suggestions for communication and mitigation of the risks.

This report summarises the first stage of a multi-stage project. Work is expected to be undertaken on the next stage of research, including detailed physics-based modelling of landslides and tsunami in Piopiotahi / Milford Sound, in the second half of 2026. Subsequent stages are anticipated to cover probabilistic hazard assessment, quantitative loss modelling and risk assessment and evaluation of risk-mitigation options.

1.0 Introduction

Piopiotahi / Milford Sound is one of New Zealand's premier tourist destinations, receiving over one million visitors per year, a high proportion of which (around 80%) are from overseas (Dirga 2025). Tourists are drawn to the Sound by the dramatic scenery, with towering mountains draped in native bush descending very steeply into the waters of the sound.

The same geological forces that produced the stunning landscape also present hazards. In addition to the known earthquake shaking hazard, and the hazard posed to people directly in the path of landslides, at least 16 substantial deposits have been found at the base of the Sound in recent years that are believed to have been the result of rock avalanches falling from the slopes above into the waters, in events that are likely to have triggered tsunami.

This report was requested by Emergency Management Southland with support from the National Emergency Management Agency (NEMA). This report summarises the known information about the tsunami hazard in Piopiotahi / Milford Sound and places it in the context of what is known about landslide–tsunami hazard in fiords[1] in other countries, most notably in Norway and Alaska, United States of America (USA). Pathways and methods for developing a better quantification of the hazard are presented, drawing on overseas and domestic experience. International experience with risk mitigation is also presented and provides context for the requirements and options for risk reduction at Piopiotahi / Milford Sound.

An overview of the hazard chain, illustrating key nomenclature used in this report, is provided in Figure 1.1. Appendix 1 contains an explanatory glossary of technical terms and acronyms.

1 We use the New Zealand spelling of 'fiord' when the context is specific to New Zealand or is without reference to a specific location. Where the context is specific to a country where the usual spelling is 'fjord', this variation has been used.

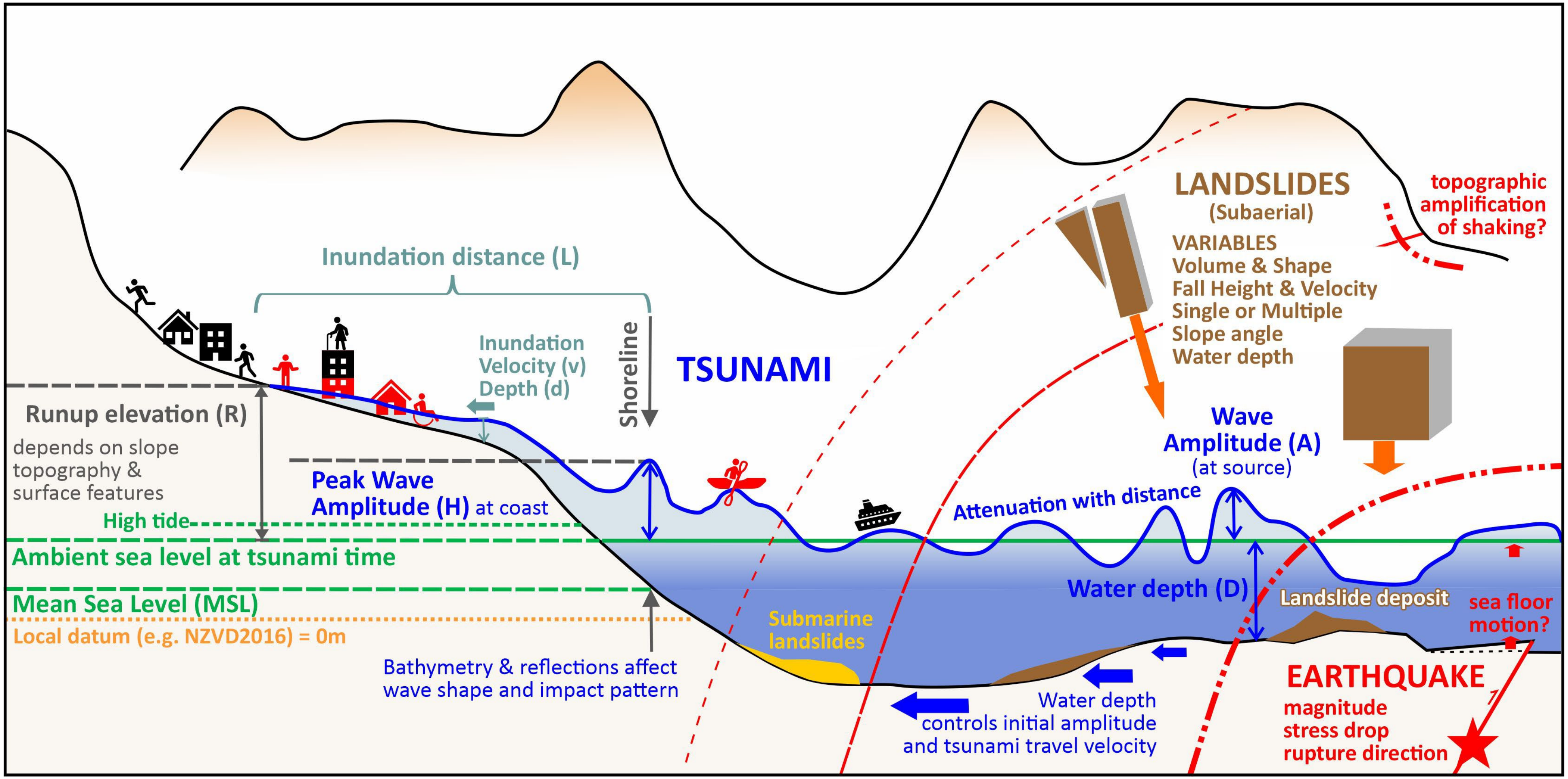

Figure 1.1 Schematic overview of the process by which a tsunami is generated by earthquake-induced landslides, outlining nomenclature used in this report. In this figure, the tsunami wave is initiated on the right, in this example by an earthquake triggering a landslide that displaces a large volume of water. In the middle of the diagram, the wave travels ('propagates') across the body of water. Its speed and height are controlled by the water depth, and, as it travels, the wave loses some energy ('attenuation'). As the wave approaches the shore it piles up ('shoals') and gets higher. The height at the coast is described in terms of the peak wave amplitude (H). The inundation distance (L) indicates how far the water travels inland, and the run-up elevation (R) is the vertical height that the water reaches onshore compared with the normal sea level. The impacts onshore are shaped by the steepness and shape of the coastal terrain, as well as the exposure and vulnerability of people and buildings.

2.0 Outline of Potential Hazard

Geophysical surveys of Piopiotahi / Milford Sound have identified 16–18 very large rock-avalanche deposits on the floor of the sound (Dykstra 2012; Dick 2021) (see Section 4.5 for more details). These range in volume from approximately 0.2 to 20 million cubic metres and are widely distributed across the base of the Sound (a view of part of the Sound is shown in Figure 2.1). All of these are thought to be the result of landslides that occurred since the last ice age, approximately 17,000 years ago, as, prior to that time, the rocks would have fallen onto, or have been eroded away by, glacier ice.

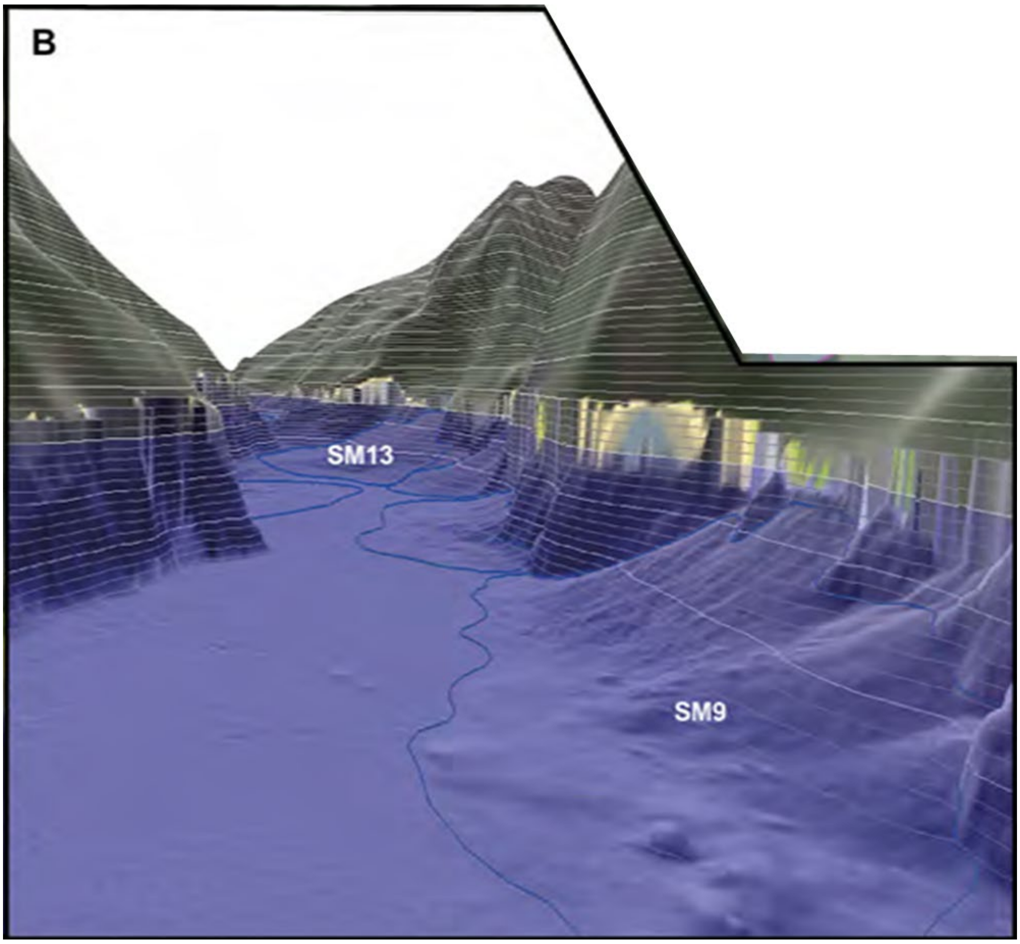

Figure 2.1 Bathymetric view of the western end of Stirling Basin, illustrating examples of the rock avalanche deposits on the floor of Piopiotahi / Milford Sound (reproduced from part of Dykstra [2012; Figure 4.2]). The location viewed corresponds to the white dashed rectangle in our Figure 4.3; SM9 and SM13 are labels for particular deposits identified in that figure.

Waves are generated when a rock avalanche falls into a body of water, and the size and spread of these waves will depend on the properties of the landslide and shape of the water body. An indication of the possible consequences for a rockslide falling into Piopiotahi / Milford Sound was given on 11 August 2003 when the M_W7.2 Fiordland earthquake caused a rockslide into the Gold Arm of Charles Sound in Fiordland. Fortunately, this is an uninhabited area, as the resulting tsunami crossed the sound and stripped soil from the opposite banks to a height of 4–5 m above the high-tide line (Figure 2.2).

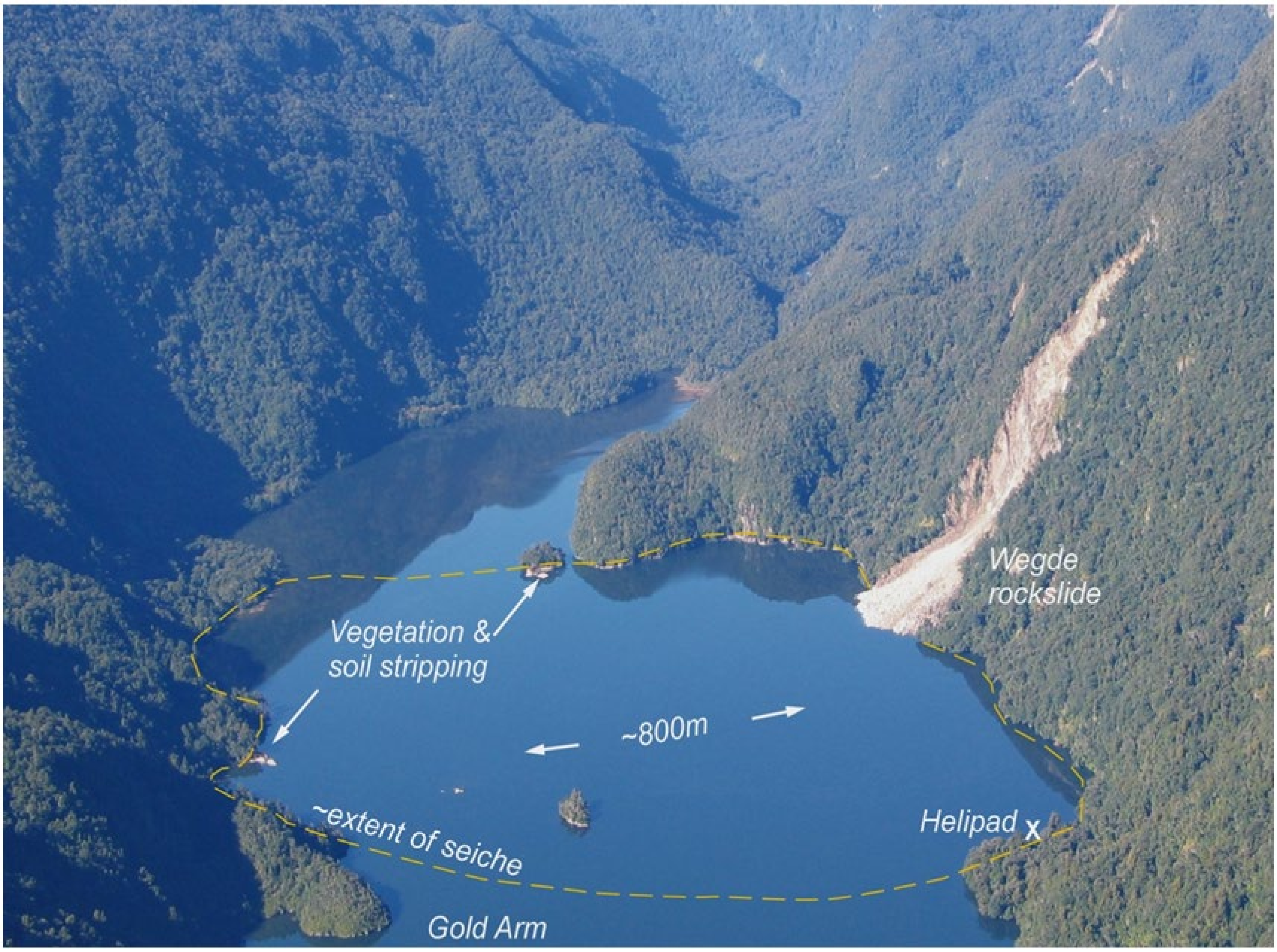

Figure 2.2 Rockfall of ~200,000 m^3 and subsequent tsunami impacts following the 11 August 2003 $M_W7.2$ Fiordland earthquake in the Gold Arm of Charles Sound (Hancox et al. 2003).

It should be kept in mind that the Gold Arm rockslide was comparable in size to only the very smallest of the rockslides identified in Piopiotahi / Milford Sound and that the largest rockslides identified there are approximately 100 times larger in volume, so could plausibly generate much larger tsunami.

An indication of the potential consequences of these larger tsunami can be gleaned by studying the tsunami caused by landslides of these larger volumes elsewhere in the world (e.g. in Dohmen et al. 2025a, 2025b), with particular focus on those events taking place in fiords. Fiords (or fjords) are long, narrow, steep-sided ocean inlets usually formed by the submergence of formerly glaciated valleys. Many of the world's largest tsunami run-up heights have occurred in fiords due to the potential for large masses of rock and/or ice to fall into a confined volume of water.

For a more precise estimate of the hazards that such landslide–tsunami pose, modelling can be undertaken. Studies so far of Piopiotahi / Milford Sound have taken an empirical approach that involves scaling the properties of historical tsunami or laboratory-scale experiments to estimate the tsunami properties (Section 4), particularly at the Cleddau Delta where tourists and workers are present in the largest numbers. Initial indications from these studies are that there is a high level of risk posed to these people. More precise estimates of the hazard are likely to require numerical modelling of the physical processes behind tsunami generation, propagation and inundation (Figure 2.3).

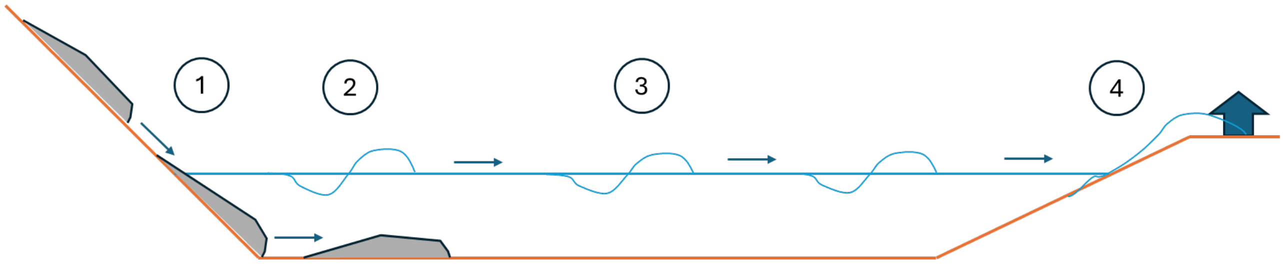

Figure 2.3 Schematic showing stages of the landslide–tsunami process. (1) Landslide initiation and motion. (2) Wave generation. (3) Wave propagation. (4) Inundation and run-up.

A tsunami wave has a long duration, usually several minutes, compared with conventional wind waves, which typically have durations of tens of seconds. In a tsunami, the water is moving at all depths, from the seabed to the surface, in contrast to wind waves, where the motion is concentrated near the surface. For these reasons, tsunami are able to travel further onshore and cause greater damage.

To go from the physical hazard, in this case, the likelihood of different tsunami inundation depths and extents, to the risk posed to people and property, we also need to consider the number of people and buildings exposed, as well as their susceptibility to injury or fatality (to people) or damage (to buildings). Improvement to assessment of the hazard is an important step but is also only one part of the whole risk-assessment process.

3.0 International Review

Landslides are recognised as the second most common cause of tsunami, and these may be either initially sub-aerial (starting above water) or entirely submarine (or in lakes entirely sub-lacustrine). See Dohmen et al. (2025) for a recent global review of landslide-induced tsunami. Most landslides that create tsunami in fiords are sub-aerial (initiated above the water).

In the following sub-sections, we briefly summarise how the known hazards of tsunami in fiords and glacial lakes are dealt with in other countries as a useful starting point for further discussion of this type of hazard in New Zealand. The primary focus here is on Norway and Alaska, two regions that have long histories of tsunami in their fjords and which have seen extensive research undertaken to understand and then mitigate the associated risks. Greenland is also given prominence due to recent hazard events and subsequent mitigation efforts. The situations in Chile and other remaining countries with fiords are briefly summarised.

3.1 Country Summaries

3.1.1 Norway

Norway is famous for its fjords, of which there are over 1700 distributed along the world's second longest coastline. The mountain ranges that encompass the fjords were formed in the Caledonian orogeny about 400 million years ago. The occurrence of earthquakes is rare compared with New Zealand, as Norway does not sit on a plate boundary, although these still occur in part due to glacial rebound from the end of the last ice age. The climate is generally colder than that of New Zealand and ranges from an oceanic climate in the south to a sub-arctic climate in the north.

The Norwegian fjords are more populated than New Zealand's, with a wide variety of towns and villages at the head, and along the sides, of the fjords. Several of these towns are also tourist hotspots, with large transient populations of visitors coming to see the fjords and travelling on cruise ships. Major historical disasters have occurred due to landslides into the fjords, notably the Tafjorden tsunami of 1934, which killed 40 people, and the Lake Loen disaster in 1936, in which a catastrophic rockfall from the Ramnefjellet mountain caused a tsunami, leading to 74 fatalities (technically Lake Loen is not a fjord but a glacial lake; however, the tsunamigenic processes involved are very similar). Longer historical records suggest that there have been two to three catastrophic events every century over the past 400 years or so (Harbitz et al. 2014).

The Norwegian Geotechnical Institute, the Geological Survey of Norway and the University of Oslo have been leading research into the potential for future tsunami in the Norwegian fjords. Studies have been completed looking at the Åkerneset rock slope on the flanks of Sunnylvsfjorden using numerical modelling to predict the consequences of failure of rock volumes of up to 50 million m^3 and potential threat posed to the tourist centre at Geiranger (which has more than 700,000 visitors and 150–200 cruise ships per year), as well as at failure of the Hegguraksla rock slide at nearby Tafjorden (Harbitz et al. 2014). Key slopes that have been identified as potential failures are continuously monitored, such as the Åknes Landslide at Synnylvs fjord on the west coast (Aspaas et al. 2024) and at Tussafoten in Eidfjord (Eian 2024). An early-warning system is in place for the tourist town of Geiranger, with warnings disseminated by sirens, SMS alerts and local media (as managed by the Norwegian Water Resources and Energy Directorate [NVE]). A tsunami could arrive in around 10 minutes; the risks are well known to local residents and evacuation plans are in place.

Another example of an early-warning system is in the fjord communities in Lyngen, where a known rock slope, which could generate a tsunami if it failed, is deforming by 4–5 cm a year (Goeldner-Gianella et al. 2017). Scenario hazard analysis has indicated that the rock-slope collapse may be between 11 and 22 million m^3 in volume and generate a wave that could reach 33 m high (run-up elevation) in the village of Lynseidet. The slope itself is extensively monitored with over 70 instruments. Once a certain threshold of movement (>15 mm/day) is reached, the slope is placed on a 'red level'. Final warning is given at least 72 hours before the rockslide and subsequent tsunami should occur. From this case, Goeldner-Gianella et al. (2017) found that, while residents possessed a solid understanding of natural hazard processes, tourists remained unfamiliar with landslide-induced tsunami risk and evacuation procedures. Despite extensive public-education campaigns, both groups, especially tourists, exhibited limited knowledge of warning systems. Importantly, people expressed a strong need for warnings to specify the time available for evacuation and clear guidance on where to go. Confidence in authorities also varied, with greater trust placed in hazard monitoring than in risk communication or emergency management.

Using four examples from sub-arctic and arctic communities in Norway and Greenland that are exposed to avalanches, landslides and tsunami, Johannessen et al. (2025) showed that successful evacuation outcomes depended on the 'co-creation of risk', where authorities, residents and experts share an evolving understanding of both the hazard and its consequences. This analysis also found that continuous communication during prolonged periods of elevated risk was found to reduce tension and increase patience with management decisions.

The risk assessment for the rockslide tsunami hazard from the Åkerneset rock slope was found to be higher than the acceptable thresholds for development by the Norwegian Planning and Building Act 2008, when multiple risk assessments were conducted in the early 2000s (see summary in Harbitz et al. 2014 [and references therein]). This presented obvious drawbacks to a region reliant on coastal activities, and the Act was amended to allow specified development to take place contingent on various requirements, such as there being no alternative location, critical facilities not being located in the most hazardous zones, a warning system being in place, evacuation plans in place and public awareness heightened (Harbitz et al. 2014). In Norway, the Norwegian Building Code defines allowable annual probabilities of landslide occurrence and associated impacts for municipal and project-scale zoning approvals (Norwegian Building Authority 2017). However, a recent report (NGI 2023) has highlighted substantial variation in risk-tolerance criteria across the public sector, suggesting that the fragmented governance of natural-hazard management across eight ministries, and the responsibility for risk-tolerance criteria, is distributed across four government agencies (NVE[2], NPRA[3], the Norwegian Railway Directorate and Bane NOR[4]).

3.1.2 Alaska

Alaska's fjords have seen several of the largest recorded landslide tsunami. The geology of Alaska is very complicated, with the accretion of landmasses over vast geological timescales partially overwritten by relatively recent glacial and volcanic features. Additionally, Alaska lies on the subduction interface between the Pacific and North American tectonic plates and, as such, experiences very large subduction earthquakes, such as the M_W9.2–9.3 1964 Alaska earthquake. Numerous active upper-plate faults are present, such as the Denali fault. The climate varies from maritime in the south, to extreme continental in the centre, to polar in the north. Most of the known landslide–tsunami activity occurs on the southern coasts, where the climate is a maritime one with cool, wet summers and cold (but not extreme) winters, with daily high temperatures fairly consistently below freezing due to the high latitude.

2 Norwegian Water Resources and Energy Directorate.

3 Norwegian Public Roads Administration.

4 Bane NOR SF is the Norwegian government agency responsible for owning, maintaining, operating and developing the Norwegian railway network.

For the most part, the fjords are sparsely populated, with just a few small settlements. However, there are also a few larger towns and industrial locations situated in or near fjords, such as Valdez and Whittier in Prince William Sound and Seward in Resurrection Bay.

Historically, the very largest run-up heights from landslide–tsunami in Alaska (and globally) have been associated with glaciers that are retreating in the present day. The most famous of these is the 1958 Lituya Bay tsunami that reached a run-up height of 524 m, as evidenced by the destruction of forests on slopes around the bay (Miller 1960). Another similar landslide and tsunami occurred in in Taan Fjord in 2015, associated with a large rock avalanche from the Tyndall Glacier, where run-up heights reached 150–193 m (George et al. 2017; Corsa et al. 2022).

A further reminder of the ongoing hazard from landslide-generated tsunami in glaciated fjords came in August 2025, when a >64 million m^3 rockslide collapsed into Tracy Arm fjord in southeast Alaska, generating a 'mega-tsunami' with a maximum measured run-up of 481 m on the opposite side of the fjord (Shugar et al. 2026). The event occurred adjacent to the rapidly retreating South Sawyer Glacier and was interpreted as being strongly pre-conditioned by long-term glacier thinning and retreat linked to anthropogenic climate warming. The tsunami produced an initial breaking wave travelling at more than 70 m/s, stripped vegetation from fjord walls over tens of kilometres and generated hazardous currents and surges throughout the fjord system frequented by cruise ships and tourism vessels. The event attracted substantial international media and scientific attention because it represented a near-miss in a heavily visited tourism area, and because seismic instruments detected precursory microseismic activity in the hours to days before failure. The Tracy Arm event has therefore become an important contemporary example of the growing international focus on landslide–tsunami hazards in glacier-retreat environments, on the implications of climate-driven slope destabilisation and on the potential role – and limitations – of future monitoring and early-warning systems in fjord environments.

Closer parallels to what may be expected in Piopiotahi / Milford Sound are to be found in the tsunami that followed large earthquakes. The M_W9.2–9.3 1964 Alaska earthquake caused local tsunami through more than 20 local landslides (submarine and sub-aerial) impacting the coastal towns of Whittier, Seward and Valdez, in some cases before the shaking had even finished. This was followed by a more widespread tsunami caused by the earthquake deformation. At least 82 of 122 tsunami fatalities are thought to have been caused by the local landslide–tsunami.[5] Maximum reported run-ups were up to 52 m in the Valdez Arm.

Numerous studies have been conducted to examine the potential for future landslide tsunami in the fjords of Alaska; many of these have been organised by the United States Geological Survey (USGS), such as a study of the potential for landslide–tsunami in the Barry Arm of Prince William Sound, which could potentially affect the town of Whittier (Barnhart et al. 2021; see Section 3.4.6).

Management of the risks from tsunami in Alaska takes place under the umbrella of the United States National Tsunami Hazard Mitigation Program, involving the Alaska Department of Natural Resources Geological and Geophysical Surveys, the Alaska Division of Homeland Security and Emergency Management and the National Oceanic and Atmospheric Administration.[6] This also includes collaborative research with the USGS. A particular concern is to mitigate the dual effects of earthquake- and landslide-induced tsunami, which have different characteristics in terms of geographical spread, localised intensity and travel time. Monitoring devices are being developed to detect precursory movement of potential landslides in key locations such as Barry Arm (Rosen 2025), and tide gauges have been installed for tsunami monitoring (Barnhart et al. 2021). The USGS and partner agencies also communicate the hazard to the public through a status update website[7] (USGS 2021).

5 https://earthquake.alaska.edu/about-tsunamis-alaska

6 https://dggs.alaska.gov/hazards/tsunamis.html

7 https://dggs.alaska.gov/hazards/barry-arm-landslide.html

3.1.3 Greenland

The coast of Greenland has one of the most extensive fjord systems in the world, with over 150 named fjords. The interior of Greenland is covered by a huge ice sheet and has an arctic climate. However, the coasts are milder due to the warming effects of ocean currents and experiences a tundra climate and biome. Warming of the climate is taking place relatively quickly in Greenland compared with the global average.

Several landslide tsunami have been observed in the past 30 years. As Greenland has a small and scattered population of around 57,000, earlier landslide–tsunami may not have been recorded or reported prior to modern instrumental networks – for example, the 2023 mega-tsunami in Dickson Fjord was noteworthy for the very unusual seismic signal that it generated (Svennevig et al. 2024). Landslides may be caused by the retreat of glaciers buttressing the slopes, or by freeze-thaw action weakening of slopes, so it is also conceivable that climate change may be accelerating the rate of events (Svennevig et al. 2024).

Key historical events include the 2000 landslide and tsunami in Paatuut on the west coast of Greenland, in which 90 million m^3 of material slid from 1000–1400 m altitude, of which approximately 30 million m^3 entered the sea. The resulting tsunami had run-up heights of around 50 m close to the location of impact and 28 m at the abandoned mining town of Qullissat about 20 km away (Dahl-Jensen et al. 2004). It is thought that the proximal trigger for the event was the re-freezing and subsequent expansion of meltwater in pre-existing cracks.

Another major landslide–tsunami occurred at Karrat Fjord, also on the west coast, in 2017. In this event, the landslide volume is estimated at around 50 million m^3. Run-up was estimated at >90 m near the landslide; ~50 m on the opposite side of the fjord; and ~10–12 m at the village of Nuugaatsiaq 32 km away, where 11 houses were destroyed and four people were killed (Fritz et al. 2018; Paris et al. 2019).

In 2023, a mega-tsunami occurred in Dickson Fjord on the east coast of Greenland. This was initially noticed due to the unusual seismic signal that it caused. The landslide is inferred to have been of around 25 million m^3 in volume and triggered by glacial thinning (and so of less direct relevance to Piopiotahi / Milford Sound). Initial backsplash is inferred to have reached around 200 m, with subsequent waves of up to 110 m. Seiching (sloshing) within the sound is inferred from seismic data to have continued for over nine days, repeating a 92-second oscillation (Svennevig et al. 2024).

The 2017 Karrat Fjord tsunami was the first known event of its type to impact an inhabited settlement in Greenland (Strzelecki and Jaskolski 2020) and has prompted discussion of the potential risks posed by future events. The governments of Greenland and Denmark offered to build houses in new locations for those who were evacuated; however, the houses would only be available for renting (not ownership), and choices were limited. Matti et al. (2023) describe the engagement processes for the planned re-location and recommend a pivot from top-down decision-making to one that supports more community agency. Matti et al. (2023) also examined planned re-location from landslide-induced tsunami in Iceland and, in both countries, emphasised that transparent governance, adequate compensation and clear timelines are essential to maintaining trust and social cohesion.

In the Karrat Fjord area, local low-tech solutions, such as human lookouts and awareness training, have been implemented (Johannessen et al. 2025). Officials have also conducted exercises/drills to help with preparedness.

3.1.4 Chile

Patagonia on the west coast of Chile contains an extensive network of fjords. The climate varies from temperate in the north to polar in the south. Although quite similar to New Zealand in latitude, it is generally much drier than Fiordland. There is a subduction interface between tectonic plates off its coast, leading to large earthquakes such as the M_W9.3–9.5 1960 Chile earthquake.

The most notable recent landslide–tsunami occurred in 2007 at Aisén Fjord, when a M_W6.2 earthquake triggered hundreds of sub-aerial landslides on the flanks of the fjord (Lastras et al. 2013). These landslides in turn generated waves of several metres' run-up height, causing 10 fatalities and severely damaging salmon farms, which form the main economic activity of the region.

Several studies have been conducted to simulate the landslide-induced tsunami, including those by Scheele et al. (2013) and Uribe et al. (2025).

3.1.5 Other Countries

Other countries with fjords and subsequent potential tsunami hazards include Iceland, Canada and Antarctica.

The coasts of Iceland contain an extensive network of fjords; however, the most prominent rockslide-caused tsunami in recent history was in the different environment of the volcanic Lake Askja. A 2014 rockslide of around 20 million m^3, of which approximately half entered the lake, caused a tsunami with maximum run-up heights near the slide of 60–80 m and run-up heights of 10–40 m typical around the lake (Gylfadóttir et al. 2017). Cracks appearing in the Svínafellsheiði mountainside in the Öræfi district of southeast Iceland have led to concerns that a large section of the slope is unstable, with the potential for a 60 million m^3 rockslide falling onto the glacier below. It is considered possible that ice from the glacier could be incorporated into the debris flow, which might enter the glacier lake below and cause flooding or a tsunami. Matti et al. (2023) discuss engagements undertaken with the local community in response to the risk, which is expected to increase over time as the glacier retreats and the glacier lake increases in size.

The fjords of the west coast of Canada are geologically an extension of those in Alaska and so are consequently exposed to similar hazards and risks. In 1975, a landslide on the west fjord wall of the Kitimat Inlet occurred contemporaneously with collapse of the Kitimat River delta, which further mobilised fjord sediments, leading to a wave – estimated at its peak as being 8.2 m from crest to trough – that caused damage to wharves and boats at Kitimat settlement (Clague et al. 2000).

While fiords are present in Antarctica, especially on the Antarctic Peninsula, little appears to be known about the potential tsunami hazard, with most Antarctic tsunami research focused instead on the potential for tsunami caused by glacier-calving events.

3.2 Major Historical Events

Some of the very largest historical tsunami, such as those at Lituya Bay and Taan Fjord in Alaska, have occurred where glaciation remains an active process and glacier retreat has destabilised adjacent slopes. Tsunami also occur in fiord settings where glaciation is no longer an active process, where they may be triggered by earthquakes or the collapse of volcanos or where they may occur spontaneously due to destabilisation of slopes.

Table 3.1 Notable historical tsunami caused by sub-aerial landslides or volcanic collapse. Key sources are Slingerland and Voight (1979), Ward and Day (2010) and Heller and Ruffini (2023); see also Dohmen et al. (2025a, 2025b).

Location	Year	Reported Run-Up Height on Land (m)	Notes: Volume, Wave Height, Cause, Reference
Mount Unzen, Japan	1792	~100 (estimated)	Debris flow from volcano flank collapse; ~15,000 fatalities (Slingerland and Voight 1979; Sassa et al. 2016). Historical sources and compilations describe very large local waves, with maximum heights up to ~330 ft (~100 m) and ~187 ft (~57 m) in places; these are effectively local run-up/wave heights on the shore.
Tafjorden, Norway	1934	62	Volume ~1.5 × 10^6 m^3. Near-source wave height is commonly quoted at ~60 m run-up near the slide but much lower for run-up onto land at inhabited locations (~15–17 m at Tafjord village, 6 km distance) (Hermanns et al. 2006).
Lake Lovatnet (Loen), Norway	1936	74	Following an earlier event in 1905, approximately 1 million m^3 of rock detached from an over-steepened glacial carved face on Mount Ramnefjellet and fell into a lake. Wave height unclear, run-up 74 m; caused 74 fatalities. No major earthquake trigger (Jørstad 1968; Slingerland and Voight 1979; Waldman et al. 2021).
Lituya Bay, Alaska, United States of America (USA)	1958	524	M_W7.7 earthquake of 9 July 1958 induced a 30.6 x 10^6 m^3 landslide to fall 914 m into Lituya Bay near the terminus of Lituya Glacier. It generated the largest ever measured tsunami run-up of 524 m (1.35 km across the bay). Run-up was attenuated to 9.7 m at 12 km. Eyewitness account suggests a wave front of 15–22 m (50–75 ft) but only 7–15 (25–50 ft) wide, followed by turbulent chaotic sloshing. Areas where soil and vegetation were stripped are still clearly visible in Google Earth imagery. Prior to the event, D. Miller (United States Geological Survey) had found evidence for at least four previous waves estimated at 1936, 1899, 1874 and 1853 (Miller 1960; Slingerland and Voight 1979; Ward and Day 2010; Barnhart et al. 2021).
Vajont Dam, Italy	1959	235 (overtopping 245–270)	Subaerial block slide; wave ~10 m at dam (Panizzo et al. 2005a; Crosta et al. 2016). Reconstructions show that the wave eroded the opposite valley side up to ~235 m above the then lake level.
Lake Rupanco, Chile	1960	>10	Major earthquake triggered a landslide into a glacial lake (not a fjord).
Xintan, Yangtze River, China	1985	54	Three Gorges region (Huang et al. 2009). Back analysis gave a run-up height of about 54 m (Wang and Xu 2009). Some sources mention a wave height of 49 m.
Papua New Guinea (Aitape)	1998	10–15	Controversial submarine landslide and/or earthquake source out to sea (Tappin et al. 2008; Heinrich et al. 2001).
Paatuut, Greenland	2000	50	Rock avalanche (Dahl-Jensen et al. 2004). Run-up of ~50 m near the slide and ~28 m at Qullissat across the strait.
Stromboli, Italy	2002	<11	Volcano flank collapse (Tinti et al. 2006). Event produced near-shore/local tsunami waves in the ocean with maximum heights of ~10–20 m near Stromboli; modelling often quotes ~10 m at the coast.
Qianjiangping, Three Gorges Reservoir, China	2003	39	Large sub-aerial landslide of ~20–24 million m^3. Observed run-up to 175 m above sea level (Yin et al. 2015).

Location	Year	Reported Run-Up Height on Land (m)	Notes: Volume, Wave Height, Cause, Reference
Charles Sound, Fiordland, New Zealand	2003	5	M_W7.2 Secretary Island earthquake induced a large (150,000–200,000 m^3) wedge failure in gneiss bedrock with a vertical fall of 300 m on a 45° slope. This generated a small tsunami that crossed Charles Sound (800 m), damaged vegetation and soil up to 4–5 m above high-tide level and stripped vegetation off a small island. It also damaged a helipad ~250 m west of the slide. Affected area of ~0.45 km^2 (Hancox et al. 2003, 2004).
Aisén Fjord, Chile	2007	Multiple, locally large	The 2007 M_W6.2 earthquake triggered numerous landslides and tsunami-like displacement waves. Wave heights have been suggested to be up to ~50 m (Sepúlveda and Serey 2009).
Lake Lucerne, Switzerland	2007	Unknown	Potential lake tsunami in 1601 and 1687 with 4–5 m waves. Subaqueous slides (Fuchs and Boes 2010)
Gongjiafang, Three Gorges Reservoir, China	2008	13.1	Max run-up of 13.1 m on the opposite bank, decreasing upstream (Huang et al. 2012, 2014).
Eqip Sermia, Greenland	2014	50	Ice-glacier calving produced an iceberg–tsunami amplitude ~45–50 m near the glacier face; run-up on the opposite shore 4 km away was only ~10–15 m, where infrastructure was damaged (Lüthi and Vieli 2016; Gylfadóttir et al. 2017).
Lake Askja, Iceland	2014	71	Rockslide into volcanic lake. Field surveys show vertical run-up of typically 10–40 m, with local maxima ~60–80 m near the impact area (Gylfadóttir et al. 2017).
Taan Fjord, Alaska	2015	150–193	Large rock avalanche from Tyndall Glacier (Corsa et al. 2015; George et al. 2017).
Three Gorges Reservoir, China	2015	6	Rapid sub-aerial landslide from the reservoir bank, unrelated to an earthquake. Detailed modelling and field observations show maximum run-up ~6.2 m on the opposite shore (Xiao et al. 2018). Considered to be one of several important landslide-generated wave events associated with long-term slope adjustment caused by rapid drawdown and refill cycles around the Three Gorges Reservoir.
Karrat Fjord, West Greenland	2017	10	Rock avalanche/tsunami. Run-up of >90 m near the landslide, ~50 m on the opposite side of the fjord and ~10–12 m at Nuugaatsiaq (Paris et al. 2019).
Anak Krakatau, Indonesia	2018	2–13	Lateral flank collapse of ~100–300 million m^3 of Anak Krakatau volcano into the sea (Grilli et al. 2019). Coastal run-up was mostly in the 2–13 m range on Sumatra and Java.
Jinsha River, China	2018	Unknown	Landslide–dam failure system (Hu et al. 2020). 140 m dam height, lake level and flood discharge (not run-up).
British Columbia, Canada	2020	114	Elliot Creek landslide into coastal fjord (Geertsema et al. 2022).
Dickson Fjord, East Greenland	2023	200 (wave)	Massive landslide. Week-long sloshing observed seismically (Svennevig et al. 2024). Reports describe an initial backsplash with run-up of ~200 m and subsequent waves up to ~110 m, with the seiche oscillating for days.
Tracy Arm, Alaska, USA	2025	481	>64 million m^3 rockslide adjacent to the rapidly retreating South Sawyer Glacier (Shugar et al. 2026).

3.3 Landslides, their Dynamics and Tsunami

We provide here a technical review of the current understanding of landslides and their potential to generate tsunami waves, citing recent global research, laboratory experiments, numerical modelling and case studies from Norway and Piopiotahi / Milford Sound. Some of the content is highly technical, and non-specialists may prefer in a first read-through to cover only the high-level summary in the Introduction (Section 3.3.1) before moving ahead to Section 3.4.

3.3.1 Introduction

This section explains, in some detail, that the size of a tsunami generated by a landslide depends not only on the volume of material involved but also on how rapidly and coherently the mass fails, the angle and velocity at which it enters the water, the depth and geometry of the water body and the physical properties of the sliding material. Sudden, high-velocity rock avalanches – particularly those triggered by earthquakes – are generally more capable of producing large waves than slower, rainfall-induced failures because these deliver mass impulsively and with greater momentum. Most people will have an intuitive understanding of these principles from their experiences jumping or diving into water (Figure 3.1). The size of the resultant splash and wave can be quite variable.

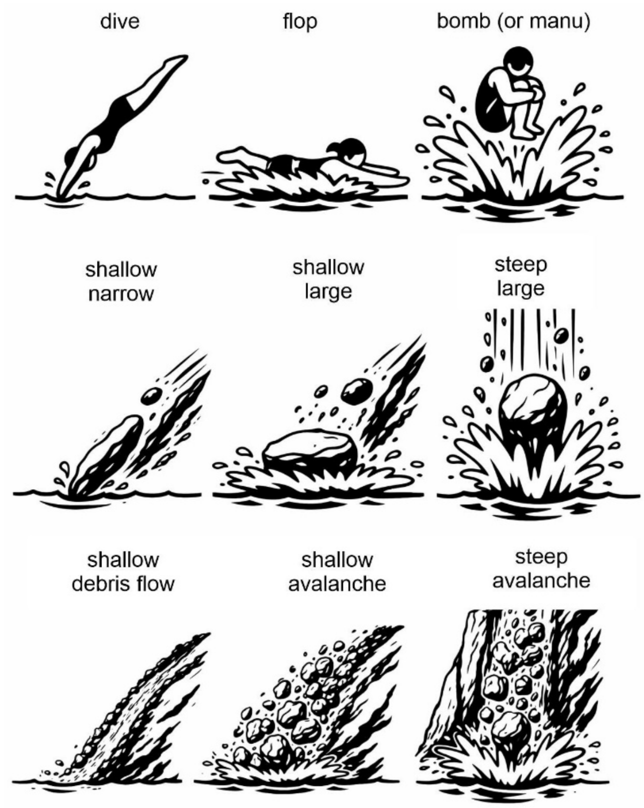

Figure 3.1 Schematic illustration of entry into water of swimmers (top row), individual rocks (middle row) and landslides (bottom row) to highlight the effect of shallow and steep entry angles and an object's shape on the resulting wave. Clearly mass and volume are also important in the resultant wave. (Cartoon generated by ChatGPT AI, under instruction by Simon Cox).

The section also explains how the stability of slopes can be identified and monitored using geomorphic mapping, lidar, satellite InSAR and historical landslide catalogues, noting that steep terrain can introduce bias and uncertainty in hazard assessment. Statistical magnitude–frequency relationships are used to characterise how often landslides of different sizes occur, while empirical scaling relationships link earthquake magnitude to the number and size of triggered landslides. Evidence of numerous large post-glacial rock avalanches on the floor of Piopiotahi / Milford Sound is indicative that very large failures have occurred in the past.

Finally, the section outlines approaches used to model landslide-generated waves, ranging from simplified equations based on field observations to more complex rheological and numerical models that account for slide deformation and water–air–sediment interactions. Tools such as the SPLASH run-up formula are widely used in hazard assessment but contain significant recognised uncertainties, so dynamic numerical models are generally preferable for detailed site work. Given the variability in landslide behaviour and the limitations of available data, this section emphasises the importance of incorporating uncertainty into tsunami-hazard analysis and suggests that conservative assumptions may be warranted where consequences are high and knowledge remains incomplete.

3.3.2 Overview

There are several recent reviews on landslide-induced tsunami, including global occurrences and modelling approaches (Heller and Ruffini 2023; Dohmen et al. 2025a). A global database of 317 landslide-induced tsunami (including landslide properties and causes, generated wave heights and the resulting economic damage and fatalities in affected coastal communities) was developed by Dohmen et al. (2025b). Using simple statistical analysis, Dohmen et al. (2025a) clearly showed that landslides with the highest volumes do not necessarily trigger the largest waves. Landslides with giant (10^9–10^{12} m^3) or monster (10^{12}–10^{15} m^3) volumes have generated tsunami with water heights on the order of tens of meters, while the highest waves were triggered by smaller (also known as large 10^6–10^9 m^3) landslides.

Key parameters on which tsunami are considered dependent (Heller and Ruffini 2023) include:

- Bulk slide volume V_S [or the slide grain volume $V_g = (1 – n/100)V_s$ *(n = porosity)*].
- Bulk slide density ρs [or the grain density $\rho g = \rho s/(1 – n/100)$].
- Landslide shape (thickness, length and width).
- Slide impact velocity.
- Slide impact angle.
- Water depth (at the slope toe).
- Density of water (into which the landslide falls).
- Landslide rheology and slide model (block versus granular slide, grain-size distribution, friction angles, porosity, permeability, rheology parameters, cohesion, etc.).
- Mass movement type (sliding, flowing, falling, toppling, spreading).
- Water body bathymetry and geometry (2D, 3D, intermediate geometries, etc.).
- Any seiching produced by the earthquake shaking.
- Topography and vegetation on land surrounding the waterbody (e.g. lake or fiord).

The amplitude and frequency of any initial wave(s) resulting from a landslide falling into a body of water are strongly controlled by the combination of volume, geometry, entry angle, velocity and landslide rheology. At the top of the slope, these parameters can vary markedly depending on the slope collapse failure mechanism, which affects the rate of supply of material into the moving mass.

Studies of Norwegian rock-slope failure areas subdivide landslides into three principal types to help promote this understanding: (1) rockfall, (2) rockslide and (3) complex fields (Figure 3.2).The angle of the slope, friction along the runout path, runout distance and material characteristics subsequently change the velocity, geometry and rheology of a landslide by the time that it reaches the base of a slope and/or water. Once a tsunami(s) is generated, wave propagation depends mainly on the geometry and bathymetry of the waterbody, amplitude and frequency.

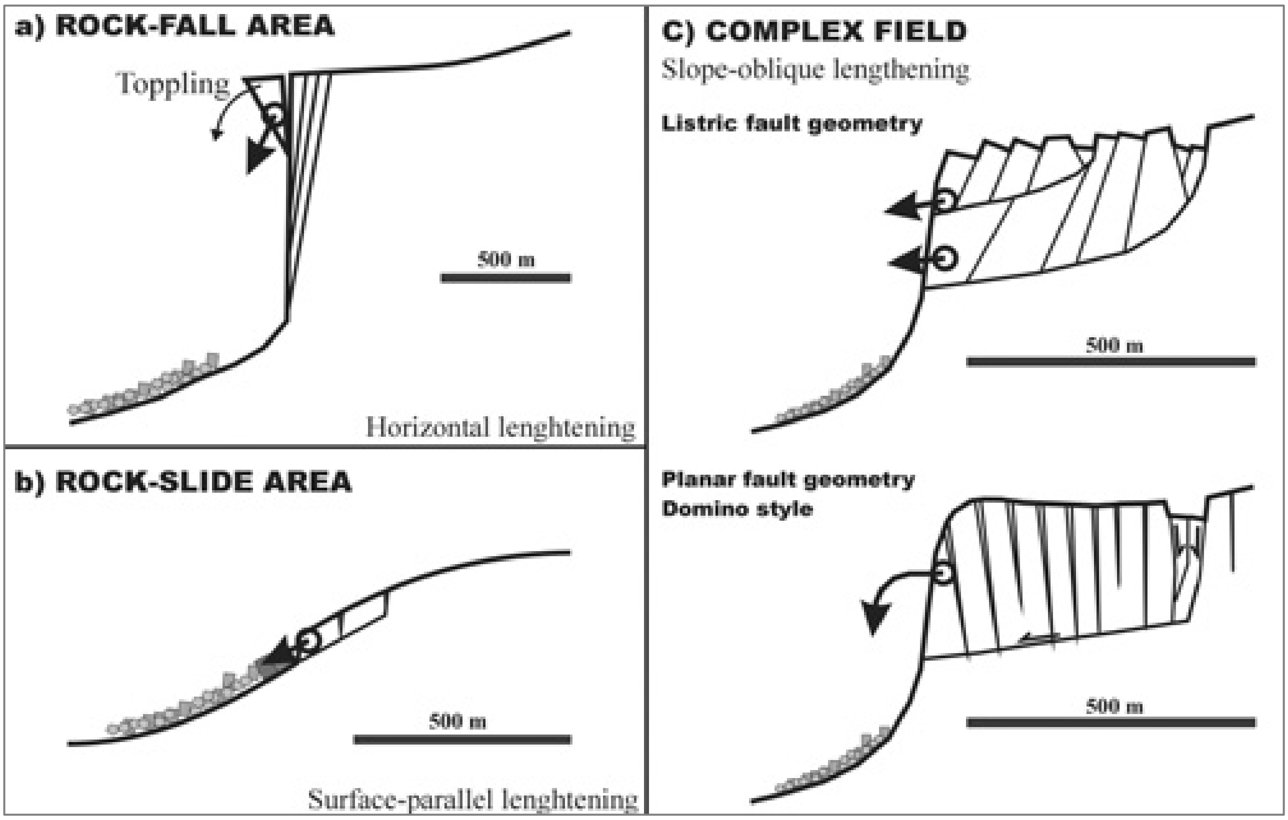

Figure 3.2 Examples of a variety of types of rock-slope failures, showing how different joints, extension fractures, shear fractures and faults can be exploited to result in different styles of landslide (Braathen et al. 2004 [Figure1]).

3.3.3 Landslide Mapping and Hazard Identification

The potential for slopes to collapse, or be susceptible to collapse, can be investigated through observations of topography, topographic features, fracture density and orientation. If slopes have already started to deform and move under the influence of gravity, these may express geomorphic features or changes in location that can be measured. Precise surveying by repeat lidar or InSAR methods can highlight present slope creep and acceleration over time. The presence of landslide and rockfall deposits at the base of a slope, as well as the location and size of the deposit material, provide evidence of past events. Catalogues and mapping of past failures can be used to develop models of the susceptibility of slopes to fail, providing information on past failures that can be used to understand places where there is potential for future slope failure.

Concern about an apparent disparity between past events and slopes deemed presently unstable recently led the NVE to review its database (n = 423) of past events compared with Norwegian Geological Survey (NGU) mapping of unstable slopes (n = 1144) (Kristensen et al. 2025). They found significant discrepancies between mapped and monitored unstable slopes when compared with known historic or prehistoric rock avalanches. A greater number of instabilities tended to be mapped on gentler slopes, whereas recent failures statistically seem to originate on steeper slopes (Table 3.2). The issue of planimetric mapping of landslides on steep slopes, and the uncertainty this can create, has also been noted in Fiordland (Cox et al., in prep. [a]). The very steep topography may be important when defining hazard from slopes in and around Piopiotahi / Milford Sound.

Table 3.2 Some notable ‘problematic’ examples of hazard on steep slopes in Norway.

Event	Scale	Comment
Fortunsdalen 2021	150,000–180,000 m^3 landslide on very steep slopes created a dam.	Not mapped as an unstable slope, no INSAR, not very visible in lidar.
Geiranger Fjorden 8 May 2017 https://youtu.be/vrX0WRTcxz0	A major rockslide in spring without an obvious trigger in terms of a seismic event or heavy rainfall. About 167,000 m^3 with detached rocks falling in front of the main body caused a tsunami of ~1 m.	Considered beforehand to possibly be an unstable slope. Little satellite or INSAR data before.
Koppartind 2024	Rockfall activity from a buttress slowly collapsing.	The actual area of failure is much larger than identified in prior mapping.
Skarfjellet 2025 https://www.youtube.com/watch?v=sgoE7MXyNCo	Continued active rockfall, releasing noticeable volumes and generating fresh debris, provided warning. Modelled at ~4 million m^3. Closed trail.	On the edge of a post-glacial failure previously mapped. Clearly visible in InSAR. Moving 20–40 cm/day, then slowed.

The case histories in Norway highlight that there can be an inherited bias when mapping and monitoring slopes, particularly those that are known to be creeping. Steep slopes require less movement before failure, and the development of geomorphic features used to recognise that failure is occurring (or imminent) is less pronounced. Steeper slopes tend to be much less visible in satellite monitoring (InSAR) and also have failures with smaller planimetric areas in aerial photos than shallow or moderately angled slopes.

There can also be bias and uncertainty in apparent variation in magnitude and frequency over time. High-resolution bathymetric mapping and seismic reflection data revealed the presence of at least 18 very large (10^6–10^7 m^3) post-glacial rock-avalanche deposits that blanket ~40% of the bottom of Piopiotahi / Milford Sound (Dykstra 2012). There are also at least 10 additional, terrestrial landslide deposits of 10^6–10^8 m^3 in the lower Milford catchment, defined by geomorphic mapping and field investigations. These landslides are interpreted to have occurred during the post-glacial period, with many of the dated deposits inferred to be Holocene in age (~9–1 ka) (Dykstra 2012). By way of comparison, recent moderate and large historical earthquakes in Fiordland (e.g. 1988, 1993, 2003, 2007 and 2009) have caused widespread superficial landsliding over very large areas, particularly from steep slopes near the earthquake epicentres, but none have triggered very large (≥10^6 m^3) landslides in bedrock.

There are valid reasons why landslides and tsunami into fiords might have been more frequent and larger as glaciers retreat, as ice withdrawal removes support for the sides and base of fjord walls. Pre-historic earthquakes and shaking may also have been significantly higher than that experienced during the recent Fiordland earthquakes. There will always be some uncertainty as to whether the geological record of processes in the long-term are a reasonable representation of the future, particularly as climate evolves. But this is an international science question that is yet to be fully resolved or implemented in operational policy. Of concern would be the potential that this might be used, politically or in management and policy, as a reason for future inaction. In the absence of clarity, it may be better to adopt a conservative approach, assuming that the worst-case scenario is still a credible possibility.

3.3.4 Landslide Magnitude–Frequency Distribution

Specific treatment of landslide volume and mobility influences modelled tsunami heights (Barnhart et al. 2021). Estimation of a landslide failure plane, and the volume above it, can be achieved after a landslide has failed by reconstruction of pre- and post-failure elevation models (change detection). Where landslides are old and accurate pre-event elevation models are not available, volumes are commonly estimated using the sloping local base level method (Jaboyedoff et al. 2020). Other interpolation methods are also proposed and used (Singh and Sepúlveda 2025). The uncertainty in all volume calculations tends to increase markedly as slopes become steeper, particularly where mapping is restricted to 2D planimetric view (Marc et al. 2016).

Measurement of relative magnitude (M) and frequency (F) of historical rockfall and landslide volumes is now relatively straightforward from landslide catalogues and is fundamental to hazard assessment. Depending on the type of bedrock and spacing of jointing, these are commonly approximated by the formula:

$$logF = a + b.logM \quad \text{Equation 3.1}$$

where F is the cumulative frequency per year, M is the volume (m^3), a is an empirically determined constant that depends on the exposure of a region to landslides and b is the slope of the power-law relationship. The a and b values vary from one geological setting to another. Deviations from straight power laws often occur as a result of completeness issues (particularly detection of small landslides), but there is variance also caused by local geology and process information (topographic amplification, lithology, runout dynamics). For hard plutonic rocks in British Columbia, Hungr (1999) empirically determined a and b values of 0.77 and -0.43, respectively. The approximately 1000-year, pre-historic landslide inventory developed for Milford Sound had a and b values of 0.56 and -0.54 (Dykstra 2012).

A key statistical concept for earthquake-induced landslides is that the universal magnitude scaling relationship M_L is directly proportional to $\log(N_{LT})$, where N_{LT} is the total number of landslides associated with a triggering event and M_L is the local magnitude of the earthquake (Keefer 1984; Malamud et al. 2004). A more recent study (Tanyaş et al. 2018) has used a larger collection of earthquake-induced landslide inventories and shows that size distributions are more variable than previously assumed, presenting a new model that incorporates uncertainty. These empirical relationships are useful for understanding the general scale of landsliding associated with earthquakes (Sepúlveda et al. 2010) but do not account for factors such as slope and geological susceptibility (see also Hancox et al. [2002] and Massey et al. [2018, 2020a]).

3.3.5 Landslide Velocity

The transport velocity of a landslide is a function of driving forces (primarily gravity) and resisting forces (friction and viscous drag), which are influenced by physical and environmental factors. Some common considerations include: geometry and topography (steeper slopes and greater vertical drops lead to higher potential energy conversion into kinetic energy, increasing velocity), rheology (material properties and pore-water pressure dictate how a slide deforms and moves; viscous drag acts as a major dissipative resistance force) and erosion and entrainment (which add mass and energy to the flow; can enhance mobility and amplify acceleration).

Landslide velocity is also controlled by how quickly the mass is supplied into the moving system. Catastrophic failures inject mass impulsively, promoting inertia-dominated motion and dynamic weakening, whereas progressive or episodic failures produce supply-limited velocities that remain sensitive to hydrological and frictional controls. Consequently, there is fundamental distinction between earthquake-induced landslides and rainfall-induced failures (Keefer 1984; Cruden and Varnes 1996; Iverson 2000). Earthquake-induced landslides have high rates of failure, high initial velocities independent of slope angle and near-synchronous collapse over large areas in an inertia-dominated regime. In contrast, rainfall-induced landslides commonly fail at lower rates and are often progressive or episodic, with velocity strongly modulated by pore-pressure diffusion.

Catastrophic rock avalanches (impulsive supply) will behave fundamentally differently from progressive rockfalls, even on identical slopes (Davies and McSaveney 2009). Rock avalanches have near-instantaneous mass delivery, high initial velocities, strong-dynamic weakening and long runout (high mobility). Their failure rate dominates early velocity, while fragmentation-driven processes and basal processes control their runout. A rapid, coherent collapse injects high momentum quickly, high normal and shear stresses at the base and elevated pore pressures (due to undrained loading). In contrast, a slow/progressive disaggregating collapse, such as rockfall, allows stress dissipation and pore pressure diffusion, which help prevent dynamic weakening mechanisms from activating.

3.3.6 Landslide Shape

There is observational evidence that failure rates have subsequent imprint on landslide geometry and flux rate. The notion is in part based on statistics of deposit planiform shape, thickness, volume-area scaling, runout style and number-size statistics (Guzzetti et al. 2009; Larsen et al. 2010; Marc et al. 2016; Massey et al. 2018, 2020a, 2020b).

Studies commonly use a volume-area scaling relationship:

$$Volume = \alpha(Area)^{\Upsilon} \quad \text{Equation 3.2}$$

where α is a thickness proxy and Υ is a scaling exponent. Earthquake-induced landslides tend to have relatively high α values and exponents (Υ) ~1.2–1.4, whereas rainfall-induced landslides have a lower thickness proxy and exponents ~1.1–1.3.

Earthquake-induced landslide deposits are commonly described as having a tendency toward more-compact, lobate or sheet-like morphology and high volume to area ratios (Dick 2021). Conceptually, much of the landslide mass arrives together, momentum spreads material laterally rather than stretching it longitudinally and deposition occurs when the inertia dissipates. In contrast, rainfall-induced landslide deposits have lower volume to area ratios and are commonly elongated or channelised. Conceptually, prolonged or episodic supply of a landslide occurs as mass is fed incrementally, flow self-organises into channels and mass is advected downslope in a tongue shape with long runout.

Accordingly, the potential for generating tsunami waves from earthquake-induced landslides, or some other spontaneous gravitational collapse that remains relatively coherent, seems greater than it will be from rainfall-induced landslides. For the purpose of earthquake-induced landslide tsunami scenarios, the worst-case wave scenario is likely to come from a large (≥1 million m^3) rapid rock avalanche.

3.3.7 Landslide Rheology and Behaviour Models

Slide kinematics and impulsive wave features, such as wave shape, amplitude, run-up and run-down, can be defined and varied in empirical experiments. For example, Huang et al. (2014) performed laboratory tests to examine the effects of bed slope angle, water depth, slide impact velocity, geometry (three-dimensional size of the rigid block and grain size of the granular cluster) and volume on the characteristics of impulse waves. The study showed that rock-mass failure type plays a key role in tsunami characteristics, strongly influences air–fluid–solid interaction and provided different equations for estimating primary wave amplitude depending on failure types. Although the application of these derivative equations is inexpensive and efficient, they provide preliminary estimates only, with some uncertainties for complex water-body shapes and changing rheological behaviour of landslides at different scale. Prototype specific physical model tests are suggested to be more reliable (Heller and Ruffini 2023).

Some landslides have been modelled with simple rigid block models, which slide down a slope (Slingerland and Voight 1979). Such conceptualisation has the drawback that this can be inaccurate where macroscopic deformation occurs on steep slopes, where slide volumes are very large or where a non-linear complex three-phase (water–air–soil) flow is generated close to the impact area. There is a big difference between a rigid rock plunging into water and a granular cluster sliding into the water. Numerical tools used to model waves may conceptualise a landslide as either a rigid or deformable mass (Yavari-Ramshe and Ataie-Ashtiani 2016). The rheology is very important for controlling the volume, shape and rate at which a landslide may enter a water and, therefore, create a tsunami. Landslides can be considered as a homogeneous single phase, mixtures or a multi-phase fluid. Widely applied rheological flow models (see Appendix 1) include Newtownian, Bingham, Bagnold or bi-linear for granular flows, or Newtonian for mudslides and debris flows. Coulomb or Voellmy rheologies are also popular, used to describe behaviour of granular mixtures of solids and fluids.

To most accurately estimate landslide-induced waves caused by sub-aerial landslides, especially at the wave-generation stage, landslide deformation needs to be considered. Such models tend to presume either a single layer containing a mixture or multi-phase fluid; or a two-layer domain that includes a layer of granular material beneath a layer of water, where each layer is described as a homogeneous, mixture or multi-phase fluid with its own rheology.

Numerous studies have demonstrated frictional behaviour when landslide sizes are small to moderate (i.e. thousands of cubic metres), but include velocity-dependent terms in their behaviour once these become large or giant (e.g. greater than millions of cubic metres). Adding a velocity-dependent term allows models to simulate both stopping and long-runout behaviours and can be used to predict deposit morphology (Dick 2021). Voellmy rheology describes the flow resistance as a combination of Coulomb friction ($\mu\sigma$ that is a constant friction component μ proportional to the normal stress σ) and a velocity-dependent friction (with a turbulence/roughness coefficient times velocity squared; ξV^2). Other approaches suggest modifying Voellmy rheologies when landslides undergo spatial and temporal changes in solid–fluid composition (Meyrat et al. 2023) or to account for slope- or height-dominated regimes within the flow of a rock avalanche (Hergarten 2024). Confinement along the flow path can also influence the landslide rheology and generate long runout in moderate-sized rock avalanches (Strom et al. 2019).

In many hazard and risk studies, the exact rheology and nature of landslides may be very difficult to predict. Empirical observations of landslide deposits and runout geometry can potentially be used to provide an indication of, or calibrate, landslide rheology (Dick 2021). However, where the exact nature and style of collapse is not known, or may vary from site to site, relatively simple and generic empirical equations from laboratory and numerical tests, or field occurrence and historical observations, may be a sufficient method of determining the scale of resultant tsunami waves (for discussion, see Heller and Ruffini [2023]). A framework for analysing uncertainties emerging from the landslide source process was proposed by Løvholt et al. (2020), which employs event trees to conduct tsunami uncertainty analysis and probabilistic tsunami-hazard analysis. Their approach combines empirical landslide data with expert judgement to come up with probability maps for tsunami inundation. They propose that landslide tsunami-hazard analysis contains significant epistemic uncertainties caused by incomplete knowledge (cf. those caused by natural randomness), which can be incorporated in the probabilistic framework, including inundation-height-exceedance maps.

3.3.8 Empirical-Wave-Amplitude Formula

Attempts to describe and model landslide-induced impulse waves have been made using numerical simulations based on theoretical mathematical relationships and empirical data based on either physical model experiments or field observations (Slingerland and Voight 1979; Fritz et al. 2004; Panizzo et al. 2005b; Enet and Grilli 2007; Abadie et al. 2008; Ataie-Ashtiani and Shobeyri 2008; Di Risio and Sammarco 2008; Gisler 2008). A useful summary of wave equations has been provided by Di Risio et al.

(2011). Approaches generally adopt some form of the relationship where the amplitude of the initial wave, for a given water depth, is related to the impact speed and mass of a given landslide at the air–water boundary. However, landslide entry angle and surface geometry are also important variables on wave amplitude, as illustrated simplistically in Figure 3.1.

The closer that a landslide speed is to the shallow-water phase velocity (or celerity of a tsunami in water of a particular depth), the higher the wave amplitude. A useful equation for celerity is:

$$c = \sqrt{gd}$$ Equation 3.3

where g is the gravitational acceleration and d is water depth. The Froude number is the ratio of the landslide velocity (v) to the tsunami phase velocity $F = v/sqrt(gd)$.

A common approach to modelling displacement waves is to derive a landslide impact velocity, which can be based on theoretical analysis of a rigid block in freefall (Noda 1970) or sliding on an inclined plane (Slingerland and Voight 1979). Downslope movement a rigid block on a plane can be modelled with the simple equation of gravity motion, modified to allow for frictional resistance of the sliding block:

$$V = \sqrt{2gl\,[sin(\alpha) - \,tan(\sigma)cos(\alpha)]}$$ Equation 3.4

where V = velocity, g is gravitational acceleration, l is slide path length, α is the failure plane angle and σ is the angle of dynamic bed friction. The equation provides a reasonable estimate of maximum impact velocity for steep landslides on relatively simple, planar failure planes, but it may over-estimate (by as much as 100%) the maximum velocity of a block traveling over multiple planar segments of significantly differing slope angle.

The Slingerland and Voight (1979) best-fit linearised regression formula was utilised at Piopiotahi / Milford Sound by Dykstra (2012) (see Section 4.6). However, this best-fit application also ignores the variance in the original sample population used in the regression, so Taig and McSaveney (2015) recommended adopting the 84th percentile coefficients (the values at the mean plus one standard deviation) for which only 16% of the population is likely to exceed.

There are other predictive models based on granular mass movement, where internal frictional resistance is considered (Walder et al. 2003; Fritz et al. 2004). These approaches require knowledge of slide geometry (e.g. failure-slope angle, slide distance, dynamic bed friction angle) and bulk material properties (e.g. density, internal friction angle). The method of Heller et al. (2009) was implemented in a GIS-environment by Cannata et al. (2012), who generated a module for the open-source GRASS GIS-program named *r.impact.tsunami* to study landslide tsunami. This uses empirical equations to estimate initial wave characteristics based on landslide parameters such as mass volume, density, slide thickness and impact slope. Outputs from this initial step are a set of initial conditions for the wave, including its height and velocity, which are then used to simulate propagation and run-up using a set of shallow-water equations.

Physical laboratory models can also be used to understand the generation of tsunami waves but need to be modelled with Froude similarity (Hughes 1993) in that the gravity and inertial forces need to dominate over the kinematic viscosity of water V_w (Reynolds number $R = g^{1/2}\,h^{3/2}\,/V_W$) and surface tension σ_W (Weber number $W = \rho wgh^2/\sigma_W$). A certain model size is required to avoid significant scale effects.

Numerical simulations for submarine landslides are also available and quite distinct from sub-aerial landslides that impact on a water body (see Watts et al. [2005] and Løvholt et al. [2008]). Although both are derived from point sources, sub-aerial landslides generate leading positive and leading negative waves that are governed by the net displaced volume. This poses a fundamentally different property for tsunami propagation compared with the completely submerged landslides, which add zero net volume (Løvholt et al. 2008).

3.3.9 Empirical Propagation and Run-Up Formula

A semi-empirical model was generated to predict the run-up height of waves generated by a landslide (Oppikofer et al. 2019). A catalogue of landslide-induced displacement waves was used to develop semi-empirical relationships linking displacement wave run-up height (R in metres) to distance from landslide impact (x in kilometres) and to landslide volume (V in millions of cubic metres). For individual events, run-up decreases with distance according to power laws. Consideration of 10 events demonstrated that run-up increases with landslide volume, also according to a power law, and is used to generate the SPLASH equation (Oppikofer et al. 2019).

The general form of the SPLASH equation is:

$$R = aV^b x^c \qquad \text{Equation 3.5}$$

where Oppikofer et al. (2019) derived best-fitted parameters, a = 18.093, b = 0.5711 and c = −0.7419, from 10 events.

Currently in Norway, unstable rock slopes threatening settlements or water bodies with adjacent communities are hazard-classified following a standardised workflow that assesses morphology, structure and activity – but which also assumes that all slopes fail as rock avalanches (alternative failure types include rock creep flows and rotational slides). Runout distances are estimated using global runout *H/L– volume* relationships, and displacement wave run-up is evaluated with the SPLASH formula. It has been shown that this does not account very well for wave-height reduction at direction changes and has tendency to over-estimate the impacted area. Nonetheless, it is simple in application and useful and used for susceptibility mapping. Other GIS-based models for tsunami generation and propagation include *r.impact.tsunami* in the GRASS GIS mentioned in Section 3.3.8 (Cannata et al. 2012).

3.4 Numerical Modelling

This section contains a review of numerical techniques used for modelling landslide-induced tsunami in fiords internationally. Some of the content is highly technical, and non-specialists may prefer in a first read-through to cover only the high-level summary in Section 3.4.1 before moving ahead to Section 3.5.

3.4.1 Introduction and Overview

Numerical modelling of landslide–tsunami involves the solution of physical equations governing the motion of the landslide and tsunami. It contrasts with empirical modelling, which involves interpolation or extrapolation from sets of observational data of past landslide–tsunami at other locations – this is the approach used previously for Piopiotahi / Milford Sound (see Section 4.6). A major advantage of numerical modelling is that it can be adapted to the specific context of a particular location (e.g. topography, bathymetry, rock properties) to an extent that empirical modelling generally cannot.

In numerical modelling of landslide–tsunami, a landslide can be modelled separately from a tsunami and used as a determined input to a tsunami model, or a landslide and tsunami can be modelled together in a ‘coupled’ model. Coupled models would generally consider both the landslide causing movement of the water and also the presence and motion of the water affecting the motion of the landslide once it has submerged.

Landslide motion is typically modelled as either a rigid block or as a dense, viscous, debris flow, as described in the previous section. Ideally the choice of model reflects expectations of the form and nature of prospective landslides – whether these are expected to break and fall as a solid piece of rock, to break up into many smaller pieces or to be better represented by a debris flow (see discussion in Fine et al. [2003]). In all likelihood, reality will likely involve some combination of the above, with the slide breaking up into both small flow-like pieces and occasional larger parts. Where a landslide is modelled as a debris flow, there are different possible numerical representations of friction at the base of the flow and of the rheology, which are properties that strongly affect how materials deform and flow.

Tsunami generation occurs when the landslide enters the water and continues as the slide travels beneath the water surface. Generated waves may include a 'splash' component of short-duration waves that remain close to the site of impact (Walder et al. 2003; Han et al. 2022) and a 'tsunami-like' component that is able to efficiently propagate large distances. While the 'splash' can be hazardous in the near vicinity of the landslide, it is generally the tsunami-like waves that hazard assessments are concerned with because their long range and travel expose locations of interest (e.g. Milford township) to waves from a greater number of potential landslide locations.

Numerical models of tsunami propagation solve the equations of water motion. Typically, these models fall into two categories depending on whether or not they incorporate the effects of frequency-dispersion. Frequency-dispersion is a process by which the shape of the wave may become separated into different components and which takes place when the wavelength (distance between consecutive wave peaks) is not much longer than the water is deep. In this situation the shorter-period (higher-frequency) components of the wave travel more slowly than the longer-period (lower-frequency) components, stretching out the sequence of waves. This is a cumulative effect that increases with the distance travelled. However, numerical solution of dispersive wave equations is much more complicated and resource-consuming than modelling non-dispersive waves (see discussion in Esposti Ongaro et al. [2021]).

Once a tsunami encounters land, it can cause inundation, and, particularly when steep slopes are present, the momentum of the tsunami may cause it to run up to greater heights against the slope. Run-up can also be accentuated when the tsunami inundates into a narrowing valley, in which case the water volume is 'squeezed' into a smaller space and the surface height increases to compensate. Numerical inundation modelling allows for the flow around detailed topography to be accounted for and requires specialised algorithms for modelling the boundary between wet and dry locations.

Sometimes the different stages – generation, propagation, inundation – are modelled using different software, although this requires careful transfer of boundary information between the different sub-models. Alternatively, some software packages model the whole process within a single integrated computation, which avoids the need for transferring boundary conditions.

Sections 3.4.2–3.4.5 provide more technical detail on the stages of the numerical modelling process. In Section 3.4.6, we summarise some key numerical-modelling case studies.

3.4.2 Modelling Landslide Motion

As discussed in Section 3.3.6, landslide motion is typically approximated as either that of a slope-descending rigid block or represented by modelling the motion of a dense viscous granular flow. Ideally, the choice of representation would be made to best approximate the actual anticipated landslide behaviour, i.e. whether the slide is likely to remain rigid or become broken into many smaller pieces in a debris avalanche (Fine et al. 2003).

For the rigid-block case, the landslide is assumed to be cohesive and non-deformable, and the equations of motion are typically those governed by the action of gravity on an inclined plane with resistance coming from base friction (Section 3.3.7). Once submerged, the equations of motion should also take into account buoyancy, hydrodynamic friction and drag forces (for details, see Watts [1998]; Grilli and Watts [1999] and Enet and Grilli [2007]). Application of this model may treat the moving block as a time-varying sea-floor (or lake-floor) disturbance or be used to define an initial water-surface displacement (see Section 3.4.2).

The dynamics for a debris avalanche modelled as a viscous or granular flow are sensitive to assumptions of landslide rheology (Section 3.3.6), for which there are many formulations. Typically, modelling proceeds using a two-layer approach, with the lower layer (the only layer when sub-aerial) representing the granular flow and the upper layer representing the water body above the landslide.

The equations used by Heinrich et al. (2001) for modelling generation of the 1998 Papua New Guinea tsunami by a submarine slump are conveniently similar to those used for modelling tsunami propagation (Section 3.4.4):

$$\frac{\partial}{\partial t}(hu) + \alpha\frac{\partial}{\partial x}(hu\,u) + \alpha\frac{\partial}{\partial y}(hu\,v) = -\frac{1}{2}\kappa\frac{\partial}{\partial x}(gh^2cos\theta) + \kappa ghsin\theta_x - \tau_{xz}$$

$$\frac{\partial}{\partial t}(hv) + \alpha\frac{\partial}{\partial x}(hv\,u) + \alpha\frac{\partial}{\partial y}(hv\,v) = -\frac{1}{2}\kappa\frac{\partial}{\partial y}(gh^2cos\theta) + \kappa ghsin\theta_y - \tau_{yz}$$

$$\kappa = 1 - \rho_w/\rho_s$$ Equation 3.6

where ρ_w and ρ_s are the water and slide densities, respectively (ρ_w is taken as 0 for sub-aerial slides). Here, x and y are in a slope parallel coordinate scheme. θ is the local maximum slope, and θ_x and θ_y are the slope angles in the x and y directions, respectively. α relates to the over-thickness velocity profile and is taken as 1 for granular flows (uniform velocity profile) or 6/5 for viscous flows (parabolic velocity profile). g is the gravitational constant, u and v are the depth-averaged velocities in the slope-parallel x and y directions and h is the slide thickness perpendicular to the slope. τ is shear stress at the bed surface for the granular flow case:

$$\tau_{xz} = \kappa gh\ cos\theta\ tan\varphi\frac{u}{\|u\|}$$ Equation 3.7

where φ is the friction angle between the rock bed and the landslide mass.

For viscous flows:

$$\tau_{xz} = -3\mu u/(h\rho_s)$$ Equation 3.8

where μ is the dynamic viscosity.

This set of equations, with minor variations, forms the basis for several landslide–tsunami studies, both initially sub-aerial and entirely submarine, conducted using the COMCOT (Cornell Multi-grid Coupled Tsunami) model (Mountjoy et al. 2019; Hughes 2025).

3.4.3 Modelling Wave Generation

As discussed in Section 3.3.7, the Froude number, defined as the ratio of the landslide velocity (v) to the tsunami phase velocity *F = v/sqrt(gd)*, plays an important role in tsunami generation by landslides. When the Froude number is close to 1, the landslide and tsunami are propagating at similar speeds, which is most efficient for the build-up in amplitude of the leading tsunami wave (Fine et al. 2003).

Landslides that are entirely submarine do not generally approach speeds such that the Froude number is close to 1 (exceeding 1 is the underwater equivalent of going ‘supersonic’). Whereas, for initially sub-aerial landslides, there is always a point in time after these become immersed when the Froude number is close to 1 and energy is passed efficiently to the tsunami (Fine et al. 2003). A further consideration, especially for enclosed or partially enclosed water bodies, is the additional volume that the landslide adds to the water body.

Experimental studies have found that, for sub-aerial landslides, the landslide frontal area (Fritz et al. 2003), mass and slope angle (Heller et al. 2008; Bullard et al. 2019) and length (Enet and Grilli 2007) all also play a role (Løvholt et al. 2020).

As mentioned in Section 3.4.2, there are in general two approaches for numerical modelling, one in which the landslide is represented as a coherent body retaining the same shape and the other where it is modelled as a fluid-like debris avalanche. In the rigid-body case, one approach is to represent the body as a moving boundary condition in the bathymetry, which appears in the tsunami propagation equations via the $\frac{\partial h}{\partial t}$ term in Equation 3.9. In such a representation, the landslide body can be allowed to deform in a limited way such that it can be made to follow the changing gradient of the lake or sea floor. An alternative approach is to apply tsunami initial conditions derived from experimental studies that are scaled to match the anticipated landslide (Enet and Grilli 2007) or derived from 2D (vertical slice) numerical modelling applying the Navier-Stokes equations to the rigid-body problem (Lane et al. 2016).

Where the landslide has been represented by a granular or viscous-fluid debris flow, the solution to the landslide model represents in effect a time-series of changes to the lake bed. These may then also be incorporated into the tsunami equation of motion (Section 3.4.4) via the $\frac{\partial h}{\partial t}$ term in Equation 3.9.

3.4.4 Modelling Wave Propagation

Water-propagation modelling for tsunami is most commonly performed by solving the nonlinear shallow-water equations. In spherical coordinates, these equations can be represented as (Wang and Power 2011):

$$\frac{\partial \eta}{\partial t} + \frac{1}{R cos\varphi}\left\{\frac{\partial P}{\partial \psi} + \frac{\partial}{\partial \varphi}(cos\varphi Q)\right\} = -\frac{\partial h}{\partial t}$$

$$\frac{\partial P}{\partial t} + \frac{1}{R cos\varphi}\frac{\partial}{\partial \psi}\left\{\frac{P^2}{H}\right\} + \frac{1}{R}\frac{\partial}{\partial \varphi}\left\{\frac{PQ}{H}\right\} + \frac{gH}{R cos\varphi}\frac{\partial \eta}{\partial \psi} - fQ + F_x = 0$$

$$\frac{\partial Q}{\partial t} + \frac{1}{R cos\varphi}\frac{\partial}{\partial \psi}\left\{\frac{PQ}{H}\right\} + \frac{1}{R}\frac{\partial}{\partial \varphi}\left\{\frac{Q^2}{H}\right\} + \frac{gH}{R}\frac{\partial \eta}{\partial \varphi} - fP + F_y = 0$$

Equation 3.9

where H is the total water depth and $H = \eta + h$, F_x and F_y represent the bottom friction in the x and y directions, respectively. Typically, these are evaluated using Manning's formula:

$$F_x = \frac{gn^2}{H^{7/3}} P(P^2 + Q^2)^{1/2}$$

$$F_y = \frac{gn^2}{H^{7/3}} Q(P^2 + Q^2)^{1/2}$$

Equation 3.10

where n is the Manning's roughness coefficient, which may be spatially variable to represent the roughness of different surfaces. η is the water-surface elevation, P and Q are the volume fluxes in the x (west to east) and y (south to north) directions, φ and ψ are the latitude and longitude, R is the radius of the Earth, g is the gravitational acceleration, H is the water depth and f is the Coriolis force.

These or similar equations are typically solved using either a finite difference scheme implemented on a regular rectangular mesh (e.g. COMCOT [Wang and Power 2011]) or by a finite volume scheme over an irregular mesh usually formed of triangles (e.g. ANUGA [Roberts et al. 2013]). Some schemes also apply adaptive grid or mesh refinement, i.e. changing the size of grid cells or mesh triangles as needed (GeoClaw; Arcos and LeVeque 2015).

If the wave length of tsunami waves are not long compared with water depth, a situation more likely to occur for landslide-induced tsunami than those caused by earthquakes, an effect known as frequency-dispersion occurs. In this process, the high-frequency components of the wave travel more slowly than the low-frequency ones, leading to changes in the shape of the wave that accumulate over time. There are various techniques for incorporating frequency dispersion, although these come at a significant cost in computational time and model complexity. See Esposti Ongaro et al. (2021) and Kirby et al. (2022) for comparison of different techniques.

3.4.5 Modelling Run-Up and Inundation

Numerical modelling of inundation and run up extends upon the equations of motion for tsunami wave propagation (Section 3.4.4) by tracking and updating the boundary between water and dry land with each time step of the model. There are various schemes for achieving this; see, for example, Cho (1995), Liu et al. (1995) and the COMCOT implementation in Wang and Power (2011).

3.4.6 Modelling Case Studies

There have been several numerical modelling studies of landslide-induced tsunami in fiords. Below, we summarise three examples linked to the country summaries in Section 3.1.

Barnhart et al. (2021) studied the potential for large landslides on an unstable slope of the Barry Arm of Prince William Sound, Alaska. The potential landslides occur where the Barry Glacier has only very recently retreated (since about 2012), leaving slopes that were previously buttressed by the glacier no longer supported in this way. Should the slopes fail, these would now fall into the fjord located where the glacier was previously. Four scenarios have been studied; these involve larger (689 million m^3) and smaller (290 million m^3) volumes and two representations of the landslide mobility.

Modelling was conducted using D-Claw a relative of the GeoClaw (Arcos and LeVeque 2015) software originally developed for tsunami modelling. D-Claw simulates the coupled evolution of fluid and solid phases in a depth-averaged model. The landslide is treated as a fully saturated granular material. In the absence of a landslide, the equations for a tsunami reduce to the nonlinear shallow-water equations.

The larger volume (689 million m^3) and higher-mobility scenario produced the largest tsunami heights (i.e. water-surface elevations above background level). In the largest scenario, tsunami heights reach 200 m in the 'splash zone' in the northernmost part of Barry Arm and run-up heights in excess of 500 m on the opposite fjord wall. The subsequent tsunami is estimated to take 26 minutes to reach the town and port of Whittier approximately 60 km away (distance over water). The tsunami height in Passage Fjord, 500 m offshore of Whittier, is estimated to peak at just over 2 m.

Harbitz at al. (2014) studied the potential for rockslides and subsequent numerical tsunami modelling for the Åkerneset landslide in Storfjorden, Norway, and of the nearby Hegguraskla rockslide in Tafjorden. In inner Storfjorden 108 rockslide deposits have been mapped. Of these, 21 are equal or larger than the one that caused the 1934 Tafjord disaster, but only six of these occurred in the Holocene (last 10,000 years). For Åkerneset, the 1:5000-year event is assumed to be 54 million m^3 and the 1:1000-year event is assumed to be 18 million m^3. For Hegguraskla, the 1:5000-year event is assumed to be 3.5 million m^3 and the 1:1000-year event is assumed to be 2 million m^3.

Modelling of tsunami generation and propagation was conducted with the GloBouss or DpWaves software solving the Boussinesq equation, and a one-way-nested MOST model was used for inundation. Rockslides were represented by either a moving 'rounded box' of fixed trajectory or the output of numerical rockslide models. Validation and calibration were made against physical experiments and reconstruction of historical events. Twenty-three (23) locations were considered by the study, including the popular tourist centre of Geiranger (similar to Milford) and Tafjord, the site of a landslide–tsunami disaster in 1934. Outputs included maximum inundation height, maximum current velocity and maximum flow depth.

At the time of the study, the hazard was found to be higher than the acceptable threshold for development by the Norwegian Planning and Building Act. This presented obvious drawbacks to a region reliant on coastal activities, and the Act was amended to allow specified development contingent on various requirements, such as there being no alternative location, critical facilities not being located in the most hazardous zones, a warning system being in place, evacuation plans being in place and public awareness sustained.

Scheele et al. (2013) studied the tsunami generated in Aysen Fjord, Chile, by rockslides following the M_W6.2 earthquake in 21 April 2007. Over 300 landslides were triggered in the area, with three of the largest reaching Aysen Fjord and causing tsunami. Two of these tsunamigenic landslides were modelled for the report, with volumes of about 18 x 10^6 and 22 x 10^6 m^3.

The maximum tsunami run-up measurement was ~50 m in close proximity to one of the two large tsunamigenic landslides. The most distant measurements were around 15 km away. Modelling was performed using COMCOT. Inundation and run-up was not computed, but, allowing for this, the model results provided a reasonable match to the observations. A following study by Uribe et al. (2025) used NHWAVE and FUNWAVE-TVD software to allow for frequency dispersion and considered both a viscous flow and solid landslide model; these changes improved comparisons with observations, particularly at more distant locations.

While there is a lack of numerical modelling studies of landslide–tsunami specific to New Zealand's fiords, landslide–tsunami modelling studies have been made (or are being made) for lakes and offshore islands that use comparable techniques:

- The Waihi Fault scarp above Lake Taupō is believed to be responsible for at least three major landslides into the lake. Wang et al. (2013) used COMCOT and a simplified tsunami initial condition to make modelling comparisons with the tsunami caused by the most recent landslide in 1910.
- Mountjoy et al. (2019) considered a variety of sub-aerial and delta collapse scenarios in Lake Tekapo in the Mackenzie Basin. For that study, they used the COMCOT software and a two-layer (landslide + water) approach.
- In her PhD thesis 'Reconstructing Lacustrine Tsunami Hazard in High-Seismicity Regions of New Zealand's South Island', Hughes (2025) used primarily geological and geophysical techniques to reconstruct past potentially tsunami-generating mass movements in South Island lakes. The thesis also includes numerical modelling of collapse of the Lake Rotoroa delta using the COMCOT two-layer approach.
- Current research in the 'Beneath The Waves' Ministry of Business, Innovation and Employment (MBIE) Endeavour project is studying tsunami risk posed to the Bay of Plenty by landslides on the flanks of Whakaari / White Island (Hughes et al. 2025). Geophysical studies have been used to identify potential failures using the limit equilibrium method, and modelling of landslides and subsequent tsunami is being performed using the COMCOT two-layer approach.

3.5 International Risk Tolerance and Management Approaches

Risk tolerance refers to individual or societal willingness to bear a risk. In many countries, risk management uses risk-tolerance criteria to evaluate risk and determine whether risk-mitigation measures are required to reduce this risk. For landslides, risk-tolerance criteria typically focus on life-safety risk, including both individual risk (such as annual individual fatality risk) and societal risk (probability of multiple fatalities occurring, often expressed as an F-N chart). Several countries and guidelines have proposed risk-tolerance criteria, most notably Hong Kong (ERM 1998) and Australia (ASG 2007). New Zealand approaches are discussed in Section 5.1.4.

Hong Kong has proposed societal risk tolerance criteria (Figure 3.3). The criteria provide a means to plot landslide risk for groups of people, expressed in terms of landslide probability and potential loss of life. This approach supports decisions on whether a given level of risk can be accepted (broadly acceptable), requires mitigation irrespective of cost (unacceptable) or should be reduced only where further measures are not "grossly disproportionate" to the benefits gained, consistent with the ALARP (as low as reasonably practicable) principle.

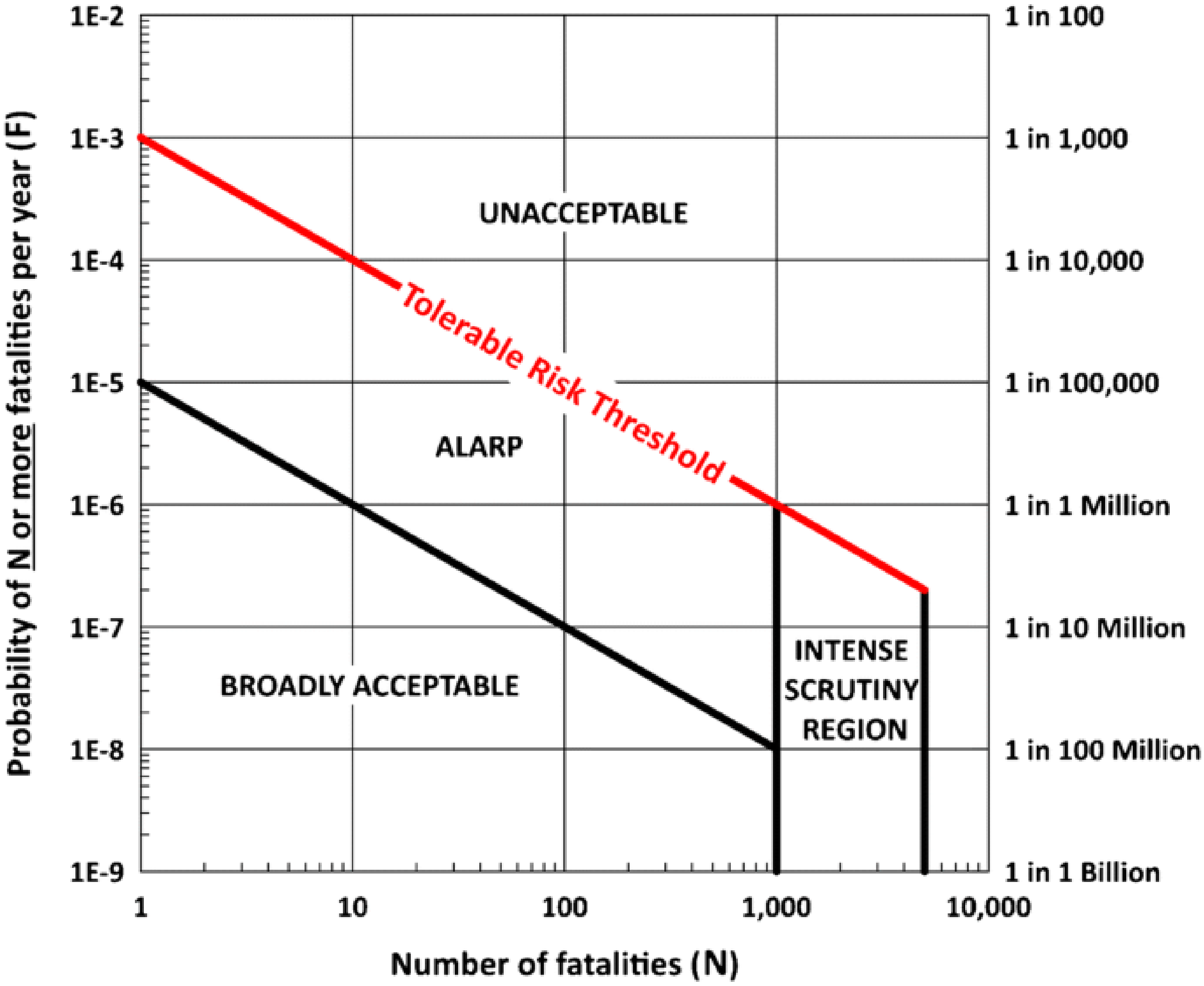

Figure 3.3 Societal risk-evaluation tool for direct losses from landslides (F-N criteria) developed in Hong Kong (ERM 1998), although a different version without the 'broadly acceptable' zone is more widely used in Hong Kong (Strouth and McDougall 2021).

Sim et al. (2022) provide a review of global landslide societal risk-tolerance criteria. They note that many countries adopt frameworks developed elsewhere, especially from Hong Kong and Australia. However, they observe a frequent mis-match between official criteria and how it is implemented (or not) in practise. Similarly, Strouth and McDougall (2021) demonstrate how applying Hong-Kong's societal F-N criteria (which was developed in the wake of fatal anthropogenic slope failures) in western Canada has proven problematic, often generating unaffordable risk management and mitigation requirements. The Hong Kong criteria, in particular the tolerable-risk threshold line in Figure 3.3, was developed for an area affected by a single (anthropogenically modified) slope segment that threatens hundreds to thousands of people and covers up to a 1000-year-return period, and therefore may be less relevant for hazards that threaten many more people or have a return period greater than 1000 years. Strouth and McDougall (2021) argue that such criteria should serve as guidelines rather than strict thresholds, as well as that risk-evaluation tools should be transparent to provide a framework for communicating 'why' each decision was made. They also argue that there should be an emphasis on cost-effectiveness and an acknowledgement of resource constraints. Strouth and McDougall (2022) also examined and evaluated individual life-safety criteria and found that these are also often adopted from other jurisdictions or hazard types without considering local context (for an overview of international individual risk-tolerance criteria, see Table 5.1 in de Vilder et al. [2024]). The individual life-safety risk-tolerance criteria were often unachievable, particularly for existing developments, and may not be representative of the whole population (i.e. homeowners who may accept greater risk to stay in their homes). A list of international papers reviewed are shown in Appendix 4.

Winter and Bromhead (2012), using examples from the United Kingdom, Hong Kong, Japan and Jamaica, showed that societal acceptance of landslide risk is shaped by social, economic and political conditions, proposing a ternary ‘willingness’ model to capture the willingness to accept risk, pay for risk reduction and modify the environment. Tappenden (2014) provides an analysis of the involvement of the public in setting risk-tolerance criteria as part of the District of North Vancouver’s Landslide management strategy following a fatal landslide. This analysis shown that expert education sessions, public open houses and an online survey allowed for public input on risk tolerability.

4.0 Review of Piopiotahi / Milford Sound Landslide–Tsunami Studies

The potential for tsunami hazard in Fiordland has been documented and evolved in published literature during the past two decades. A geomorphic record of some very large (10^6–10^8 m^3) post-glacial rock-avalanche deposits has been discovered at the bottom of Piopiotahi / Milford Sound and nearby terrestrial valleys. This region of exceptionally steep topography sits astride a very active plate boundary. Intense levels of shaking, either from an Alpine Fault rupture or other earthquake source, are imminent and sufficient to generate a large number of landslides. It seems there is little doubt that a very realistic and credible tsunami hazard exists from rock falling into the fiord, to which a large number of Piopiotahi / Milford Sound visitors and staff may be exposed.

Potential natural hazards generating visitor risk at Piopiotahi / Milford Sound include earthquakes, ocean-source tsunami, delta collapse, landslides and landslide-induced tsunami, while liquefaction and gradual effects of sea-level rise are of concern for assets and infrastructure (Grindley et al. 2007). Flooding, erosion, sedimentation, rainfall-induced landslides and avalanches are localised hazards that also affect the Milford road and valleys of Fiordland.

While there are many potential hazards and hazard cascades locally, the possibility of an earthquake-induced landslide(s) causing a tsunami has been highlighted due to the high level of associated societal risk (Otero and Almanzar 2024; Davies and Dykstra 2025). Notable uncertainties in the tsunami hazard remain due to limitations in available data and modelling and potential evolution of the hazard over time. Here, we review the existing body of work on tsunami hazard and risk in Piopiotahi / Milford Sound, with a focus on the earthquake-induced landslides triggering tsunami events, summarising key findings and uncertainties that have relevance for improved modelling.

4.1 Historical Observations

In Fiordland, there have been few direct observations of tsunami, due in part to the remote location, as well as the relatively short period of record keeping (<200 years). New Zealand's written record of day-to-day events is short and insufficient to allow a reliable assessment of hazards associated with return time of hundreds to thousands of years. Descriptions of damage from landslides and possible tsunami in Fiordland are listed in Table 4.1. Possible early tsunami events were reviewed by Downes et al. (2005) and Dykstra (2012) as part of a preparatory work for their field reconnaissance. No big landslides have fallen into Piopiotahi / Milford Sound to create large waves in the brief <200-year written history of the area (Taig and McSaveney 2015).

Table 4.1 Compilation of direct observations of tsunami in Fiordland.

Date	Description	References
1820s	Māori oral history, as recorded and interpreted by 20th century European historians, refers to an apparent tsunami in which a group of Māori were killed while walking along the coast near Orepuki in Southland during the 1820s. In unrelated documents, sealers in Dusky Sound, Fiordland, recorded a large earthquake in 1826 (with aftershocks extending into 1827) that caused a probable tsunami, many landslides in the mountains and possibly coastal deformation. The exact dates and sources of these events remain unknown, but they are considered consistent with a large Fiordland subduction zone earthquake(s).	Downes et al. (2005)
1987	A massive slip at Deep Cove (in Doubtful Sound) was reported in *The Southland Times* of 23 May 1987 to have occurred the previous day, creating a 2–3-m-high wall of water that lifted a 17 m boat onto a wharf. It is possible that this is the same event referred to by Downes et al. (2005) – "… a landslide into Deep Cove in May 1987, which did not occur in association with an earthquake, also caused localised 3 m waves" – and as a large rockfall in 1988 that lifted a 40 tonne boat 4 m onto a wharf, noted in Dawe (2007).	Dykstra (2012)
1988	The 31 May 1988 Fiordland M_W6.1 earthquake caused collapse of some lake deltas and a sub-aerial landslide that generated a 1-m-high wave in Lake Te Anau.	Forsyth et al. (2006); Turnbull and Beanland (1988)
2003	The M_W7.1 Secretary Island earthquake in 2003 generated 1852 mapped landslides. A tsunami was generated when a wedge-failure collapse of ~200,000 m^3 gneiss fell from a 40° slope into Taiporoporo Charles Sound (Hancox et al. 2003). The wave travelled directly across Gold Arm, where it stripped vegetation up to 5 m above the high-tide limit ~800 m away, and along the fiord ~250 m, where it displaced a helipad on piles and an adjacent and wharf. Landslides fell into many fiords and rivers during the earthquake, leaving these turbid and dirty with plant debris for weeks. It seems likely many would have generated local waves. A small tsunami wave (0.3 m peak to trough) was also recorded at Jackson Bay 190 km northeast of the epicentre in South Westland and travelled across the Tasman Sea to Port Kembla (0.17 m peak to trough) on the east coast of Australia.	Hancox et al. (2003); Leonard (2004); Power et al. (2005)
2009	The 2009 M_W7.8 Dusky Sound earthquake directed energy offshore and generated only 313 mapped landslides, significantly fewer than the 2003 earthquake. Close to the earthquake epicentre, waves and strong currents were experienced by boats in Dusky Sound (see Wilson et al. [2009] and Appendix 1 witness reports). Locally, GPS stations showed evidence of 220 mm land subsidence. At Passage Point cove, marine organisms were transported onshore and plants damaged up to 1.16 m above and 7.5 m inland of the spring high tide, estimated to be from a wave 2.3 ± 0.2 m. A wave of 1 m was measured at the Jackson Bay tide gauge, and the tsunami was detected in eastern Australia and propagated as far away as the west coast of the United States of America.	Wilson et al. (2009); Clark et al. (2011); Uslu et al. (2011)

4.2 Field Investigations of Tsunami Deposits and Sedimentation

As the record of historic tsunami events is too incomplete to reflect the complete range of possible tsunami events that may have occurred, observations have been augmented with fieldwork (mostly test pits in flat-lying coastal sites) to explore for paleo-tsunami deposits. Potential evidence of earthquake uplift and possible tsunami preserved in sedimentary sequences was found by Downes et al. (2005) (investigations at Cascadia, Martins Bay and Goose Cove) but remains reconnaissance in nature. Other flat sites around Piopiotahi / Milford Sound with potential to store tsunami deposits were identified and investigated by Dykstra (2012), but none showed any obvious evidence of past tsunami.

That fieldwork has been unable to definitively locate evidence of pre-historic tsunami in Fiordland is not entirely surprising. Deposits associated with the 2009 M_W7.8 earthquake tsunami were composed of fragile material (including plants and marine organisms) and other materials difficult to distinguish from normal storm deposits (Wilson et al. 2009). Loose material is also not always available around the fiord margins to create distinctive deposits, and the open coast is exposed to regular large swells and extreme seas. Tsunami deposits in Fiordland may be particularly difficult to identify and unlikely to last long (Clark et al. 2011).

Piopiotahi / Milford Sound has a locally high sedimentation rate, averaging ~1.3 mm/yr for the basin over the past 1340 years (Knudson et al. 2011) compared with much of Fiordland. But sedimentation rates for Milford (and the rest of Fiordland) are relatively low by global standards, even compared with the fjords of Norway where sedimentation rates are around 4–9 mm/year (Paetzel and Dale 2010) despite similar resilient bedrock geology and little contemporary glacier cover. Deltas have grown seaward (prograded) into the head of Piopiotahi / Milford Sound during the Holocene due to ample sediment supply (~109 tonnes/km^2/yr; Pickrill 1993) from its relatively large mountainous catchment. The Cleddau and Arthur river deltas at the head of the fiord, and the Harrison delta on the north shoreline, are large by Fiordland standards and extend to the bottom of Stirling Basin (-290 m). Depositional rates are sufficient that post-depositional deformation, foreset bed slumps and turbidity currents occur on the Cleddau Delta front (Brodie 1964; Dykstra 2012). Given the young age and unconsolidated nature of the delta, there is potential for delta collapse – whether induced by an earthquake or simply due to growth and loading – to cause a tsunami.

4.3 Distal-Source Tsunami

There is potential for some of the tsunami recorded elsewhere in New Zealand (Downes et al. 2017; Orchiston et al. 2025) to have affected Fiordland waters, be these from distant or regional sources or even local faults offshore of Fiordland. Expectations of wave amplitude and wave heights can be projected based on the nature of fault patterns, earthquake displacement, ground shaking and local landslides in comparison to landslide-induced tsunami elsewhere in the world (i.e. empirical models and calculations generated from observational experience).

The New Zealand National Tsunami Hazard Model (NTHM) 2021 provides revised hazard curves and de-aggregation plots of various tsunami wave amplitudes at the open coast entering Piopiotahi / Milford Sound, based on input parameters from distant and regional sources, local subduction zones and crustal faults (Power et al. 2023; Coastal section 210). The model does not include landslide-induced tsunami waves nor is it of sufficient resolution to accurately represent geographic attenuation and/or amplification as tsunami travel within Piopiotahi / Milford Sound. The maximum amplitude of a 1-in-1000 year return interval wave is estimated to be around 5 m (50th percentile), potentially 6.4 m (at 85th percentile), but larger waves should be expected over longer timeframes (at lower probability) (Figure 4.1). The study results are unable to identify whether this maximum amplitude occurs within the Sound itself[8] or on the open coast around the mouth of the Sound.

8 The numerical modelling underpinning the NTHM includes a representation of the interior of Milford Sound, although the narrow entrance to the sound is poorly resolved at the resolution used. It is in the aggregation of these model results into

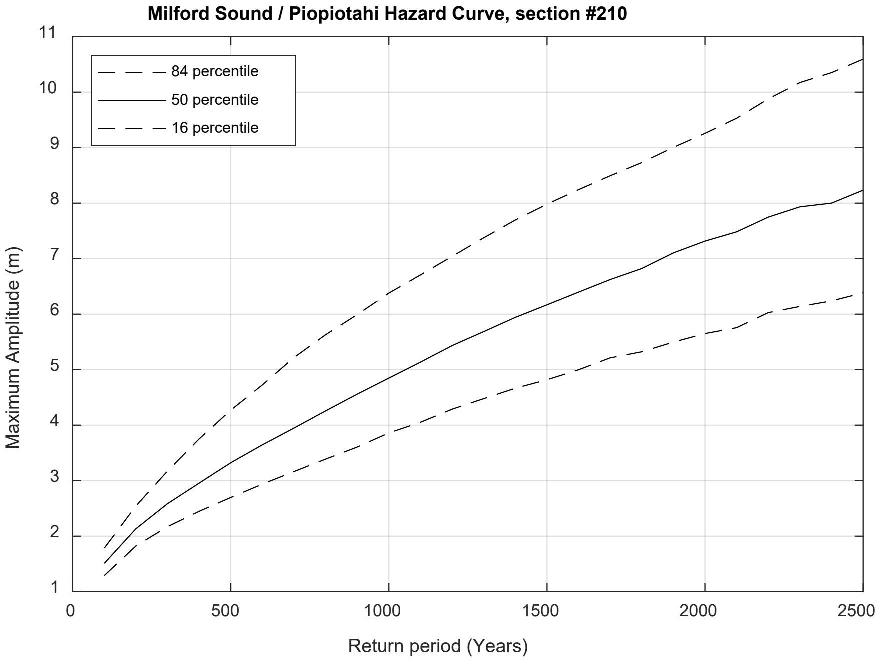

Figure 4.1 Wave-amplitude frequency hazard curve for Piopiotahi / Milford Sound for tsunami sourced from distal-, regional- and local-source earthquakes (reproduced from Power et al. [2023]; Coastal section 210).

The hazard from distal tsunami travelling within the sound to Milford Village / the Cleddau delta was reviewed by Grindley et al. (2007). Based on wave-height predictions for the Fiordland open coast during a subduction-zone earthquake, they calculated maximum run-up heights of 5.7 m on the basis of solitary wave run-up theory. Proximal tsunami sourced from sub-aerial or submarine landslides were not considered in this assessment.

A second Milford Village / Cleddau delta hazard review by Mabin and Tipler (2008) simulated solitary 2D waves travelling from the coast to the site without reflection or refraction within the fiord. This study adopted offshore wave heights from other studies, assuming that wave run-up is approximately equal to wave amplitude. Small waves (<1 m) were expected to attenuate ~10%, while larger waves (~5 m) amplified to 10 m. The report considered large slope collapses in Milford and, while thinking them ‘unlikely’, that proximal sources warranted further work.

4.4 Earthquakes and Shaking

The spectacular mountainous topography of Piopiotahi / Milford Sound owes its origin to both active tectonics and past glaciation. The Alpine Fault traverses beneath the western end of the fiord (Turnbull et al. 2010) and is part of one of the fastest-moving active plate boundaries in the world. Strike-slip rate estimates of 29.6 (-2.5/+4.5) mm a^{-1} since c. 270 ka were averaged along the onshore section immediately to the north (Barth et al. 2014) and 27.2 (-3.0/+1.8) mm a^{-1} to 31.4 (-3.5/+2.1) mm a^{-1} since c. 17 ka along the offshore southern and Resolution sections (Barnes 2009; Barnes et al. 2013). A large number and regularity of past earthquakes on the fault demonstrates that the next event is inevitable, while the time since the last event provides statistical probability that the next earthquake is of a much higher magnitude than the long-term average and should be expected soon (Berryman et al. 2012; Howarth et al. 2018, 2021). Fault rupture and displacement of the sea floor can result in ocean-source tsunami. Strong shaking can also be expected to occur in the area from other earthquakes, such as on the subduction-zone plate boundary further southwest or other faults in the Fiordland region.

coastal sections for probabilistic analysis – in this case, combining the interior of the sound with about 20 km of open coast – that prevents identification of where the maximum occurs.

The National Seismic Hazard Model (NSHM)[9] (Gerstenberger et al. 2024) provides estimates of the probability of different levels of earthquake ground shaking being exceeded over time. At Piopiotahi / Milford Sound, shaking levels thought capable of triggering landslides in bedrock terrain (~0.2–0.3 g peak ground acceleration [PGA], after Hancox et al. [2002]) have an approximate annual exceedance probability of 0.01, equivalent to an average recurrence interval of about 100 years. The NSHM derives these ground-motion probabilities from a range of earthquake sources, including the Alpine Fault, the Puysegur subduction interface, crustal faults and distributed seismicity.

Different hazard curves for sites of bedrock (V_{s30} = 1000 ms^{-1}, also known as subsoil Class B), very dense soil / soft rock (V^{s30} = 500 ms^{-1}, also known as Class C) and stiff soil (V^{s30} = 200 ms^{-1}, also known as Class D) are relevant for interpreting the triggering of landslides in Fiordland (Hancox et al. 2002). Example shaking probabilities calculated for Milford Village (V^{s30} = 1000 ms^{-1}) are illustrated in Figure 4.2. For comparison, strong-motion seismographs at Milford (subsoil category B) recorded PGA_{max} = 0.072 g during the 2003 M_W7.2 earthquake (77 km source distance; Reyners et al. 2003) and 0.026 g during the M_W7.8 Dusky Sound earthquake (110 km source distance; Fry et al. [2010]). There were no landslides recorded from these earthquakes in Piopiotahi / Milford Sound and, at this level of shaking, there should be a very low opportunity for earthquake-induced landslides (Hancox et al. 2002).

The ground acceleration needed to trigger landslides is, very approximately, 0.2–0.3 g (Hancox et al. 2002). The annual probability of exceeding this level of ground shaking in Piopiotahi / Milford Sound is approximately 1% (0.01), corresponding to an average recurrence interval of about 100 years (Gerstenberger et al. 2024). This suggests that an earthquake with sufficient energy and ground motion to generate landslides has at least a 1% chance of occurring in any one year at Piopiotahi / Milford Sound, and, on average, there will be some large coseismic landslides generated every 100 years.

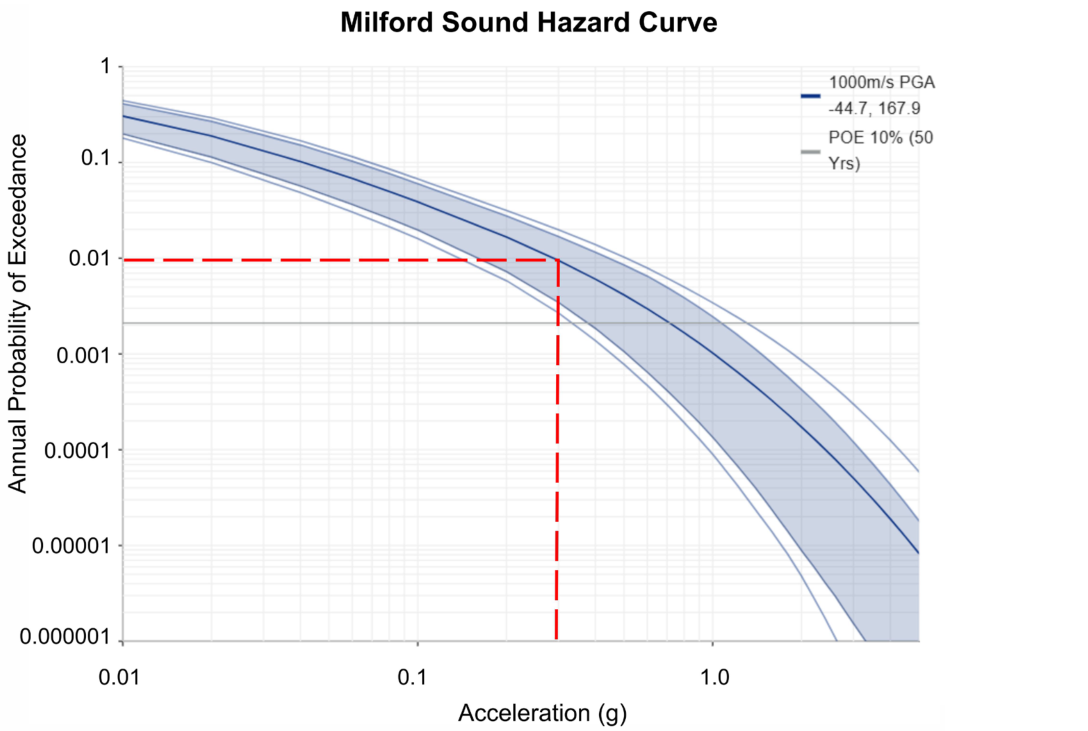

Figure 4.2 The hazard curve for a V_{s30} = 1000 m/s (Class B site) at Piopiotahi / Milford Sound as exported from the National Seismic Hazard Model website[9] (Gerstenberger et al. 2024), with axes annotated for this report. If we assume that there is a moderate opportunity for earthquake-induced landslides in solid bedrock to start to occur at about 0.2–0.3 g (Hancox et al. 2002), as shown by the red dashed line, then that level of shaking can be expected about once every 100 years.

9 https://nshm.gns.cri.nz

However, the NSHM considers only known 'active faults' and background seismicity, and these probabilistic calculations do not fully account for time since last rupture. There is now widespread recognition within the scientific community that another major Alpine Fault earthquake is inevitable and effectively imminent within planning timeframes (Orchiston et al. 2018; Howarth et al. 2021), with suggestions that landslides and rockfall could occur throughout Fiordland and the Southern Alps (Robinson et al. 2016).

The Alpine Fault is commonly described in terms of six distinct structural sections, each with distinct slip behaviour and slip rates (Barth et al. 2013; Howarth et al. 2018). In a re-examination of the past 20 earthquakes on the Central section of the Alpine Fault, Howarth et al. (2021) evaluated whether these also ruptured the South Westland section or terminated at a change in character along-strike. The study presented paleoseismic evidence that not all ruptures carry through the segment termination, interpreting that the fault has different modes of earthquake and temporal clustering of both major (M_W7–7.9) and great (M_W≥8) earthquakes. In turn, this will influence the levels of shaking experienced in Piopiotahi / Milford Sound. The strongest shaking scenarios for Fiordland generally involve multi-segment ruptures that propagate southward onto the South Westland and Fiordland sections of the Alpine Fault, although there remains considerable uncertainty regarding the precise rupture extent and segmentation behaviour of the next earthquake.

The recurrence interval for the Central section of the Alpine Fault was calculated at 249 ±58 years (1σ, 15 events, with a coefficient of variation of a risk index [COVRI] of 0.22 [0.12–0.37 (95% confidence interval)]), which makes this the most periodic fault section documented on Earth (Howarth et al. 2021). The corresponding probability of rupture on the Central section (single or multi-segment) in the next 50 years is 75% (29–99% [95% confidence interval]). A best-fit model simulation suggests an 82% (64–95% [95% confidence interval]) probability that the next event will be a M_W≥8 multi-section rupture, but Howarth et al. (2021) cautioned that more work is needed before this forecast can be operationalised. Recent work by Mere et al. (2024) contributes geomorphic fault expression mapping to support the notion of segmentation, but there is still some uncertainty as to whether the next earthquake will be M_W7–8 or M_W≥8.

Regardless of the next earthquake's magnitude, a very important result from research is the high probability of a major earthquake on the Central, and possibly entire, Alpine Fault in the next 50 years. This means that the Alpine Fault dominates the shaking and hazard probabilities throughout much of the southern and western South Island. The current earthquake probability of 75% in 50 years (i.e. 0.015, or 1.5×10^{-2}) is higher than the long-term background average of shaking from other possible earthquake sources.

Site shaking during an Alpine Fault earthquake can be estimated from different individual rupture-scenario models. For example, a ShakeMapNZ M_W8.1 earthquake model returned 0.4 g at Milford village (Class B) and 0.8 g where the Alpine Fault crosses the mouth of Piopiotahi / Milford Sound (Horspool et al. 2023). Such calculations contain numerous assumptions and should only be seen as indicative. These cannot account for complex interference of seismic waves and amplification that may occur due to the extreme topography in Fiordland, which is an important factor for triggering landslides that is yet to be understood in any detail. Recent work has also illustrated the importance of rupture direction and length for the different style of Alpine Fault earthquakes, aftershocks and ground-motion simulations (Bradley et al. 2017). Differences in directivity and stress drop are part of the explanation for the large number of landslides generated by the 2003 M_W7.2 Secretary Island earthquake (n = 1852 landslides) compared with the 2009 Dusky Sound M_W7.8 (n = 313) (Hancox et al. 2010; Cox et al., in prep. [a]). Although the precise distribution and intensity of shaking will vary depending on rupture extent, directivity and local topographic effects, the available evidence indicates that a major Alpine Fault earthquake would likely generate shaking levels sufficient to trigger at least moderate landsliding in the Piopiotahi / Milford Sound area (Hancox et al. 2002). A detailed discussion of segmentation of the Alpine Fault, and its implications for hazard calculations, is included in Appendix 3.

4.5 Fiordland Landslides

The narrow valleys and extremely steep topography in Fiordland contain a relatively high concentration of very large (>1 million m^3) pre-historic landslides (Hancox and Perrin 2009; Korup 2005; Turnbull et al. 2010). Factors that may have preconditioned slopes to failure include gravitational stresses due to post-glacial slope de-buttressing and river incision, localised reduction of rock-mass strength due to faulting and earthquake shaking, and slope dilation following precursory landsliding. Landslide triggering mechanisms include seismic ground shaking, fluvial undercutting, groundwater and pore pressure fluctuations, loading from forest growth, high-intensity rainstorms and saturation.

High-resolution bathymetric and seismic-reflection data revealed the presence of at least 18 very large (10^6–10^7 m^3) post-glacial rock-avalanche deposits that blanket ~40% of the bottom of Piopiotahi / Milford Sound, as well as four submarine slope collapses. At least 10 additional terrestrial landslide deposits of 10^6–10^8 m^3 have been identified in the lower Milford catchment by geomorphic mapping and field investigation (Figure 4.3) (Dykstra 2012). Identification in bathymetric data was supported by seismic-reflection data and short cores of fiord sediments, which show lithological variation and sedimentary structures consistent with submarine slope failures and sedimentation from rocky slope collapses. It was suggested that most, if not all, of the landslides would have been earthquake-induced and that some of the deposits might be formed by more than one landslide (Dykstra 2012).

Offshore cores and terrestrial exposure dating provide some constraints on some landslide ages (Dykstra 2012). A conservative maximum age constraint of ~17 ka was assigned for the sub-aqueous deposits based on reconstructed deglacial chronology – anything older is assumed to have fallen on, or been eroded by, glacial ice. A further 11 subaerial landslides that fell on land were identified in valleys around Piopiotahi / Milford Sound, some of which have ages constrained by cosmogenic exposure age dating.

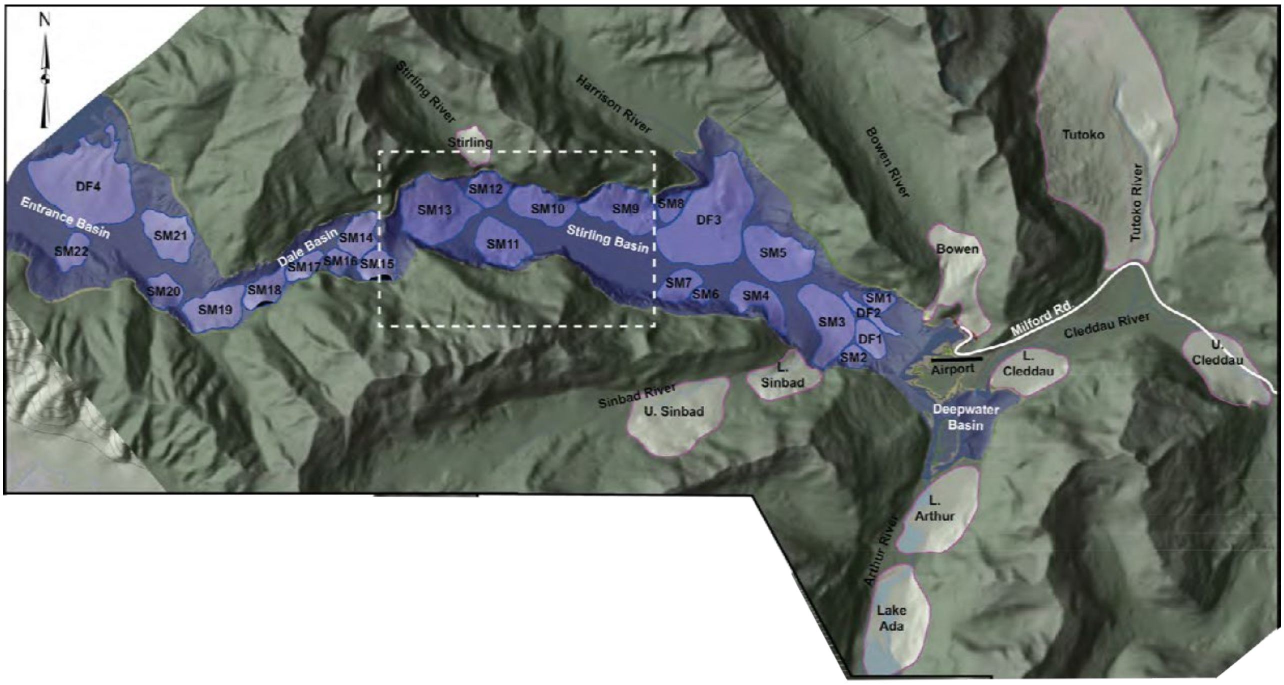

Figure 4.3 Map of landslides in the vicinity of Piopiotahi / Milford Sound (reproduced from Dykstra [2012]; Figure 4.2). Landslide names have the following prefixes: DF = submarine density flow; SM = subaerial source with submarine deposit.

Re-mapping of the deposits in Piopiotahi / Milford Sound by Dick (2021) revised the total number of sub-aerial rock-avalanche deposits to 16, down from the 22 identified by Dykstra (2012), as some deposits were thought more likely to be sub-aqueous fans or non-rock-avalanche failures. Those features identified as rock avalanches vary considerably in volume, runout and deposit geometry. Landslide mobility (H/L_{max}) appears to be toward the low end of rock avalanches globally. Factors suggested by Dick (2021) to affect emplacement dynamics are related to the lack of topographic confinement, together with runout down the steeper sub-aerial fiord walls onto the much flatter fiord bottom. An abrupt change in slope dissipates energy at the front of the avalanche, slowing the spreading edge to result in proximally thick lobate deposits that spread both laterally as well as forward. In contrast, runout over a shallow-gradient sub-aerial path onto the steeper fiord bottom has resulted in more elongated deposits. There may also be drag, as masses enter the water, and interaction with fiord-bottom sediment.

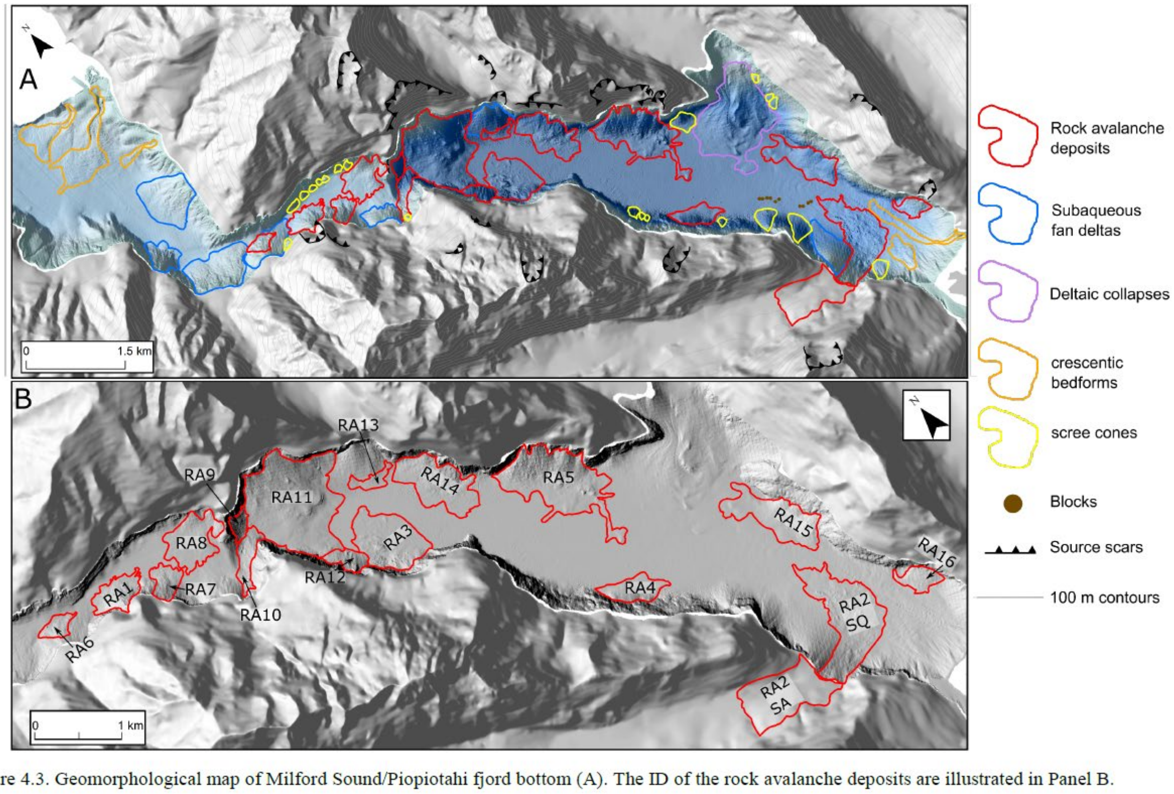

Figure 4.4 Classification of landslide and other submarine features in Piopiotahi / Milford Sound by Dick (2021), based on mapping by Dykstra (2012). Reproduced from Dick (2021; Figure 4.3) under CCBY 4.0 licence. Detailed diagrams and maps of individual deposits and source areas are provided in Dick (2021; Appendix A). Note that the interpretation and identification of rock avalanche (RA) deposits differs from Dykstra (2012).

A series of reconnaissance observations of slopes both from the air and from the ground (and climbing), were made by Dykstra (2012) to help identify source areas and features that may be indicative of failure modes. Many source areas could be identified above larger submarine deposits based on geomorphic features (e.g. failure scarps, dislocated ridgelines, wedge- or basin-shaped depressions). Landslides appeared to be characterised by deep-seated failures along steeply dipping failure planes that are parallel or sub-parallel to face aspects. Exfoliation (removal of outer sheets) of shallow slabs and wedge failures have occurred, some slumping on foliation, but rotational-type failures are not present. Obvious indicators of incipient failure (including tension cracks or slumping) and deep-seated failures were not seen, but some evidence for possible progressive weakening was found. Features of sheeting joint and slab failure appear dominant, mostly on slopes of 50–70°, and many extend to ridgelines. Landslides commonly fell from heights of 500–1500 m directly into the fiord. Further refinement of landslide chronologies may ultimately be possible through approaches such as submarine coring, dendrochronology and improved geochronological investigations of terrestrial deposits.

Placing empirical observations of these very large (>1 million m^3) landslide deposits into a present-day context is not entirely straightforward. For example, while these have been treated as if they had been earthquake-induced and single events for hazard and risk assessment, there is a possibility that some could have other causes or are the result of multiple events. Inventories of Fiordland landslides induced by earthquakes during 2003 and 2009 have been recently reviewed and improved. Although there were large numbers of landslides (n = 1852 and 313 for 2003 and 2009, respectively [Cox 2024a]), their volumes appear to have been considerably smaller (<0.7 million m^3) than the pre-historic deposits in bathymetry (Dykstra 2012) and mapped on land (Hancox and Perrin 2009; Dykstra 2012) (see discussion in Hancox et al. [2010]). It is conceivable that there has been an evolution of slope stresses over time and/or with changing climate conditions, or else that past shaking was significantly greater than experienced during the recent M_W7.2 and M_W7.8 earthquakes to enable such large volume collapses.

The inventories of landslides during the 2003 and 2009 earthquakes have been used to determine regional-scale earthquake-induced landslide susceptibility (Cox 2024b; Cox et al., in prep. [b]). A logistic regression model was trained on eight predictive parameters (PGA, elevation, slope, aspect, curvature, local slope relief, land cover and geology) during the two earthquakes. Albeit tuned on ground accelerations that may not be as great as could be expected during an Alpine Fault earthquake, landslide-susceptibility maps for the entire Fiordland region were generated using a prediction of PGA from the NSHM (Gerstenberger et al. 2024). The maps show spatial variability in the probability of landslide occurrence at a 10%-in-50-year probability of exceedance. The highest probabilities of landslide occurrence are predicted from slopes about Piopiotahi / Milford Sound (Figure 4.5).

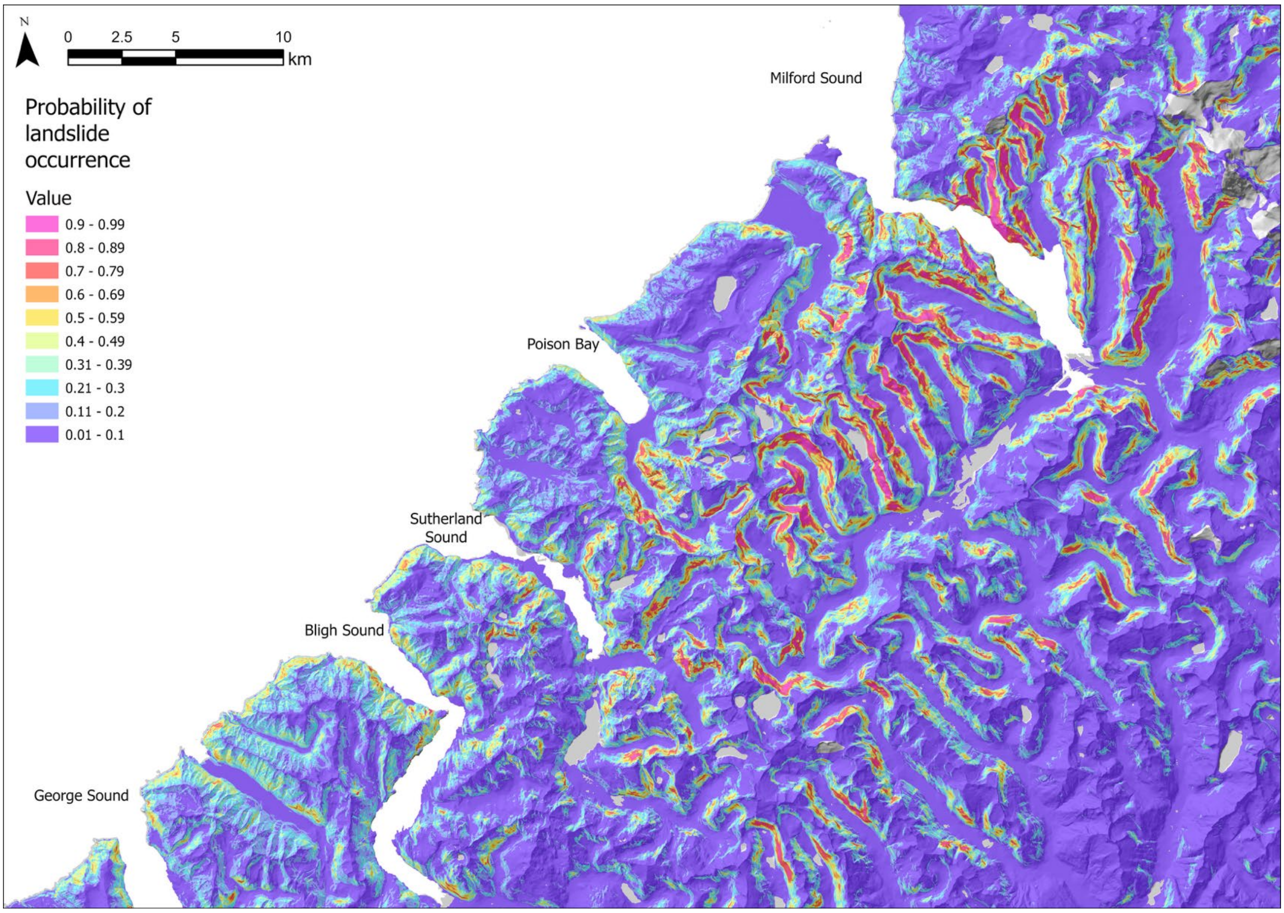

Figure 4.5 Earthquake-induced landslide-susceptibility map for the region between Piopiotahi / Milford Sound and George Sound (from Cox et al., [in prep. (b)]). The probability of occurrence is based on PGA conditions with a 10%-in-50-year probability of exceedance from the NSHM (Gerstenberger et al. 2024).

4.6 Landslide-Induced Tsunami

4.6.1 Initial Landslide and Wave-Amplitude Models (Dykstra 2012)

The PhD thesis by Dykstra (2012) was innovational in gathering evidence for historical landslides in Piopiotahi / Milford Sound, utilising bathymetric and seismic data, cores from the then National Institute of Water & Atmospheric Research (now part of Earth Sciences New Zealand; unpublished work of Barnes and Pickerill), together with field work and exposure-age dating. Modelling was undertaken to assess hazard and risk at Milford, suggesting that collapses of 3 million m^3 would generate waves ~4 m with a maximum local run-up of 17 m and that landslide-induced displacement waves can travel the length of the fiord in less than five minutes. Long-term risk to life was estimated at 0.38 deaths/year (assuming no prior warning) based on landslide magnitude and frequency and the numbers of visitors and resident/worker populations estimated at that time. The risk seemed surprisingly high.

To establish a landslide magnitude–frequency relationship for landslides in the Piopiotahi / Milford Sound area, Dykstra (2012) extracted physical landslide characteristics derived from 3D models (including the aspect and gradient of slope failure, deposit area and volume, fall height and runout distance). The following equation:

$$logY = -0.54logX + 0.56 \qquad \text{Equation 4.1}$$

was derived, where Y is cumulative frequency per 1000 years and X is landslide magnitude in millions of cubic metres.

Note that, on one hand, the volumes used may be a conservative estimate of magnitude, as seismic data suggested that some landslide deposits were partially buried and could have been larger than those now exposed in Piopiotahi / Milford Sound bathymetry. Calculated deposit volumes were 'sense-checked' (verified) against reconstruction of possible source locations and the geometry of slopes above the fiords (Dykstra 2012). On the other hand, the deposits might be liberal representations of collapse volumes, as these may have been the net result of multiple small failures, instead of one single large (wave-forming) event. Either way, their scale is considerably larger than landslides induced during the 2003 and 2009 earthquakes in Fiordland.

Resulting tsunami wave terms (see Figure 1.1 and Appendix 1) were estimated using analytical solutions that consider landslide volume, impact speed, maximum water depth (where material fell into the fiord), initial wave amplitude, attenuation and amplification, shoreline arrival wave height and run up. Velocity of landslides was estimated using a simple sliding block model equation, with gravity motion modified to allow for frictional resistance of the sliding block. It requires that the blocks will remain rigid and semi-intact and some coefficient of bed friction to be measured or assumed. Dykstra (2012) varied dynamic bed friction between 27° and 30°, which, at lowest observed slope failure angles, reduces impact velocity by ~20–25%, thereby reducing corresponding wave amplitudes by ~30–35% depending on slide path length. For steeper slope angles, the frictional braking affect is small, reducing wave amplitude by ~2–3%. Relatively high-impact velocities are expected for sub-aerial landslides at Milford, as many have travelled down slopes of over 60° inclination.

In addition to impact velocity, wave amplitude at source is dependent on water depth and geometry of the bottom, landslide-material density and porosity (assumed to be zero for solid block models) and, to a lesser extent, wetness and the ability of the material to deform. The complexities of these interactions are not easily quantified. Like many studies, Dykstra (2012) simply assumed that a solitary wave would be generated by impact as a landslide enters the water, which pushes the fluid ahead to generate a positive seaward wave that radiated outwards from the impact site.

Wave height is potentially also influenced by the shape as well as volume and density of an intact or semi-intact mass of sliding blocks. Notwithstanding these complexities, Dykstra (2012) approximated the initial maximum wave amplitude using equations incorporating landslide volume, density, impact velocity and water depth (Noda 1970; Slingerland and Voight 1979). The amplitude of a tsunami wave at source was taken as being directly related to the landslide speed and shallow-water celerity [*c=(gd)^0.5*] – the square root of water depth (*d*) multiplied by gravitational acceleration (*g*) (Sorensen 1993).

The regression equation for maximum first wave amplitude developed by Slingerland and Voight (1979) is derived from a combination of physical 3D laboratory model and field observations of actual landslide-induced tsunami. It uses a dimensionless calculation of landslide kinetic energy that is dependent on the landslide volume and velocity, the density of a landslide and water, the water depth (D) and gravitational acceleration. The equation provides a simple and practical way to estimate source wave amplitudes from landslides. It was adopted by Dykstra (2012) for Piopiotahi / Milford Sound assuming constant slide densities of 2 t/m^3. Uncertainties in amplitudes using conceivable bulk slide debris densities (from 1.6 to 2.5 t/m^3) are ±20–25%. The amplitude of waves at Cleddau delta estimated by Dykstra (2012) from landslide deposits mapped on the floor of Piopiotahi / Milford Sound (Figure 4.3) ranged from 0.3 to 65.1 m (Figure 4.6).

Waves may be caused directly from submarine landslides, as well as the sub-aerial landslides that fall into water. Predicting wave amplitudes from submarine landslides is also nuanced, with variables that create equal, if not more, uncertainty. A mathematical equation based on a dynamic balance of inertia, gravity, buoyancy, friction and hydrodynamic forces developed by Watts et al. (2005) was applied by Dykstra (2012) to approximate the four density-flow deposits interpreted to be submarine mass failures in Piopiotahi / Milford Sound ('SM' in Figure 4.3). The wave amplitudes calculated at source were relatively small (0.3–1.3 m), lower than all but two of the amplitudes calculated for sub-aerial landslides (Dykstra 2012; Table 4.3), reproduced here as Figure 4.6. However, note that these results could not be replicated by Taig and McSaveney (2015), who instead calculated amplitudes of 1.3–9.0 m.

Deposit ID	V=Vol. (x 10^6 m^3)	d=Water depth (m)	v=impact velocity[a] (m/s)	Distance[b] (km)	A_{max}= Amp.[c] (m)	Runup[d,e] (m)	
Subaerial source with submarine deposit						R_{max}	R_{inn}
SM1	1.0	200	86	1.2	6.2	27	27
SM2	0.5	170	47	1.2	2.4	8	10
SM3	2.2	240	85	1.7	8.0	41	38
SM4	4.6	270	70	2.7	8.2	42	39
SM5	4.8	270	109	2.8	15.8	93	82
SM6	0.2	280	36	3.8	0.3	1	1
SM7	1.5	290	74	4.2	3.5	15	15
SM8	0.7	290	52	4.8	1.2	4	5
SM9	11.0	290	81	5.3	16.4	97	85
SM10	4.3	290	72	6.6	7.2	37	35
SM11	2.3	290	120	7.1	9.5	49	46
SM12	4.9	290	38	7.5	3.2	14	14
SM13	18.5	290	99	8.3	31.5	186	164
SM14	1.7	130	100	9.3	25.7	152	26
SM15	3.9	130	127	8.9	65.1	456	65
SM16	0.8	130	104	9.5	16.3	96	16
SM17	3.0	130	49	10.3	14.0	71	14
SM18	4.9	130	103	10.9	56.9	398	57
SM19	6.7	130	79	11.6	49.0	343	49
SM20	2.3	130	67	12.5	17.9	105	18
SM21	4.3	130	68	13.5	28.3	198	28
SM22	0.9	130	50	14.2	6.0	26	6
Tafjord[f]	3.0	200	69	NA	**10**	**61** (62)	NA
Lituya[g]	30.6	140	74	NA	**96** (~100)	**540** (542)	NA
DW1[h]	*1.0*	*50*	*86*	*1.0*	*82*	*460*	*460*
Submarine density flows (granular)							
DF1	0.5	190 (20)	NA	1.2	1.3	4	4
DF2	0.2	220 (20)	NA	1.0	1.4	5	5
DF3	14.2	290 (55)	NA	4.2	1.2	4	4
DF4	13.2	130 (55)	NA	15.1	0.3	1	0.3

[a] estimated impact velocity assuming dynamic bed friction angle θ=27°(see text).
[b] distance from impact site to Cleddau delta.
[c] estimated maximum first-wave amplitude, assuming slide density ρ=2.0 g/cm^3 (see text).
[d] R_{max} = estimated max. near-field runup, 45°shoreline amplification, see text and Fig. 4.16.
[e] R_{inn} = inundation; maximum runup at Cleddau delta, 10°shoreline amplification. Grey highlighted values are waves originating from the outer basins (Dale or Entrance), which are not scaled for shoreline amplification, due to expected attenuation by Stirling Basin (see text).
[f] Tafjord, 1934 simulation, parameters: ρ=2.0 g/cm^3, θ=27°, slope failure angle α=60° (Hermanns et al., 2006; Jorstad, 1968). Values in brackets are observational data.
[g] Lituya Bay, 1958 simulation, parameters as per Fritz (2002); Miller (1960): ρ=1.6 g/cm^3, θ=14°, slope failure angle α=40°, 610 m slide path. Values in brackets are observational data.
[h] Hypothetical landslide into Deepwater Basin, and displacement wave (see text).

Figure 4.6 A reproduction showing the range of landslide volumes, water depth, impact velocities, maximum wave height/amplitude and run-up at the Cleddau delta estimated by Dykstra (2012; Table 4.3) from landslide deposits on the floor of Piopiotahi / Milford Sound. The table distinguishes those inferred to be sub-aerial, which fell into the water, from those inferred to be submarine slope collapses. Examples of Tafjord, Lituya Bay and a hypothetical DW1 landslide (Mt Sheerdown-Deepwater Basin) are provided for reference.

4.6.2 Wave Run-Up and Initial Hazard Estimates (Dykstra 2012)

Studies of wave run-up in fiord environments reviewed by Dykstra (2012) included observational data of events, physical laboratory experiments (e.g. scaled 3D physical models of fiord basins), and analytical and numerical methods. Around 10 references (cited by Dykstra as the "bulk of literature") suggested that maximum wave run-up is between two and five times the wave height when it nears the shoreline. There are certainly exceptions to such 'rules of thumb', with examples of very large waves and run up in historic time (e.g. observed in Norway, Alaska / British Columbia and Chile). When displacement waves are directed nearly perpendicular to shore, refraction and wave entrapment can result in secondary waves with larger run-up than the initial waves, which require complex modelling of the water dynamics.

Two equations for run-up at shorelines (Pedersen and Gjevik 1983) were applied for wave run-up by Dykstra (2012) (Figure 4.6), which assumed a solitary wave without reflection and/or entrapment: (1) R_{max} estimate based on run-up at the nearest shoreline, assuming near-perpendicular wave arrival, a 45° shore slope and no wave attenuation during crossing of the fiord; (2) R_{inn} inundation at Cleddau delta, assuming near-perpendicular wave arrival and a 10° slope (Figure 4.6). The general trend from the equations is for greater amplification as waves get larger, but steeper shorelines cause less amplification of smaller waves than shallow (nearly flat) shorelines, then the trend reverses as waves get larger than about 3 m.

On one hand, R_{inn} values at Cleddau delta potentially over-estimate the run-up – Dykstra (2012) suggests by between two and four times for waves initiated in the shallow outer basins due to possible attenuation of waves as these travelled through the deepwater Stirling Basin (so used unscaled source amplitude for the nine landslide–tsunami). On the other hand, the equations could under-estimate, as these do not account for wave amplification due to fiord geometry and/or standing wave oscillations. Run-up calculations were tested with historical observations of very large waves at Tafjord (1934 Norway) and Lituya Bay (1958 Alaska) (Figure 4.6). Note that state-of-the art hydrodynamic modelling can now instead be based on detailed bathymetry and high-resolution lidar topography now available, rather than single, simplified values of slope and allows for multiple waves and their interference.

Tsunami magnitude–frequency relationships were developed as first-order approximations for hazard at Milford by Dykstra (2012; Figure 4.18 using Table 4.3). These were based on estimated cumulative frequency (per 1000 years) using calculated wave heights ('amplitudes') and run-ups (Dykstra 2012; Table 4.3 – reproduced here as Figure 4.6) and an assumption that the mapped landslide deposits were all generated within 17 ka since ice withdrawal. The log-normal distributions (reproduced in Figure 4.7) were used to derive maximum expected tsunami amplitude and run-up heights for long return periods using the best-fit regressions on a range of values (e.g. 1–164 m in Figure 4.6). A selected example of a 1-in-1000-year proximal tsunami amplitude of ~4 m at Milford was highlighted, with an estimated run up at the Cleddau delta of ~17 m. Note that this chosen number seems to have become ingrained in the literature and discussions, but larger waves and/or run-ups are possible.

Waves with an amplitude of 20 m and maximum localised run-up up of 100 m may have occurred once every 2000 years. The scenario of a landslide (e.g. from Sheerdown Peak) into the shallow waters of the Deepwater Basin beside the Cleddau delta could hypothetically generate an even larger wave and run up. Multiple landslides may have occurred at any one time and could be expected during an earthquake, along with complex amplification of waves by reflections and entrainment. The hazard curve does not include the probability of offshore tsunami from distal sources.

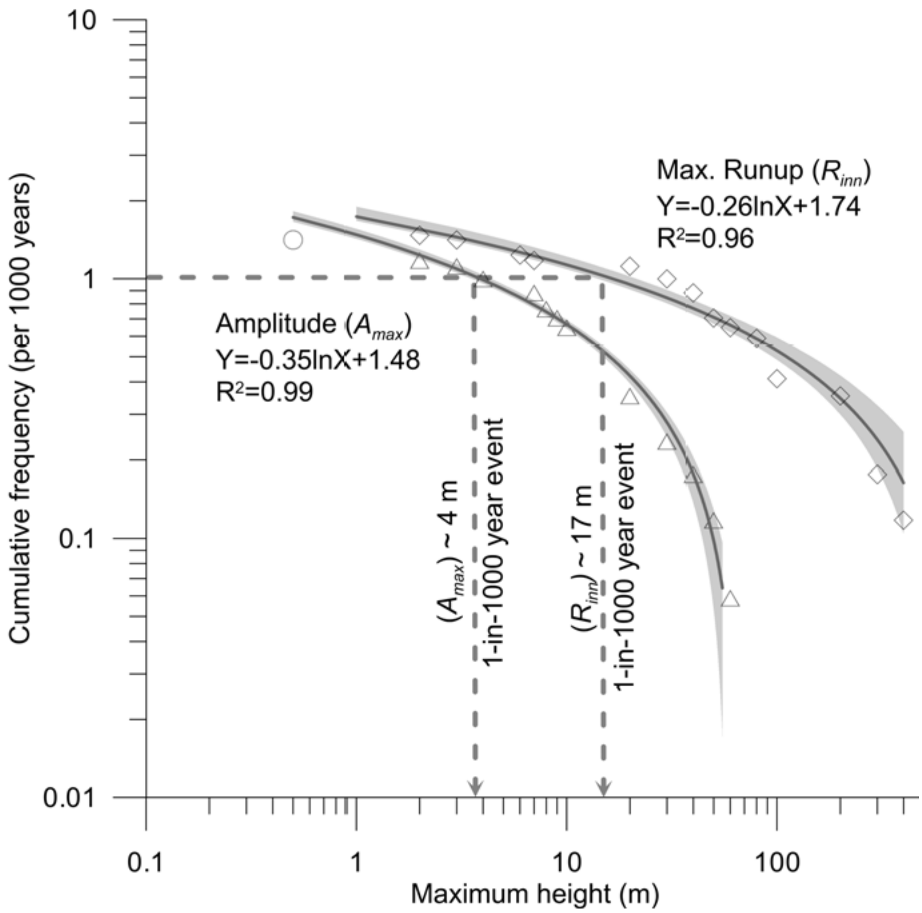

Figure 4.7 Simulated tsunami magnitude–frequency relationship for Piopiotahi / Milford Sound (reproduction of Figure 4.18 from Dykstra [2012]).

4.6.3 Model Refinement (Taig and McSaveney 2015)

In a review of the landslide-induced tsunami risk at Milford, Taig and McSaveney (2015) argued that, within the reasonably foreseeable future, it is inevitable that Piopiotahi / Milford Sound will experience an earthquake with destructively strong ground shaking, that this shaking will further damage the rock mass walls of the fiord and that bits of rock will fall to the valley floor. If sufficiently large masses enter the water, these could generate large waves that would affect much of the fiord and shoreline. Because fully coupled numerical modelling of tsunami generation, propagation and run-up for all mapped landslide scenarios was not feasible at the time, Taig and McSaveney (2015) instead adopted simplified empirical attenuation relationships as first-order approximations for wave decay within the fiord. These subsequently recommended that detailed numerical or physical modelling of representative tsunami scenarios should be undertaken in future studies.

Taig and McSaveney (2015) argued that the use of the Slingerland and Voight (1979) ‘best-fit’ regression coefficients meant that, other than waves originating in the outer fiord, the Dykstra (2012) calculations had under-estimated maximum tsunami wave amplitudes by about 24%. As 50% of the generated waves will be larger than those calculated from a ‘best-fit model’, a systematic error was introduced by ignoring the variance. Taig and McSaveney (2015) state a widely accepted convention to incorporate the effect of sample variance is to adopt 84th percentile coefficients (mean plus 1 standard deviation), from which only 16% will exceed. They revised the range of amplitude estimates to be between 0.2 and 87 m at point of origin and calculated substantially larger maximum amplitudes for tsunami waves generated for submarine density flows (using Watts et al. [2005]). They also noted that all calculations use present-day sea level, but some material may have fallen during the past 17,000 years when sea level was lower and water depths would have been shallower, generating significantly larger tsunami at the time.

The need to consider attenuation of tsunami wave amplitude with travel distance in the fiord was also raised by Taig and McSaveney (2015). Attenuation between the source amplitude (A) and the shoreline wave height (H) was shown to be significant for tsunami generated in Three Gorges Reservoir in China and for physical models (Huang et al. 2012, 2014), as well as even greater attenuation at Loenvann (Norway) (Slingerland and Voight 1979). Both events had rapid attenuation (to 50% and 25%) within the initial 1 km distance to the impact source, then lower attenuation over the next 3 or 6 km of travel.

Two different empirical attenuation relationships were used to revise wave heights from around 0.1 to 10 m and tsunami run-up between 1.1 and 47 m on land (Tables 4.2 and 4.3, after Taig and McSaveney 2015). The calculations assumed that waves maintained their initial maximum amplitude within the first 1 km of travel, then reduced rapidly to 50% or 25%, from where they decreased exponentially with decay constants of 0.19 per km and 0.144 per km. The state of tide, which has a 2.5 m range at Piopiotahi / Milford Sound, was also considered for hazard on land, although not for boats.

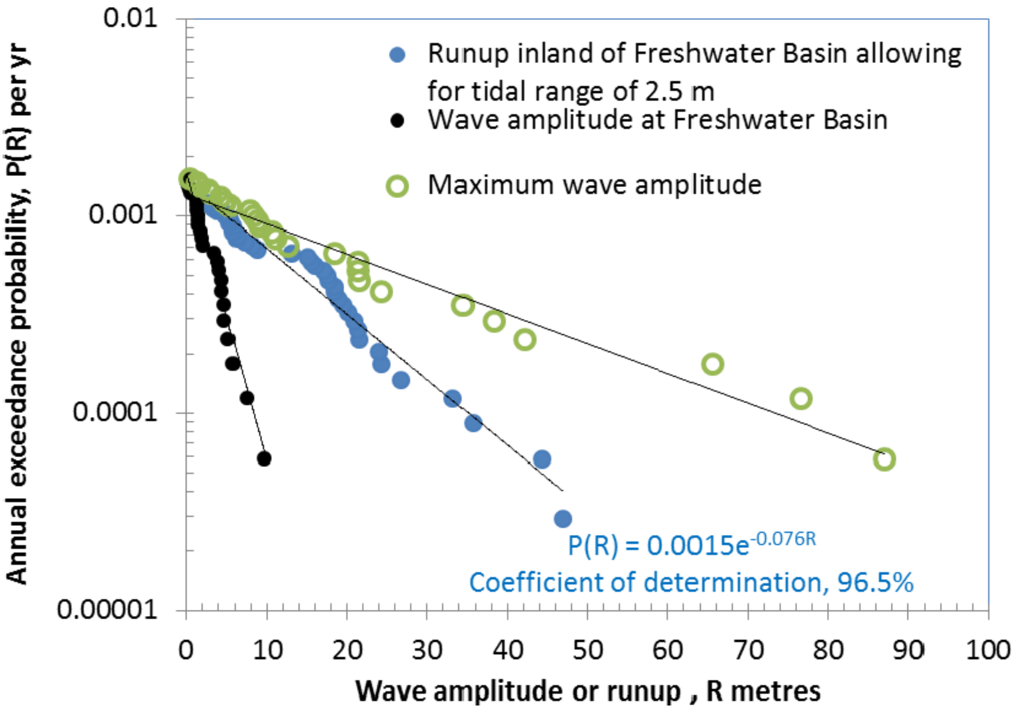

Figure 4.8 Quantitative measures of tsunami hazard at Piopiotahi / Milford Sound allowing for wave attenuation from source and one landslide for each underwater deposit, using the Three Gorges attenuation curve. Blue dots are wave run-up (*R* in Figure 1.1), allowing for a 2.5 m tidal range. Black dots are wave amplitude (height *H*, in Figure 1.1), whereas green dots are maximum amplitude at source (*A*, in Figure 1.1). Reproduced from Taig and McSaveney (2015; Figure 8).

Risk calculations completed by Taig and McSaveney (2015) were based on the conclusion that the past frequency and future probability of *not* having a significant landslide-induced tsunami occur in Piopiotahi / Milford Sound during Alpine fault earthquakes is 56%, or higher if some past earthquakes generated more than one landslide into the fiord. They suggested that 44% of Alpine Fault earthquakes over the past 17,000 years have generated waves ranging from 0.2 to 87 m at source, which attenuate to wave heights of perhaps 0.3 to about 10 m in Freshwater Basin and have a run-up ranging between 1.1 and 47 m on land. They recommended that an agency should be commissioned to undertake numerical or physical modelling of a substantial selection of tsunami scenarios based around the submarine deposits mapped by Dykstra (2012) to improve knowledge of wave height, travel and decay over time in the fiord.

Note that hazard and risk calculations in Dykstra (2012) and McSaveney and Taig (2015) are also based on a 2012 estimate that the Alpine Fault has a 27% chance of a large rupture ($M_W \geq 8$) in the next 50 years (Berryman et al. 2012; Biasi et al. 2015). This value is now considered to be quite a bit higher (Craig and

Chinn 2021). The revised and presently used metrics for an Alpine Fault earthquake are 75% (29–99% [95% confidence interval]) in 50 years (Howarth et al. 2021). Charlton et al. (2025) used the updated Alpine Fault rupture probabilities and re-calculated Taig and McSaveney (2015)'s risk calculations. Using this simplified approach, the risk metrics increase almost threefold using the updated rupture probabilities (Charlton et al. 2025).

Table 4.2 List of underwater landslide deposits and submarine debris flow deposits identified by Dykstra (2012), with revised wave amplitude and run-up. The amplitude at Freshwater Basin is calculated by the Three Gorges attenuation model, which is a more conservative model with a slower rate of attenuation and therefore calculated higher risk. Reproduced from Taig and McSaveney (2015; Table 1).

Source	Distance from Delta (km)	Volume (million m^3)	Slide-Path Length (m)	Water Depth (m)	Slope (°)	Maximum Amplitude[1] (m)	Amplitude at Freshwater Basin[2] (m)	Run-up at Milford[2] (m)
Subaerial Landslides with Submarine Deposits								
SM1	1.2	1.0	560	200	64	8.7	4.2	18.5
SM2	1.2	0.5	390	170	42	3.0	1.5	5.8
SM3	1.7	2.2	560	240	63	10.7	4.7	21.0
SM4	2.7	4.6	460	270	56	11.0	4.0	17.6
SM5	2.8	4.8	970	270	61	21.3	7.6	35.7
SM6	3.8	0.2	120	280	56	0.4	0.1	0.4
SM7	4.2	1.5	480	290	58	4.7	1.3	5.0
SM8	4.8	0.7	250	290	56	1.6	0.4	1.3
SM9	5.3	11	440	290	68	21.5	4.8	21.4
SM10	6.6	4.3	280	290	67	7.9	1.4	5.3
SM11	7.1	2.3	1060	290	65	12.6	2.0	8.1
SM12	7.5	4.9	130	290	58	4.3	0.6	2.2
SM13	8.3	18.5	650	290	70	42.2	5.3	24.0
SM14	9.3	1.7	1640	130	43	34.4	3.6	15.5
SM15	8.9	3.9	1950	130	49	87.2	9.7	46.9
SM16	9.5	0.8	980	130	57	21.3	2.1	8.7
SM17	10.3	3	190	130	61	18.4	1.6	6.3
SM18	10.9	4.9	1490	130	46	76.6	5.8	26.8
SM19	11.6	6.7	1820	130	36	65.6	4.4	19.5
SM20	12.5	2.3	1310	130	36	24.3	1.4	5.4
SM21	13.5	4.3	1200	130	37	38.3	1.8	7.2
SM22	14.2	0.9	820	130	35	8.2	0.3	1.1
Granular Submarine Density Flows								
DF1	1.2	0.5	1100	20	22	2.7	1.3	5.2
DF2	1	0.2	1600	20	25	9.0	4.5	20.2
DF3	4.2	14.2	2400	55	28	5.3	1.5	5.7
DF4	15.1	13.2	1500	55	25	1.3	0.04	0.1

[1] Using Equation 10 of Slingerland and Voight (1979) with 84th percentile coefficients a = -1.132 and b =+0.71.

[2] The values listed here are for the attenuation relationship determined from the Three Gorges Reservoir model.

Table 4.3 Estimated first arrival wave amplitudes at Freshwater Basin and Cleddau delta for three attenuation models. Reproduced from Taig and McSaveney (2015; Table 2).

Source	P(H)*/yr	Wave Amplitude at Freshwater Basin (m)			Run-Up at Cleddau Delta (m)		
		Three Gorges[1]	Loenvann[2]	None[3]	Three Gorges[1]	Loenvann[2]	None[3]
Subaerial Landslides with Submarine Deposits							
SM1	5.3×10^{-04}	4.2	2.1	8.7	18.5	8.7	41.4
SM2	9.4×10^{-04}	1.5	0.7	3.0	5.8	2.7	13.0
SM3	3.5×10^{-04}	4.7	2.4	10.7	21.0	10.1	51.9
SM4	5.9×10^{-04}	4.0	2.2	11.0	17.6	8.9	53.7
SM5	1.2×10^{-04}	7.6	4.1	21.3	35.7	18.2	110.5
SM6	1.5×10^{-03}	0.1	0.1	0.4	0.4	0.2	1.4
SM7	1.2×10^{-03}	1.3	0.7	4.7	5.0	2.7	21.0
SM8	1.4×10^{-03}	0.4	0.2	1.6	1.3	0.7	6.6
SM9	2.9×10^{-04}	4.8	2.9	21.5	21.4	12.4	111.7
SM10	1.1×10^{-03}	1.4	0.9	7.9	5.3	3.3	37.3
SM11	7.6×10^{-04}	2.0	1.3	12.6	8.1	5.1	62.5
SM12	1.3×10^{-03}	0.6	0.4	4.3	2.2	1.4	19.1
SM13	2.4×10^{-04}	5.3	3.7	42.2	24.0	16.1	232.1
SM14	6.5×10^{-04}	3.6	2.6	34.4	15.5	11.0	185.9
SM15	5.9×10^{-05}	9.7	7.0	87.2	46.9	32.7	508.6
SM16	7.1×10^{-04}	2.1	1.6	21.3	8.7	6.2	110.6
SM17	8.8×10^{-04}	1.6	1.2	18.4	6.3	4.7	94.2
SM18	1.8×10^{-04}	5.8	4.6	76.6	26.8	20.6	442.7
SM19	4.7×10^{-04}	4.4	3.6	65.6	19.5	15.5	374.0
SM20	1.1×10^{-03}	1.4	1.2	24.3	5.4	4.5	127.5
SM21	8.2×10^{-04}	1.8	1.6	38.3	7.2	6.3	209.2
SM22	1.4×10^{-03}	0.3	0.3	8.2	1.1	1.0	39.1
Granular Submarine Density Flows							
DF1	1.2×10^{-03}	1.3	0.7	2.7	5.2	2.4	11.6
DF2	4.1×10^{-04}	4.5	2.3	9.0	20.2	9.4	43.2
DF3	1.0×10^{-03}	1.5	0.8	5.3	5.7	3.1	24.3
DF4	1.5×10^{-03}	0.04	0.04	1.3	0.1	0.1	5.0

* P(H) is the estimated probability that the estimated wave amplitude at Freshwater Basin will be equalled or exceeded assuming the Three Gorges attenuation model, and that the deposits have accumulated over 17,000 years.

[1] The Three Gorges attenuation model is a more conservative model with a slower rate of attenuation and therefore calculates higher risk.

[2] The Loenvann attenuation model is a less conservative model which has more rapid attenuation in wave height with distance of travel, and therefore calculates lower risk.

[3] No attenuation is an unrealistic model for wave propagation in Piopiotahi / Milford Sound. It calculates wave height at point of landslide impact.

4.6.4 Testing Landslide Rheology and Runout (Dick 2021)

The collapse volumes, rheology and other factors that affect fiord entry (and whether a tsunami is generated) were also examined through back analysis of runout/volume characteristics to understand landslide emplacement dynamics (Dick 2021). Best-fit numerical modelling (using a DAN3D single-phase landslide model) was applied to five of the deposits mapped by Dykstra (2012) on the floor of Piopiotahi / Milford Sound. Calibration to morphometric features required high basal friction angles and/or low turbulence parameters to retard the landslide runout. Modelling found that specific material characteristics (a Voellmy rheology) were effective in simulating the subaqueous portion of landslide runout, as varying the velocity-dependent turbulence coefficient parameter could represent the resistance to flow by the water, in contrast to the frictional rheology where resistance is governed only by basal friction angle.

The variety of morphologies and morphometries of landslides identified by Dykstra (2012) was interpreted to reflect relatively low mobility (Dick 2021). Factors such as transitioning from air to water, abrupt slope-angle changes from the steep fiord to flat basin walls and lack of lateral confinement resulting in freely spreading deposits may contribute to the apparent low mobility. The results of Dick (2021) can be used to constrain future modelling of landslides and tsunami, which previously treated the landslides as an incompressible rigid block rather than granular flows. Velocities at fiord entry points calculated by Dick (2021) were slower than those of Dykstra (2012). The work hints that near-field wave amplitudes may have been previously over-estimated and recommended re-assessment of tsunami wave heights using coupled landslide–tsunami numerical models.

4.6.5 Other Considerations

Hazard calculations in Dykstra (2012) and McSaveney and Taig (2015) were based on an early estimate that the Alpine Fault has a 27% chance of a large rupture ($M_W \geq 8$) in the next 50 years (Berryman et al. 2012; Biasi et al. 2015). This value is now widely accepted to be nearly three times higher at 75% (Howarth et al. 2021). This was considered in the review of hazards for the Milford Opportunity Project (Craig and Chinn 2021) and needs to be incorporated in all future work.

The hazard models to date have not had access to high-resolution lidar data that are now available for inundation modelling, and the simplistic calculations have not utilised the high-resolution bathymetry to its full extent.

The hazard models to date also only consider generation of a single large wave. These have been based on entry of a rigid block into the fiord, a calculated wave amplitude at source, attenuation with travel distance, then translation of arrival height directly into a run-up elevation. Back-analysis of deposits raises questions on the applicability (and potential wave-amplitude over-estimation) of using a rigid-block model to derive amplitude of waves at source (Dick 2021).

The run-up heights assume there is sufficient volume of water in the wave to cover all land up to that elevation. The local topography of the land (such as Cleddau River delta, channel and Deepwater Basin) and surface obstacles or features (e.g. forest versus open space) have not been considered. They will affect local inundation depth and velocity, and therefore affect both hazard and vulnerability.

Another factor that has yet to be included in any tsunami hazard at Piopiotahi / Milford Sound is the secondary effect of wave superposition as waves are reflected and refracted around the fiord. The first arriving wave may not be the largest wave, and reflections may persist for hours.

These effects have potential to cause spatial variation in the level of risk in and around Milford Village. They can only be examined and solved through complex numerical hydrodynamic modelling using high-resolution bathymetry and topography. Current state-of-the-art tsunami modelling has potential to highlight places and routes for evacuation, as well as potential opportunity to assess and design mitigation options.

4.6.6 Summary of Tsunami Hazard at Milford

Work to date suggests a wide range of possible tsunami wave heights, each with different probabilities of occurrence as illustrated by hazard magnitude–frequency curves. Based on 16 submarine landslide deposits, Dykstra (2012) used empirical relationships of Slingerland and Voight (1979) to estimate impact velocity and wave amplitude, calculating a 1-in-1000-year proximal tsunami amplitude of ~4 m with estimated run-up at the Cleddau Delta of ~17 m but noting that higher run-up may occur less frequently. Two attenuation models were added by Taig and McSaveney (2015) (based on less attenuation at Three Gorges and more attenuation in Norway). Initial amplitude is maintained at <1 km, then 50% maximum amplitude and exponential decay at >1 km. Wave heights of 0.3–10 m were estimated in Freshwater Basin, with run-up between 1.1 and 47 m.

Agent-based modelling of evacuation scenarios (Harris 2023) has been based on:

> *"… the estimated 44% chance of a landslide-generated tsunami occurring in Piopiotahi / Milford Sound during the next Alpine Fault rupture, with the potential for a 17 m wave arriving on shore within two to seven minutes."*

This wave height and inundation, derived from Dykstra (2012), is but one scenario. A "17 m wave" seems to have been referred to widely without clarity that this is a run-up elevation, not a wave arrival height, and is at a 1-in-1000-year annual exceedance probability (= 0.001) (Dykstra 2012).

Possible evacuation routes were assessed by Taig and McSaveney (2015) under the understanding that tsunami run-up (*R*, Figure 1.1) could reach 45 m or more. Based on the distribution and elevation of local topography (hypsometry), they suggested that every metre gain in altitude from 0 to 16 m could result in an 11% reduction in the likelihood of death, whereas every metre gain above 16 m is about a 46% reduction in likelihood of death. They recommended establishment of tsunami evacuation routes that allow people to reach a height of 50 m above sea level (if they can). Craig and Chinn (2021) use elevation contours to create a general high-level depiction of tsunami hazard areas in Piopiotahi / Milford Sound by describing three categories of possible inundation areas.

5.0 New Zealand Risk Management and Planning Requirements

Risk management is a structured process that includes activities to identify, analyse and evaluate risks, or potential threats, and then implement treatments to mitigate those risks to a tolerable level. Risks may include any potential loss of life, injury or damage to assets over a specific period of time (UNDRR 2017). Risk tolerability is more nuanced, affected by societal factors and contexts. This section provides an overview of the New Zealand risk management and planning context, including relevant policies and frameworks, risk-management approaches and options and the role of risk tolerance in decision-making. These aspects are then addressed in the specific context of earthquake-induced landslide–tsunami risk at Piopiotahi / Milford Sound, concluding with a summary of potential risk-management options discussed in the existing literature.

5.1 Risk Management and Planning Context

Natural-hazard processes, such as earthquakes and tsunami, are an innate part of our environment. The risk associated with these hazards therefore cannot easily be eliminated, but steps can be taken to mitigate the risk to levels that affected groups are willing to accept or tolerate. Disaster risk management aims to prevent such natural hazard events from culminating in a disaster, or serious disruption of the functioning of a community or society that leads to extreme losses and impacts (UNDRR 2017). The risk-management process refers holistically to policies and strategies applied to strengthen resilience and reduce loss across four stages of activity, known as the '4 Rs' in New Zealand – risk reduction, readiness, response and recovery (National Civil Defence Emergency Management Plan Order 2015; UNDRR 2017; MCDEM 2019). In this section, we focus primarily on aspects of risk reduction, including prevention, treatment and mitigation, which are often carried out after the natural-hazard risks have been thoroughly identified and analysed through investigations and modelling (see Sections 3 and 4 for examples[10]).

Strategies for risk reduction fall into five general categories:

- **Avoidance:** Eliminating the risk entirely by changing activities, projects or objectives so that the risk cannot occur (e.g. measures could include avoiding development in hazardous areas, re-locating people or assets away from hazardous areas or developing buffer zones).
- **Mitigation:** Taking proactive steps to decrease the probability or severity of a risk (e.g. adding features to reduce impact, strengthening buildings against earthquake shaking or tsunami).
- **Transfer:** Shifting the burden or responsibility to others, often through insurance, outsourcing or contracts.
- **Acceptance:** Acknowledging the risk and choosing not to act, either because the cost of action is too high or the potential benefits justifies the risk.
- **Communication:** Ensuring that individuals and organisations understand identified risks, the potential impacts of these and the response strategies (avoid, mitigate, transfer, accept).

After applying these risk-reduction strategies as part of a wider risk-management approach, any risk that remains is known as residual risk, which must also be managed, often through strategies such as acceptance and communication. Global frameworks such as the Sendai Framework for Disaster Risk Reduction (2015–2030) (UNDRR 2015) and initiatives like Early Warnings for All (EW4All) (WMO 2022) provide global over-arching guidance for implementing these strategies effectively.

10 The examples given in Sections 3 and 4 focus primarily on the assessment of the hazard, which is the priority for the next stage of research. As well as an understanding of the hazard, quantitative risk assessment requires establishing the exposure (people or assets exposed to the hazard) and their vulnerability (probability of damage to a structure, or of a person becoming a casualty, as a function of the hazard properties, which in the case of tsunami is usually the inundation flow depth), elements which are only lightly covered here.

5.1.1 Risk-Management Strategies and Approaches in New Zealand

The selection and integration of risk-management strategies in New Zealand is influenced by hazard type, geographic scale and local context. New Zealand faces many different types of natural-hazard risks due to its geological and environmental settings, comprising seven of the 25 key risk areas identified in the National Risk Register (DPMC 2025). Table 5.1 provides a structured summary of key current management and treatment options used in New Zealand to manage natural-hazard risk in the context of the '4Rs'.

National-level governance and planning is central to risk management in New Zealand, with associated legislation including the proposed Emergency Management Bill (No 2) 2025 (236-1), the Civil Defence and Emergency Management Act 2002, the Building Act 2004, the National Policy Statement for Natural Hazards (Ministry for the Environment 2025) and the Resource Management Act 1991 (RMA). Recent amendments to the RMA give immediate legal effect to proposed provisions and the RMA replacement bills seek "to safeguard communities from the effects of natural hazards through proportionate and risk-based planning". Local government statutes across New Zealand also enable councils and agencies to avoid or mitigate hazard risk through land-use controls, building standards, long-term planning and risk disclosure. These mechanisms are largely focused on risk reduction and prevention, shaping where and how development occurs, but they also support readiness and recovery through formal plans, resilience objectives and transparent communication of hazard information to communities. The Natural Hazards Insurance Act 2023; however, serves as a mechanism for transferring financial risk associated with hazard exposure.

Complementing legislative, governance and planning mechanisms are strategic, social, financial and technical approaches to managing risk, as outlined in the National Disaster Resilience Strategy (MCDEM 2019). Strategic adaptation policies, Māori-led resilience initiatives and community-based preparedness efforts aim to embed long-term adaptation, equity and local knowledge into decision-making. Engineering and nature-based solutions implemented across the country also seek to directly lessen hazard impacts through physical mitigation. Early-warning systems, such as the geohazard monitoring network GeoNet[11], Emergency Mobile Alerts[12] and public-education initiatives aim to reduce immediate risk to life by improving situational awareness and enabling timely response actions (e.g. evacuation), particularly for rapidly unfolding hazards such as tsunami and severe weather.

The breadth of strategy, policy and approaches illustrate New Zealand's layered risk-management system, in which multiple agencies and individuals act at different scales and stages of disaster risk management to collectively reduce harm and impact from natural hazards.

11 https://www.geonet.org.nz/

12 https://getready.govt.nz/prepared/ema

Table 5.1 Key New Zealand natural-hazard risk-management approaches and specific actions. Sources: LGNZ (2014); the Natural Hazards Commission Toka Tū Ake Risk Reduction Strategy (2025–2029); Saunders and Kilvington (2016). It is important to note that the wider emergency-management system is undergoing significant revision in response to the findings of the 2023 North Island Severe Weather Events Inquiry. These include reforms currently in progress, with legislative changes expected later in 2026, alongside a government-endorsed investment and implementation roadmap. Therefore, some of the actions and legislations in this table will change / be formalised. The '4Rs' are risk reduction, readiness, response and recovery. NEMA = National Emergency Management Agency; MBIE = Ministry of Business, Innovation & Employment.

Approach	Actions, Legislations	Description	Strategy	The '4Rs'	Lead Agency
Governance and Planning	Emergency Management Bill (Proposed)	Designed to replace the CDEM Act 2002. Modernises the system by strengthening iwi roles, clarifying 'lifeline utility' duties (power, water) and emphasising community-led resilience.	All strategies	All	NEMA / regional CDEM groups
	Civil Defence Emergency Management (CDEM) Act 2002	The Act mandates a proactive, risk-based approach, considering both the likelihood and consequences of hazards. It aims to manage hazards sustainably. Examples of tools: CDEM plans and risk communication.	Avoidance / mitigation	All	NEMA / regional CDEM groups
	Planning Bill / Natural Environment Bill	States its purpose is "to safeguard communities from the effects of natural hazards through proportionate and risk-based planning". It moves toward a system of 'outcomes' rather than just managing 'effects'. Examples: Regional spatial strategies.	Avoidance / mitigation	Reduction	Regional and district councils
	Resource Management Act 1991 (RMA)	Regional councils and unitary authorities administer the RMA through regional policy statements and plans. These control the use of land for the purpose of the avoidance or mitigation of natural hazards. Examples: Zoning and development restrictions in floodplains.	Avoidance / mitigation	Reduction	Regional and district councils
	Building Act 2004	Regulates building work and performance standards. Manages natural hazards in relation to the construction and modification of buildings. Examples: Seismically resilient codes and floor-level requirements.	Mitigation	Reduction	MBIE / councils
	Local Government Act 2002	Section 11A requires authorities to have regard for the core service of "avoidance or mitigation of natural hazards". Examples: Inclusion in Long Term Plans.	Avoidance / mitigation	Reduction / readiness	District and city councils
	Local Government Official Information and Meetings Act 1987	Authorities must issue Land Information Memoranda (LIM) on request. Examples: Including known hazard information (erosion, flooding) on property reports.	Communication	Readiness	District and city councils
	Health and Safety at Work Act 2015	Secures the health and safety of workers and workplaces. Notably by protecting workers and other persons against harm to their health, safety and welfare by eliminating or minimising risks arising from work or from prescribed high-risk plant; and promoting the provision of advice, information, education and training in relation to work health and safety.	Avoidance / mitigation	All	MBIE

Approach	Actions, Legislations	Description	Strategy	The '4Rs'	Lead Agency
Strategic Adaptation	National Adaptation Plan and Framework	Helps New Zealand adapt to climate change through climate-resilient development and infrastructure protection. Sets the high-level policy direction for all sectors.	Mitigation / acceptance	Reduction / recovery	Ministry for the Environment / Treasury
Māori-Led Resilience	Iwi management plans / marae preparedness	Integration of Mātauranga Māori into risk maps. Marae act as primary welfare hubs and first responders (e.g. following Cyclone Gabrielle).	Mitigation / communication	Alls	Iwi/hapū / NEMA
Financial	Natural Hazards Insurance Act 2023	The Natural Hazards Commission Toka Tū Ake (NHC) provides a 'first layer' of insurance for residential homes/land. Private insurance takes the remainder. Note: Insurance manages financial impact but cannot reduce physical hazard risk.	Transfer	Recovery	NHC
Engineering	Hard engineering and structural solutions	Actions to mitigate hazard impact via strengthening, blocking, slowing or steering. Examples: Sea walls, raising structures, stopbanks and vertical evacuation structures.	Mitigation	Reduction	Regional councils / New Zealand Transport Agency
Nature-Based	Nature-based solutions	Using natural systems to manage risk with biodiversity benefits. Examples: Dune restoration, wetland creation and mangroves.	Mitigation / acceptance	Reduction	Regional Councils / Department of Conservation
Warning Systems and Evacuation	Hazard early-warning systems, evacuation and communication	Manages immediate risk to life by converting monitoring data into actionable instructions. Examples: Tsunami warning system and messages issued through emergency-management alerts.	Avoidance / communication	Response	NEMA / Earth Sciences New Zealand / MetService
Public Education	Public awareness and readiness	Empowering individuals to take action. Examples: NHC Natural Hazards Portal, 'Get Ready' campaigns, blue tsunami lines in Wellington.	Communication	Readiness	NHC / NEMA

5.1.2 Roles and Responsibilities Within Natural-Hazard Risk Management

A range of agencies, groups and individuals at the national, regional, local and community levels contribute to the management of New Zealand's natural-hazard risk (Saunders and Kilvington 2016). Agencies and groups include the:

- Ministry for the Environment, which provides national regulatory and non-regulatory guidance on the environment and climate.
- NEMA, a departmental agency in the Department of Internal Affairs (DIA) that serves as the steward, operator and assurer of the wider emergency-management system.
- The Department of Conservation (DOC)[13], which manages visitor and worker safety on public lands through compliance, hazard identification and site-management responsibilities under the Health and Safety at Work Act 2015 (HSWA).
- The Natural Hazards Commission Toka Tū Ake (NHC), a Crown entity that seeks to reduce the impact of natural hazards on people, property and the community through research, education and insurance.
- Regional and unitary councils, which are responsible for regional or catchment-scale management.
- Territorial authorities, which manage risk, including land-use designations and decisions at the city and district level.
- Civil Defence and emergency management groups, which manage disaster preparedness and response within regions and cities.
- Engineering lifeline groups, which support infrastructure and asset management.

Additionally, the National Risk and Resilience Framework includes: the National Resilience Board (coordinated, whole-of-system governance, with a strategic focus on building long-term resilience), the National Security Board (threats to national security), the Economic Chief Executives Group (economic security), the Natural Hazard Risk Reduction Forum (including non-climate-related natural hazards), the National Emergency Management Board (emergency-management system-readiness). The latter two entities and the overarching National Resilience Board are particularly relevant.

Commercial tourism operators also have a responsibility to their customers (and staff under the Health and Safety at Work Act 2015) to assess, eliminate or minimise natural-hazard risks related to the Health and Safety at Work (Adventure Activities) Regulations 2016 ('the Regulations'). WorkSafe, New Zealand's primary work health and safety regular, advises that such risks can be reduced through control measures such as:

- Spending less time in areas with possible hazards.
- Avoiding areas that could be affected by the hazard.
- Changing the activity type.

DOC is responsible for considering the safety of any commercial operation for which it has issued a concession – for the operator, its employees and its clients (on public lands). DOC's obligations, under the HSWA, for any persons conducting a business or undertaking (PCBUs) that might be in Piopiotahi / Milford Sound, are to communicate, cooperate and collaborate with other PCBUs where it has a joint interest.

13 DOC previously commissioned GNS Science to create a risk-analysis methodology to help them make decisions about natural-hazard management. See more here: https://www.doc.govt.nz/about-us/our-role/managing-conservation/recreation-management/visitor-risk-management/assessing-risk-from-natural-hazards-at-visitor-sites/

Individuals are also central to hazard management, as individual decisions can help reduce risk. Co-operation between all of the above entities is essential to ensure a streamlined and holistic national approach to planning and mitigating for natural hazards (Saunders and Kilvington 2016).

5.1.3 Risk-Management Case Studies and Recent Recommendations in New Zealand

Hazard, exposure and vulnerability vary across New Zealand, requiring a range of risk-management approaches depending on the location and context. Although every hazard event is unique, examples of natural-hazard risk management across the country can provide a lens through which to illustrate different approaches. Here, we provide an overview of management of debris flow risk at Matatā (Bay of Plenty) and rockfall risk at Cape Kidnappers (Hawke's Bay). Other notable case studies for further reading include managing crater-lake failure at Ruapehu (Keys and Green 2008) and management of land use on active faults (Bretherton et al. 2023). Please note that these examples are not directly comparable in terms of likelihood and impact to landslide-induced tsunami risk at Milford Sound. There are also relevant aspects of the management of volcanic risk in Tongariro National Park, and what is found and recommended by the Whakaari / White Island Eruption Coronial Inquiry.

Case Study 1: Matatā (Debris Flow Risk – Bay of Plenty)

Natural hazard risk: The community of Matatā is exposed to debris flow hazard from multiple stream catchments and the hills South of the area. In May 2005, a torrential rain event triggered a debris flows that destroyed 27 homes, damaged nearly 90 others (McSaveney et al. 2005) and caused the evacuation of over 500 people from their homes (Spee 2008).

Management: After the 2005 event, the causes of the debris flow were assessed, and a range of options (engineering and planning) were identified for an appropriate way forward (Boffa Miskell Limited 2018). A review after the event outlined four possible broad options to mitigate the risk of debris flows: debris detention (somewhere in the catchment); debris deflection (on the fanhead); building regulation (prohibiting of buildings in the path of future debris flows) and warning and evacuation through early detection of severe storms (McSaveney et al. 2005). Several options were discussed, including retreat, building a debris dam/detention structure or a bund, and a proposed debris detention structure was abandoned due to an independent review (Bickers 2012). In 2013, Whakatāne District Council changed its risk-management approach from an engineering- to planning-based approach (Domain Environmental Ltd 2012; Bickers 2012; de Vilder et al. 2024). In 2015, council staff worked as part of a Consensus Development Group to investigate hazard-mitigation options, identifying a voluntary managed retreat option as the best way forward (Hanna et al. 2017).

A critical challenge in this management process was the timing and communication of technical risk data. Many property owners rebuilt under the assumption that the catchment-wide debris structures would eventually be completed or conducted their own informal risk assessments without the benefit of a comprehensive, town-wide study (Whakatāne District Council 2015). It was not until 2013 that a Quantitative Risk Assessment was finalised, which revealed that a significant portion of Matatā remained subject to an 'intolerable' risk to life (Tonkin & Taylor Ltd 2013). This created a legacy issue where the 'informed consent' given by owners in the years following the disaster was found to be based on incomplete data.

Outcomes: The Matatā case study highlights the challenges of assessing different treatment options before a full quantitative understanding of the hazard is established. Engineering solutions have limits, and, if the residual risk remains intolerable, then land-use planning and managed retreat must be considered as early as possible in disaster risk management, with risk assessments shared as early as possible.

Case study 2: Cape Kidnappers (Landslides/Rockfall Risk – Hawke's Bay)

Hazard risk: A popular coastal walk in Hawke's Bay is exposed to rockfalls and landslides from 100-m-high cliffs (Shore 2020). A landslide occurred in January 2019 that seriously injured two tourists. A subsequent Quantitative Risk Assessment revealed that the risk to life was significantly higher than previously understood, bordering on levels usually associated with high-risk mountaineering rather than casual beach walking (Massey et al. 2020b).

Management: Hastings District Council and DOC are jointly managing the risks to visitors. Because the scale of the cliffs makes physical engineering or stabilisation impossible, the management strategy shifted toward a model of informed consent and exposure reduction. DOC re-classified the area as a 'Remote' rather than 'Day Visitor' site. This subtle but important change in management status shifts the burden of safety onto the individual: by reducing track maintenance and removing 'safe-looking' infrastructure, the environment communicates its own inherent danger, discouraging those who are not prepared for high-country conditions.

Outcomes: To manage the day-to-day danger, the Hastings District Council and DOC implemented a proactive trigger-based closure system (DOC 2020). Under this framework, the beach is automatically closed to the public following specific environmental events, such as heavy rainfall, significant earthquakes or the sighting of fresh debris. This was supported by enhanced, graphic signage at the Clifton entrance that clearly outlines the potential for multiple fatalities, ensuring that visitors are making an informed decision before proceeding.

Furthermore, a collaborative Experience Management Plan was established to coordinate between government bodies and private tour operators (DOC 2020). Commercial companies are now required to adhere to strict safety protocols, including the use of spotters and 'no-stop' zones in high-risk sectors. [14]

More recently, monitoring has shown that landslides were always occurring, not just during or following adverse weather. This meant that the framework that was in place and the warning signs were less effective as safety tools.

Due to the unpredictable nature of the hazard (and frequency of weather warnings), there is now (in 2026) only one operator who operates in this area, who avoids the unstable cliffs and travels overland (through private land) to a site of interest (Gannet Colony).

The case study ultimately highlights that, when a natural hazard cannot be eliminated, the most effective management tools are high-quality data, clear public communication and a realistic acceptance of residual risk. Despite management, it has also illustrated that the temporal unpredictability of hazard (and therefore risk) can ultimately drive risk reduction.

5.1.4 Risk Tolerance

Risk tolerance underpins the decision thresholds in risk management by informing the extent and type of treatment needed to reduce risk, or potential loss, to a level that an individual or society is willing to tolerate or accept (Toka Tū Ake EQC 2023a). Although risk tolerance is formerly integrated in some risk-reduction practises overseas (see Section 3.5) formal applications in New Zealand have been limited in practise.

14 DOC has recently informed the authors that risk management at this site is actively changing and visitor facilities will be reduced. For more up to date information on the situation at Cape Kidnappers, please visit: https://www.doc.govt.nz/parks-and-recreation/places-to-go/hawkes-bay/places/cape-kidnappers-gannet-reserve/cape-kidnappers-walking-track/

Until recently, risk tolerance was not explicitly considered as a step in most natural hazard and risk management approaches in New Zealand due to lack of a standardised approach for assessment (Toka Tū Ake EQC 2023b; NHC 2025). This often resulted in risk-management approaches that implicitly sought ambiguous or inconsistent targets for reduced risk levels. To address this gap, NHC developed a Risk Tolerance Methodology to enable a consistent and scalable approach for assessing 'intolerable', 'tolerable' and 'acceptable' levels of risk in New Zealand (NHC 2025). First published in 2023, and updated in 2025, the methodology proposes that risk-tolerance assessments are carried out through engagement with affected communities and stakeholders to increase the transparency and effectiveness of risk-management approaches.

Risk tolerance varies greatly across hazard contexts and scales, which has resulted in a wide range of terminology and approaches to address and describe its application. Based on a comprehensive literature review (Toka Tū Ake EQC 2023a), NHC (2025) proposes three levels of risk for use in New Zealand – 'intolerable', 'tolerable', and 'acceptable' (Table 5.2). To understand which level a corresponding risk falls into, a risk tolerance assessment should consider:

- The policy timeframe that the risk will be managed for.
- What could or has been impacted and to what extent.
- Who bears the consequences of the risk and/or risk-treatment option.
- A comparison of the timeframes and consequences of the risk threshold.

Table 5.2 Risk tolerance terminology (from NHC [2025]).

Level of Risk	Associated Risk Terms	Explanation	Descriptive Examples
Intolerable	Catastrophic Severe Unacceptable Extreme High	Risk cannot be justified except in extraordinary circumstances. Activity must cease until risk is removed or reduced	• Resilience of the land use has or will soon be exceeded beyond sustainable risk-reduction measures, with continued use of the land no longer sustainable; and/or • The coping capacity of a community or property has been exceeded, or will soon be exceeded; and/or • Life safety and/or functionality of the building is threatened beyond risk reduction measures; and/or • The consequential effects of the development on the environment will be irreversible; and/or • 'X' number of events leading to one or more of the points above have occurred in 'Y' years.
Tolerable	Significant Substantial Medium Tolerable	Risk is accepted only if the benefit gained is shown to outweigh the risk (using the 'As Low As Reasonably Practicable' principle*). Tolerable only if risk can be mitigated at a cost proportional to the benefit gained.	• The sustainable use of the land can continue with cost-effective risk reduction measures; and • Monitoring of the natural-hazard and climate-change risks is undertaken to allow changes in risks to be managed; and • Communities can cope with the impacts from natural hazard events; and • The life-safety risk and/or functionality of the land use can be managed to safeguard the future of the land use.
Acceptable	Acceptable Low Insignificant Negligible	Broadly acceptable. Monitor and maintain assurance that risk remains at this level.	• Activity can occur with limited controls or restrictions.

* For a risk to be ALARP, it must be possible to demonstrate that the cost involved in reducing the risk further would be grossly disproportionate to the benefit gained (Coster 2024).

Engagement with diverse stakeholders and Māori should support such risk-tolerance assessments (NHC 2025), and resources and frameworks have recently been developed to support these efforts, built on the 'Let's Talk About Risk' Natural Hazard and Climate Risk Engagement Framework (Brown et al. 2023, Kilvington et al. 2025). These tools provide pathways, options and guidance for practitioners seeking community and stakeholder perspectives on risk tolerance to feed into decision-making on risk thresholds.

A cornerstone example of engagement for risk-tolerance assessment in New Zealand was carried out by Kilvington and Saunders (2015), who used a series of community workshops called 'I can live with this' to understand tolerance of natural hazard risks in the Bay of Plenty. The community inputs were then used to define risk thresholds for use in the Bay of Plenty Regional Policy Statement, including thresholds for loss of life and other consequences. More-recent examples include national built environment design standards (Brown et al. 2022), climate-change adaptation planning (Hauraki District Council et al. 2023) and infrastructure asset-management planning (Marlborough District Council 2023). Engagement processes help ensure that risk-management thresholds reflect the values, preferences and risk appetites of those affected by the risk and the risk-management options.

5.1.4.1 Risk Appetite

'Risk appetite' refers to the amount and type of risk that a person or organisation is willing to pursue or retain (Aven 2013). An individual with a high risk appetite is likely to have higher thresholds for risk tolerance – a greater willingness to accept high risk for large benefits. Risk appetite can be highly variable between individuals or groups and change with time (NHC 2023; Afsari Bajestani et al. 2024). This can be observed in a tourism context through the way that individuals with a range of varying cultural and social backgrounds experience a destination. For example, solo travellers who journey with no fixed itinerary demonstrate a higher willingness to tolerate tourism risks than travellers who journey with organised package tours to comfortable resorts (Williams and Baláž 2013). Changes in risk appetite can also be observed in policy shifts, where stronger building regulations demonstrate a lower willingness to tolerate fatalities from earthquake-prone buildings in the months and years following a devastating earthquake (Henrich et al. 2018; Ball et al. 2022). Risk appetite is accordingly tied to the perceived risk of a hazard, which is dependent on a range of individual, affective, contextual and cognitive factors and biases, including previous and recent experience (Slovic 1987; Siegrist and Árvai 2020; Anderson et al. 2024). In some contexts, this variability can be addressed by using different risk thresholds for groups with different risk appetites and capabilities to deal with hazards (Taig 2022).

Societal Risk

Risk appetite, and therefore risk tolerance, shifts between individual and societal risk contexts. While individual risk refers to likelihood of loss, damage or harm to one individual from a particular natural-hazard event, societal risk refers to the likelihood of loss, damage or harm to *multiple people from one event* – for example, the chance of multiple fatalities or widespread societal loss from an earthquake or tsunami (NHC 2023). Societal risk is concerned with the collective impacts of a single catastrophic event, rather than isolated individual outcomes. Broader societal norms therefore influence thresholds for societal risk tolerability, although these norms can also be dynamic and evolve with real and perceived changes in risk (Vinnell et al. 2019; Szekely et al. 2021; Ball et al. 2022; Vriens et al. 2024).

Currently there are no legislative or agreed frameworks for assessing societal risk. Accordingly, societal risk thresholds vary widely in practise worldwide (Pitblado et al. 2012; see Section 3.5). Typically, societal risk is evaluated in the context of the frequency of the event and expected number of fatalities. Multiple fatalities are often only considered societally tolerable if the likelihood of the event is sufficiently low. For example, using the United Kingdom's Health and Safety Executive, an accident that causes the death of 50 or more people is considered intolerable if the likelihood is more than 1 in 5000 per annum (HSE 2001). In many cases, societal risk is dynamic, and whether or not such thresholds are met can change rapidly with exposure, particularly when highly mobile transient populations are exposed, such as in tourist areas or large event gatherings (Darling et al. 2025).

5.1.4.2 Tourism Risk Management

Scenic tourist destinations are often associated with high geographical exposure to natural hazards, which can interact with a complex range of vulnerabilities amongst visitors, residents and businesses (Aznar-Crespo et al. 2020). Many tourism areas in New Zealand in particular have been shaped by hazardous earth processes that are still active and pose a risk to people and assets in the area. Concentrations of transient populations in these environments exposed to hazards such as earthquakes, tsunami, volcanism and landslides can create considerable individual and societal risk levels.

Individual risk-tolerance levels are known to vary between ‘types’ of tourists (e.g. package tourists versus solo ‘drifters’) (Williams and Baláž 2013). One way of addressing this range in risk appetite is through communicating and managing risk using a range of thresholds (Taig 2022). For example, DOC manages public lands using a three-tier risk-management framework based on visitors with low-, medium- and high-risk tolerance levels (Taig 2022; DOC 2024). The framework guides risk reduction and management on DOC sites, such as the landslide risk on the beach walkway at Cape Kidnappers (see Section 1.1.3; Case Study 2). After the individual risk to day visitors was deemed intolerable and societal risk was assessed to be ‘high’, track access and communications were altered to reflect the high risk associated with the site. This sought to lower the risk by reducing exposure of low- and medium-risk-appetite day visitors, as it was considered to have a risk threshold that more closely aligned with the high-risk appetites of backcountry adventurers (Sutton and Greer 2020).

Many collaborative systems and practises exist to help manage disaster risk in tourism areas of New Zealand that help navigate the responsibilities across multiple parties (e.g. land owners, operators, emergency managers) (Danzi et al. 2025). However, there remain areas where societal risk has been identified to potentially exceed intolerable risk thresholds due to high exposure of tourist populations – notably, at Piopiotahi / Milford Sound (Darling et al. 2025; Davies and Dykstra 2025). Although these studies are limited in that they adopt overseas thresholds derived from non-tourism contexts and are based on uncertain hazard modelling (see Section 4), they suggest that there is a need to develop a better understanding of these risks in the New Zealand tourism context. The societal risk level at this iconic UNESCO (United Nations Educational, Scientific and Cultural Organization) World Heritage Area has steadily increased over the last decade due to increasing visitor numbers, and the risk is forecasted to become increasingly more intolerable with time (Darling et al. 2025) as visitors surpass one million per annum (RNZ 2025).

5.2 Risk Management for Earthquake-Induced Landslide and Tsunami in Piopiotahi / Milford Sound

5.2.1 Earthquake-Induced Landslide and Tsunami Risk

Piopiotahi / Milford Sound is exposed to extreme hazards from earthquake-induced landslide–tsunami, with limited historic analogues for comparison within New Zealand (see Section 4.1). The hazard presents life-safety risks to those visiting and working in this popular international tourism destination and UNESCO World Heritage Area. Piopiotahi / Milford Sound is remote, with limited access and egress options, and hazardous events could happen quickly with little warning. Increasingly large numbers of transient tourists visit Piopiotahi / Milford Sound, and the workers needed to support these visitor numbers suggest significant individual and societal risks. In a recent review of existing hazard and risk metrics, Charlton et al. (2025) estimate a ‘very high’ annual fatality risk for workers in the area. Recent evacuation and exposure modelling also suggests that few people would survive an earthquake-induced landslide and tsunami event during peak visitation times (Harris et al. 2024; Darling et al. 2025). In this section, we review challenges and approaches for managing this risk discussed in the literature.

5.2.2 Natural-Hazard Risk Management

Piopiotahi / Milford Sound lies within Fiordland National Park, and operations in the area are managed and overseen by a combination of government agencies, commercial entities and other organisations. Emergency Management Southland (EMS) is responsible for the delivery of Civil Defence Emergency Management (CDEM) responses throughout this region and works closely with partnering agencies to coordinate services. EMS aims to manage regional risks through six objectives, outlined in its five-year Group Plan (EMS 2026):

- Identify and understand risk scenarios to inform decision making.
- Put in place organisational structures and identify necessary processes to understand and act on reducing risks.
- Build risk awareness, risk literacy and risk-management capability.
- Address gaps in risk-reduction policies.
- Ensure development and investment practises are risk aware and do not create new risk.
- Understand the economic impacts of disaster and disruption.

The Group Plan assesses the regional risk of a magnitude 8.2 earthquake on the Alpine Fault as 'very high', noting particularly high risk in the isolated tourist areas of Te Anau and Piopiotahi / Milford Sound.

In response to the recent research on life-safety risk in Piopiotahi / Milford Sound (Harris et al. 2024; Darling et al. 2025), EMS has initiated a multi-stage project to improve understanding and management of the risk through collaboration with Milford Sound Tourism Limited, DOC, NEMA and other partner agencies (EMS 2025). Risk-communication efforts, which seek to provide clear and consistent information about the risks to support informed decision-making, have been initiated, and further work to refine risk-management approaches is underway.

5.2.3 Key Challenges for Risk Management

Chosen future risk-management strategies informed by the multi-stage project will need to develop approaches for dealing with a number of key challenges. Factors that need to be considered in future short- and long-term risk-management strategies for the area include:

- Evacuation to high ground increases an individual's chance of surviving a tsunami. However, access to high ground is severely restricted in the area by dense vegetation, steep terrain and a lack of evacuation routes and muster areas.
- Isolation and extreme weather patterns can impact hazard-response efforts and the ability to evacuate, as well as affect resourcing and the cost of risk-management strategies.
- Multiple groups with varying roles and responsibilities across time will need to be strategically aligned to manage risk effectively.
- Visitor numbers are steadily increasing, which raises hazard exposure and puts additional stress on assets and constrains viable evacuation options.
- There are many uncertainties due to a lack of historic events and the interplay of ground shaking, land instability and wave behaviour (see Appendix 2).
- Exposure timings vary considerably between seasons and daylight hours.
- Steep topography, geographic setting and land-management considerations limit construction and development of protection and evacuation structures (e.g. shelters and platforms).
- Both long-term (e.g. strategic relocations and access) and short-term (e.g. alerting and early warning) approaches will be needed to manage risk.

- Balancing the economic benefits of tourism with the societal risk of a disaster is expected to be a complex and ongoing challenge.

Risk-tolerance thresholds, uncertainty handling, and risk owners and their obligations all need to be explored. Risk-tolerance assessments can inform any future risk management approaches by setting appropriate risk-reduction goals. Recent engagement frameworks can guide these conversations with communities (Brown et al. 2023; Kilvington et al. 2025) and support decisions regarding tiered risk messaging and management.

5.2.4 Potential Risk-Management Options

5.2.4.1 Recommendations from Previous Reports and Studies

Previous reports, academic papers and reviews have proposed a range of possible risk-management options based on previous understanding of risk in Piopiotahi / Milford Sound. We summarise the main recommendations from this body of work below.

One of the most comprehensive recent studies by WSP (2024) carried out a basic risk assessment to support the Milford Opportunities Project.[15] The study suggests the following mitigation actions for earthquake-induced landslide and tsunami risk:

- **Clear and co-ordinated evacuation planning and increasing the number of evacuation points and routes:** Development of a formal evacuation plan and new evacuation routes and points based on further modelling. The study suggested that this would be supported by increased education and signage.
- **Education:** Educating the public about evacuating as soon as long or strong ground shaking is felt is therefore likely to be effective. The study noted that an increase in public understanding of tsunami risk and evacuation procedures is likely to lower life risk in Piopiotahi / Milford Sound through increasing evacuation effectiveness.
- **Vertical evacuation structures:** These may contribute to the lowering of tsunami risk in Piopiotahi / Milford Sound. This is most likely to be effective at the Visitor Centre, where the roofs of the existing three-storey buildings could be retrofitted as evacuation points. Vertical evacuation structures could also be considered at Freshwater Basin, Deepwater Basin and the Cleddau delta; however, these would need to be significantly higher than the current buildings to mitigate the risk from the potential tsunami waves, which have a potential wave amplitude up to ~10 m and higher wave run-ups (Taig and McSaveney 2015).

The WSP (2024) study also mentions options that would not be considered effective:

- **Early-warning systems:** Local-source tsunami have very limited time between formation and impact; therefore, automated warning systems may not work quickly enough for effective warnings. However, the study highlighted that mitigation measures could consider an early-warning system for distant Alpine Fault ruptures and earthquakes.
- **Seawalls and dykes:** The study stated that hard engineering approaches are unrealistic in the Piopiotahi / Milford Sound context due to the size of the structures required being in stark contrast to the natural setting.

15 https://www.doc.govt.nz/our-work/sustainable-destinations-piopiotahi/milford-opportunities-project/

A hazard and visitor risk report by Stantec (Craig and Chinn 2021) suggests the following options to manage the risk:

- **Reinforced resilient buildings:** A large 'earthquake- and tsunami-resilient' central purpose building could be constructed to reduce risk. The report suggests that strategically placed multi-purpose 'bunkers' could also be built with a low profile to withstand tsunami.
- **Improve evacuation routes:** An interim measure would be create/improve a wide clear pathway up the bluff behind the hotel to a semi-cleared muster area that could also potentially serve as a viewing point at other times.
- **Remove all overnight staff and visitors away from high-hazard zones.**
- All land-based staff should also **undergo regular training and periodic drill exercises** in conjunction with the Milford Sound Piopiotahi Emergency Response Team[16] and regional CDEM teams to put them in the best position to advise visitors quickly and with confidence.
- **Warning systems**, such as sirens or horns – without reliance on mains electric supply – should be considered, as an earthquake could cause temporary or permanent failure of the electricity supply.

The report also offers specific recommendations for boat users and cruise operators:

- Adding **an exclusion zone around the valley side for cruise ships and boats**. It suggests that a fairly large exclusion zone (>150 m) would also allow more time for pilots to react and turn their vessel to face the wave at the optimal speed and direction (apart from the very large cruise ships). Once carrying passengers, cruise boats should seek to minimise their time in the shore zone (where wave impacts would be higher) and head quickly out to deep water where there is probably a better chance of survival than in the shore zone.
- Consideration could be given to **mandating lifejackets under every seat** (for crew and visitors, with instructions upon boarding to allow for rapid deployment, instead of scrambling in a locker and passing around) or possibly even mandate wearing of life jackets.
- **Pilots should receive periodic refresher training on handling their vessel types on high waves** (say, once every three to five years) in order to improve response time and stabilising manoeuvres in waves.

Few academic research papers have commented on risk-management options. However, based on evacuation modelling, Harris et al. (2024) conclude that:

> *"Evacuating Milford Sound in the event of a landslide tsunami therefore appears infeasible (due to the combination of the limited capacity at the Lookout Platform and the distance required to travel to reach a safe location on the highway), and the primary way to reduce fatalities in such event may be to limit the number of people at Milford Sound at any given time."*

Davies and Dykstra (2025) support WSP's conclusion that an early warning system is not feasible. They state that:

> *"The only warning people at Piopiotahi / Milford Sound will receive of the potential arrival of a tsunami is the occurrence of the earthquake; while only perhaps one in three earthquakes will generate a large landslide, it is impossible to know whether any given earthquake will cause a major landslide, so every seismic occurrence must be expected to be tsunamigenic."*

16 The Milford Sound Piopiotahi Emergency Response Team is no longer active.

Davies and Dykstra (2025) note that this is different from the Norway context, as large landslides in Norway are likely to be proceeded by years to decades of warning. They state that reducing visitor numbers by a factor of about 1000 to less than 1000 per year would reduce the societal risk to acceptable levels, but this would effectively mean closing the site completely – a measure which would itself have major political, social and economic consequences (Davies and Dykstra 2025).

Darling et al. (2025) also find that there is a need for:

> *"… the risk owner (in this case, the New Zealand Government) to take an active role in managing the dynamics of societal risk in such high risk sites. In the absence of national guidance on societal risk tolerability, these insights should be used to develop specific threshold and policy advice for such high-risk areas … International experience suggests that the transfer of risk evaluation tools across sociopolitical contexts needs to be carefully applied."*

In summary, there are several strategies and approaches to managing landslide tsunami risk that have been suggested by previous research and assessments (Table 5.3). Overall, the options provided by previous studies range from doing nothing, which keeps costs low but leaves an 'intolerable' level of risk in place, to engineering solutions such as vertical evacuation structures and resilient buildings, which could reduce loss-of-life risk but may be expensive, visually intrusive and insufficient for all visitors.

Warning systems and evacuation planning offer potential benefits for non-locally-generated events but are considered ineffective for fast-onset, locally generated tsunami, and evacuation feasibility is severely limited by the landscape and capacity constraints. Education and staff training can strengthen preparedness and response but do not reduce the hazard itself and rely on rapid individual action. Options that reduce exposure to the hazard, such as restricting visitor numbers, removing overnight accommodation or limiting access, have been identified by previous Milford Sound risk assessments as having the greatest potential to reduce societal risk (Davies and Dykstra 2025). However, these measures would carry substantial economic, social, legal and reputational consequences that need to be considered. Finally, exclusion zones for boats could reduce exposure to falling debris and hazardous waves but may need to be large, especially for certain vessel types, and have not been tested in this context. Overall, the options illustrate a spectrum from low-cost but low-effectiveness measures to high-impact but high-cost and socially challenging interventions. There is also the challenge that some of these have not been tested in New Zealand and may not be feasible for this specific risk.

This page left intentionally blank.

Table 5.3 Summary of the main non-governance risk-management options for tsunami risk at Piopiotahi / Milford Sound based on previous report recommendations (Craig and Chinn 2021; WSP 2024; Harris et al. 2024; Davies and Dykstra 2025). Note that this is not a full assessment of all of the options, only ones gathered as part of this review. Positives and negatives have been sourced from previous studies where possible. These are only presented in relation to the current activities that are taking place at Piopiotahi / Milford Sound. Costs are relative and have not been accurately costed. These could be discussed and added/adjusted at a future workshop. **The below options are based on what is known about risk currently. These options could be better scoped if a full risk assessment was conducted.**

	Description	Positives	Negatives	Explicitly Recommended By:	Explicitly Not Recommended By:
Risk Acceptance	No adjustment of current management approach.	• No additional costs.	• Landslide-induced tsunami has been currently identified as an intolerable outlier in the current risk profile (Craig and Chinn 2021). • Does not reduce risk.	Not explicitly mentioned in any of the previous studies.	
Engineering and Structural Options	Tsunami resilience main hub building or vertical evacuation structures within the hazard zones (new or retrofitting existing).	• Provide safer locations during a threat. • Reduces loss of life risk. • Provides workers (and tourists) with a positive solution to reduce their risk.	• Costs could be high (relative to other options). • Could not match the natural environment. • May not be able to 'house' everyone. • May need more than one. • Would need to be linked with evacuation planning.	Recommended by WSP (2024) and Craig and Chinn (2021).	-
	Smaller 'bunkers' that are built with a low profile to withstand tsunami.	• Helps provide shelter to those who are too far away from the main hub.	• No evidence provided on how these work in practise. • People may not feel safe using them.	Craig and Chinn (2021).	-
	New seawalls and dykes.	• Could provide some protection in key low-lying areas.	• Does not fit with the natural look of the area. This type of heavy infrastructure is not considered to be in keeping with the intent of any re-development at Milford Sound. • May need to be really high. • Could lead to individuals taking no ownership of risk and relying on structures to protect them.	-	WSP (2024).
Warning and Evacuation	Implementation of monitoring and/or warning system, leading to timely evacuation.	• May provide early warning for earthquake shaking from a non-local earthquake. • Sirens or horns could potentially work if electricity is disrupted.	• Warning system would not be rapid enough for people to take protective action from a local event. • Does not remove risk. • Over-reliance on warning systems to provide alert. • Warning system may not operate in a large earthquake. • Warning systems not tested in complex cascading events like this.	Sirens and horns recommended by Craig and Chinn (2021). WSP (2024) mentions that a monitoring-based warning system could be used for regional earthquake-event warnings.	Monitoring-based warning system for local earthquakes not recommended by WSP (2024), Craig and Chinn (2021) and Davies and Dykstra (2025).
	Evacuation planning (including defining routes and points).	• Would help promote people to safety in an event. • Decreases fatality rate.	• Research by Harris et al. (2024) suggests that evacuating Piopiotahi / Milford Sound in the event of a landslide tsunami appears infeasible. • Space and geographic restrictions may limit routes and points.	Recommended by WSP (2024) and Craig and Chinn (2021).	-
Education and Training	Public and worker education on hazard and risk.	• Empowering individuals and communities with knowledge and practical skills to prepare for, respond to and recover from hazards.	• Does not remove risk. • Relies on individuals taking action. • Individuals may not have enough time to evacuate to safety.	WSP (2024).	-
	Staff training on response procedures and evacuation planning.	• Will put staff in a good position to advise visitors quickly and with confidence to improve safety outcomes for all.	• Time consuming and could incur some costs (although would be less than other options).	Craig and Chinn (2021).	-
Reduce Access	Reduce access to the area. Options range from removing overnight visitors and workers to reducing day-visitor numbers.	• Make risk more tolerable. • Reduces risk to life. • Reduces the chance of international liability actions. • Environmental benefits.	• High costs. • Impact to livelihoods. • Loss of revenue. • Legal actions. • Public disapproval. • Reputational damage.	• Craig and Chinn (2021), conditional on whether a centralised reinforced building is not possible. • Harris et al. (2024) mentions 'reducing/limited' individuals at risk as an option. • Davies and Dykstra (2025) mentioned this but highlighted the challenges with it.	-

	Description	Positives	Negatives	Explicitly Recommended By:	Explicitly Not Recommended By:
Stop Access Completely	Stop access to the area completely.	• Make risk more tolerable. • Eliminates risk to life. • Eliminates the chance of international liability actions. • Environmental benefits.	• High costs (higher than other options) in terms of lost revenue. • Significant impact to livelihoods. • Loss of revenue. • Legal actions. • Significant public disapproval. • Significant reputational damage.	-	-
Creating Fiord Exclusion Areas for Boats	Creating an exclusion zone for boats so these avoid falling debris and exposure to ‘unpredictable waves’.	• Could reduce impacts and boat capsizing, but more evidence is needed on the practicality of this in fiord settings.	• Larger zone may be needed for sail boats. • Loss of revenue. • Public/tourist disapproval of not being able to get up close to waterfalls.	Craig and Chinn (2021).	-

6.0 Workshop Summaries and Next Steps

Three workshops were held in Queenstown, Piopiotahi / Milford Sound and Te Anau between 20 and 22 April 2026. The aims of the sessions were to share the Stage 1 findings of the Piopiotahi / Milford Sound tsunami risk assessment and to discuss implications and future work with stakeholders who have an interest in tsunami risk for Piopiotahi / Milford Sound. Presentations were delivered by the Earth Sciences New Zealand team: William Power (Chief Scientist – Tsunami and Coastal Hazards), Simon Cox (Chief Scientist – Mountains to Sea), Mary Anne Clive (Hazard and Risk Social Scientist) and Graham Leonard (General Manager – Geological Hazards). Tracey Fraser (Principal Emergency Management Advisor – EMS) also contributed by providing community and regional context and supporting discussion and answers to questions at each session.

Across all sessions, discussion focused on:

- The unstable nature of steep rocky slopes in Fiordland and the evidence for past landslides that have fallen into the Sound.
- The experiences of other countries that face similar problems, such as in the fjords of Norway, Greenland and Alaska.
- The ways in which the risk to Milford Village has previously been assessed and will be more accurately evaluated in forthcoming new modelling.
- Approaches for managing the risk and the application of these to the New Zealand legislative environment.

Invitations were sent to members of relevant working and operational groups by EMS, including the Fiordland Hazard Working Group, the Te Anau–Manapouri Operational Group, the Milford Sound Operational Group, the Piopiotahi Working Group, Southland Emergency Services and local tourism operators. In total, 80 participants attended across the three sessions.

Each workshop followed the same format: a two-hour session comprising three presentations followed by discussion. The following sections summarise the key discussion points from each workshop, followed by a combined list of frequently asked questions.

At the end of this section, we briefly summarise the next steps for the programme of research and summarise some of the key lessons learnt.

6.1 Session 1: Queenstown (20 April 2026, 1:00–3:00 pm)

The first workshop was held at the Queenstown Events Centre on 20 April 2026, with approximately 35 participants. Attendees represented tourism operators and associated agencies. The session began with presentations outlining global examples of landslide-induced tsunami, the specific hazard context at Piopiotahi / Milford Sound and potential risk-mitigation approaches. This was followed by discussion focused on evacuation, project timelines, likelihood, warnings, risk tolerance and potential impacts to cruise ships.

Discussion started with a question on who is responsible for evacuation-route planning and how these routes are developed. The project team outlined roles and responsibilities for tsunami evacuation planning in New Zealand, led by CDEM, and emphasised the importance of robust hazard modelling to underpin effective evacuation planning. Participants sought clarity on the timeline of the broader project. Earth Sciences New Zealand and EMS confirmed that the current technical phase is expected to be completed by the end of the year, alongside implementation of a communication plan.

Questions were raised about how often landslide-induced tsunami might occur and whether clearer language could be used to describe likelihood. The Earth Sciences New Zealand team explained the staged nature of the science, noting that likelihood estimates will improve as new modelling and evidence become available. EMS stated that communicating probabilities at this stage remains challenging, as values are expected to change with improved science.

Discussion also covered earthquake early warnings received on mobile phones. The team clarified how the system works overseas and explained its limitations for near-source earthquakes, where warning times would be very short. Broader discussion reinforced the importance of natural warnings, strong or prolonged shaking and visible rockfall, as well as clear messaging that immediate evacuation is essential.

An audience member acknowledged the value of this work and asked who ultimately determines what level of risk is tolerable, and how risk reduction is managed over time. Tracey Fraser outlined the relevant legislation, decision-making roles and responsibilities, noting the need to balance emergency-planning constraints. The discussion also highlighted the importance of considering individual worker risk alongside potential mass-casualty risk. The Earth Sciences New Zealand team referenced comparative risk work undertaken for DOC by Tony Taig.

There was interest from the participants in further research on the impacts of landslide-induced tsunami on large cruise ships. The Earth Sciences New Zealand team noted that this could be an additional future workstream, acknowledging limited research specific to fiord environments, with Japanese response offering useful examples for New Zealand.

Participants asked what practical actions could be taken now. EMS confirmed that current guidance and priorities are set out in the Risk Communications Strategy (see Appendix 5). Examples of comparable mass-fatality risk elsewhere in New Zealand were discussed, including the large Hikurangi subduction zone tsunami scenario, although with lower likelihood. Graham Leonard also shared lessons from hazard communication approaches with DOC and tourism operators at Tongariro National Park over the last 15 years.

6.2 Session 2: Piopiotahi / Milford Sound (21 April 2026, 6:00–8:00 pm)

The second workshop was held in the evening at Milford Sound Café on 21 April 2026; 15 participants attended this session. Attendees were predominantly tourism and concession operators. The same presentation delivered in Queenstown was repeated, followed by tailored discussion focused on landslide-induced tsunami risk in the area, project stages and practical implications for mitigation.

Discussion initially focused on the staged nature of the project and the timing of future modelling. The Earth Sciences New Zealand team outlined that the next phase (Stage 2) would involve hydrodynamic modelling to test a range of landslide volumes and locations, including sensitivity analyses around runout volumes and resulting wave heights. These scenarios would then be assessed for likelihood, with results expected early next year, subject to funding.

There was exchange about the potential role of warning or alerting systems in response to reduce this risk. The Earth Sciences New Zealand team re-iterated that, in this context, the earthquake itself is the warning. Due to the very short time between an earthquake and landslide–tsunami generation, there is no practical way to detect, analyse and issue warning quickly enough to be effective. This limitation applies to both technological systems and formal emergency alerts (Emergency Mobile Alerts). It was communicated that natural warnings such as strong (shaking where you cannot stand) or prolonged (more than 1 minute) shaking and visible rockfalls are the most reliable indicators, and people must act immediately without waiting for official confirmation.

Participants asked about evacuation feasibility, including situations involving very large numbers of people (e.g. 2000+ visitors in Milford at peak times). The Earth Sciences New Zealand team highlighted that evacuation effectiveness is a critical mitigation issue and that lessons from international examples, including Japan, show that pre-planning, quick action, clear routes and public understanding are central to reducing risk. There was specific interest from participants in evacuation routes, although it was acknowledged that these require further consideration in planning.

Questions were also raised about whether specific landslide-source areas or particularly unstable slopes would be studied. The Earth Sciences New Zealand team explained that the current focus is on whether potential landslide volumes are sufficient to generate damaging tsunami, rather than identifying individual slopes likely to fail. It was noted that landslides can originate from multiple locations and that it is currently unrealistic to map with confidence which slopes may fail in an earthquake.

As in the Queenstown session, participants also asked about appropriate advice for maritime vessels, including cruise ships. The Earth Sciences New Zealand team explained that research in this area is limited, particularly for fiord environments. However, evidence from Japan suggests that vessels should keep away from fiord walls and orient towards incoming waves. It was noted by the team that waves within fiords behave differently than in open water, but keeping distance from steep walls and aligning with wave direction is considered a logical risk-reduction action.

The discussion concluded with reflections on the importance of communication. The recently released Risk Communications Strategy was highlighted by EMS as an opportunity to help provide consistent core messages to the operators while allowing updates as knowledge improves. The Earth Sciences New Zealand team also referenced successful communication examples from Tongariro National Park.

6.3 Session 3: Te Anau (22 April 2026, 10:00 am – 12:00 pm)

The third and final workshop was held at the Te Anau Club on 22 April 2026, with approximately 30 participants attending. Attendees were predominantly tourism operators and representatives from emergency services. The same presentation delivered at the Queenstown and Piopiotahi / Milford Sound sessions was repeated, followed by discussion focused on what operators can do now to communicate risk, staff training and risk disclosure, examples from Tongariro National Park and potential impacts to boats.

The discussion began with a question about differences in tsunami wave arrival time and size depending on whether a landslide occurs close to Milford Village or nearer the entrance to the fiord. The team explained that wave heights are generally larger closer to the landslide source, as there is less time and space for the wave to attenuate, although larger volumes of water may be displaced further from the village. Thus, there will be differences in time and size depending on where the landslide occurs. The Earth Sciences New Zealand team provided clarity on the currently limited feasibility of slope-stability monitoring in this environment.

Participants emphasised the value of effective risk communication, noting positive examples from Ruapehu and Tongariro National Park and supporting a similar approach for Piopiotahi / Milford Sound. A question was raised about the extent to which lessons from the 2019 Whakaari / White Island eruption are influencing current decision-making, with Graham Leonard providing an overview of how that event has shaped the wider regulatory and risk-management context.

Further discussion focused on the importance of ongoing modelling and science to inform potential engineering and mitigation options, while also highlighting the need to not lose focus on practical actions that can be taken now. Participants stressed the urgency of providing risk information to visitors earlier in their journey, rather than relying solely on long-term mitigation solutions. DOC’s obligations and shared responsibilities for communicating known risks were discussed, alongside reference to the existing communications strategy, which provides guidance that can be used immediately. Tracey Fraser highlighted the importance of staff training, awareness and appropriate risk disclosure as key components of preparedness. The collective appreciated the need and desirability of consistent messaging.

As in previous sessions, Earth Sciences New Zealand shared lessons learned from working with concessionaires and DOC at Tongariro National Park, including training approaches and effective risk-communication practises.

Discussion ended with questions about impacts to boats from tsunami. As in previous sessions, the Earth Sciences New Zealand team shared that research on this is limited but that there are some examples from Japan that we can learn from. It was confirmed that the situation would be so quick that there would not be time to evacuate boats from the Sound to the deeper ocean.

6.4 Frequently Asked Questions and Answers

The following list of frequently asked questions, with the team's responses to these, is based on questions asked during the workshop sessions or in associated conversations.

Project-Related

- **What are the next steps for the project, and what is the expected timing for future modelling?**

  We are currently scoping Stage 2, which will include hydrodynamic modelling, and hope to have most of the work completed by the end of the year, with stakeholder engagement to take place early next year. We still need to find funding commitments for future stages.

- **Is the new Risk Communication Strategy accessible and practical for operators to use?**

  Yes, it provides key consistent messages for everyone, from what to put on the website to what to tell staff. It does not use specific values, as these will be added as new knowledge is developed. This aims to reduce potential for confusion by lowering the risk of back-tracking on messaging and changing core messages within short timeframes.

Underpinning Science

- **Can we identify where future landslides are most likely to occur?**

  Yes, to some extent. We can identify which slopes are more or less likely to fail during a large earthquake by comparing Piopiotahi / Milford Sound's terrain with landslides triggered in past earthquakes elsewhere, such as the 2003 Secretary Island earthquake. Models typically combine factors such as expected ground shaking, slope angle, elevation, slope shape, geology, land cover and known rock fractures to estimate relative susceptibility to collapse. There is some postgraduate student work in progress toward this end.

  These approaches are useful for identifying broad areas of higher hazard. However, predicting exactly which slopes will fail, and how large failures may be, remains difficult in Piopiotahi / Milford Sound's extreme terrain. Ground shaking may be locally amplified or reduced by the complex topography, and many fractures and rock weaknesses are poorly mapped. As a result, there is still significant uncertainty in detailed predictions of landslide location, probability and volume.

  Given the uncertainties, we may still use the overall distribution of past landslides identified geologically in Piopiotahi / Milford Sound as a statistical guide to what might happen in future, even if individual future landslides will never be precisely the same as past ones.

- **How do tsunami wave arrival times and wave heights differ if a landslide occurs close to Milford Village compared with nearer to the entrance of the fiord?**

A landslide-induced tsunami close to Milford Village would arrive very quickly, potentially within a minute or two, leaving little warning time. Wave heights near the source are often largest because the wave has less distance over which to spread and lose energy.

A landslide nearer the entrance of the fiord would generally produce longer travel times before waves reached Milford Village, and wave heights may reduce somewhat as the wave propagates up the fiord. However, if large landslides were to occur in the outer fiord, these may still generate substantial waves that travel efficiently along the confined fiord geometry.

In general, tsunami wave height tends to decrease with distance from the source, but the final impacts also depend strongly on the size of the landslide, water depth, fiord shape and how waves reflect and focus within the fiord.

- **What would be the potential impacts of a tsunami on cruise ships or other vessels? And what should people do?**

  A landslide-induced tsunami could create very strong currents, rapid water-level changes and large waves within the fiord. The impacts on vessels would depend on the size and location of the landslide, the shape of the fiord and how close vessels were to the source. Smaller boats near the source area would generally be at greatest risk, while larger vessels may still experience dangerous surging, loss of manoeuvrability or collisions with debris or shorelines.

  People on vessels should follow the instructions of the skipper, harbour authorities and emergency-management agencies. In general, if there is sufficient warning, vessels may be safer in deeper water away from steep slopes and confined shorelines. People on land should move immediately to higher ground or follow designated evacuation procedures if strong shaking, unusual water movement or official tsunami warnings occur.

- **What is the likelihood of a landslide-induced tsunami occurring, and how should probabilities be communicated to people?**

  A landslide-induced tsunami at Piopiotahi / Milford Sound is **very unlikely during a short visit**, but it is a credible life-safety risk. The risk comes mainly from a large earthquake triggering landslides in the fiord. Current advice is to communicate this honestly: the chance is low for visitors, but the consequences could be severe, warning time may be very short and safety options are limited once people are there.

  Probabilities should therefore be kept simple and framed around decision-making, not false precision. The agreed messaging is:

  “A large earthquake or tsunami is extremely unlikely during your visit, especially a short one. Even so, these hazards do pose a risk to life at Piopiotahi / Milford Sound. If one occurs while you are there, your options to stay safe are limited. Know before you go.”

  For staff or people staying longer, the message should also say that **risk increases with time spent in the area**. Communication should be consistent across websites, booking information, staff inductions, signage and visitor materials, and it should be updated as new tsunami modelling and risk-assessment work becomes available.

- **How many of the large landslides identified in Piopiotahi / Milford Sound are known to have been triggered by earthquakes?**

  None of the ~18 very large landslides identified in Milford Sound have been individually ‘proven’ to have been triggered by a specific earthquake. Rather, the interpretation is based on the overall pattern of evidence.

No recent Fiordland earthquakes have triggered major landslides into Piopiotahi / Milford Sound, largely because their epicentres and strongest shaking have generally been more than ~80 km to the southwest. However, the large landslide and debris deposits preserved on the floor of the Sound are widely inferred to be predominantly earthquake-induced since retreat of the glaciers about 17,000–22,000 years ago. This interpretation is based on the close relationship between the frequency of Alpine Fault earthquakes and the number of large, mapped landslide deposits, together with the very high shaking expected during major Alpine Fault rupture events.

One report (Taig and McSaveney 2015) notes that “most, if not all” of the large submarine landslide deposits were probably triggered by earthquakes, but it also recognises uncertainty and that some individual landslides may have had other causes, such as extreme rainfall or progressive slope failure.

Importantly, the evidence is therefore strongest at the scale of the landscape as a whole, rather than as a confirmed causal link for each individual landslide.

Mitigation / Risk-Reduction Options

- **Is monitoring and alerting a feasible option for landslide-induced tsunami risk at Piopiotahi / Milford Sound?**

  A monitoring system for these slopes would add little value at this stage, as the main trigger is seismically induced, not sporadic rock failure due to gradual weakening. Perhaps in the future this may become feasible, with more sensitive technologies capable of monitoring a wide area. As things stand, there are limitations to creating an effective warning system in this context. There is very little time between the occurrence of an earthquake and landslide generation. At present, with technology currently available, it is unfeasible to create a warning system that could alert people in Milford Village in time. Natural warnings (ground shaking, rockfall) will be the most effective. We should encourage awareness of natural warnings. If an earthquake is long (more than a minute) or strong (hard to stand), or if there is any evidence of rockslides taking place, evacuate to high ground or inland as soon as possible. Every minute and every metre counts.

- **How would people be evacuated from Piopiotahi / Milford Sound following an event?**

  It will depend. It could be complicated depending on access and resources available. If it is an Alpine Fault event and the whole South Island has been affected, it could be a long time until resources are deployed. Locals need to have plan and be prepared to be self-sustainable for a period. Helicopters could have difficulty getting in and out. Boats may be an option but will take time. Getting involved in the Milford Operations Group can help align plans. Local emergency response depends on local volunteers.

- **How long should people remain in a safe location after a landslide-induced tsunami?**

  We need to do more research on this, but we expect it to be shorter than after a tsunami generated directly by an earthquake. There will be aftershocks, and these may be of sufficient size to trigger landslides and tsunami themselves. Wait to receive an ‘all clear’ message if possible.

- **What practical actions can be taken now if an event were to occur in the near future?**

  Start with communicating about the risk and raising awareness. Use a multi-layered approach that targets people from early in their decision to visit through to when they are in the location. An agreed set of messaging and communications pack is available from EMS.

6.5 Next Steps and Key Lessons from the Review

This report summarises Stage 1 of a multi-stage programme of work. Subsequent stages are anticipated to include:

- Initial physics-based numerical modelling of landslides and subsequent tsunami, including a study of the sensitivity of tsunami inundation in the Milford tourist centre and village to landslide location and volume, and detailed modelling of selected scenarios.
- A hazard assessment estimating the levels of inundation associated with different annual probabilities and that considers key uncertainties (for example, the degree to which the rate of landsliding has reduced over time since glaciation), as well as the latest information on Alpine Fault earthquake likelihood.
- Estimates of the probable impacts, in terms of casualties, building damage and infrastructure damage, from the modelled scenarios. When these are combined with the hazard model, this leads to a quantitative risk model.
- Quantification of the risk benefits that can be achieved through different forms of mitigation.

Some key lessons that the project team has gained from this study that will guide the future work include:

- The valuable increase in accuracy that can be obtained by adopting similar physics-based numerical modelling approaches to those used in Alaska and Norway (among others) for integrated modelling of landslides and tsunami, relative to purely empirical modelling approaches.
- Awareness that different tectonic and climatic environments affect the landslide-initiation process and that this needs to be understood and handled differently in different parts of the world. For example, dense monitoring of specific slopes deemed most likely to fail, as is done in Norway, is unlikely to be as effective here, where intense earthquake shaking can trigger landslides before these reach the same level of instability found in tectonically less-active countries. In our circumstances, we should be prepared for the possibility that future large landslides could occur on any one of many slopes. This motivates making a sensitivity study (to landslide location and volume) a priority in the next phase of work.
- Tsunami travel-time is a very important factor in determining which mitigation measures are likely to succeed. In the case of Piopiotahi / Milford Sound, tsunami travel times can be very short (just a few minutes), which implies the importance of heeding natural warnings – in particular, the need to self-evacuate from ‘long or strong’ earthquake shaking rather than reliance on instruments to provide a warning. It also puts the focus on pedestrian evacuation, as, for most people, it will not be practical to use a vehicle in the time available.
- Uncertainties about the changing likelihood of landslides post-glaciation, and about their modes of failure, are significant and will need to be accounted for in future work. Plausible ranges can be considered, varying from conservative ‘worst case’ assumptions (e.g. no change in landslide rates over time and landslides always occur in single events) through to more optimistic ones. A parametric approach could be used to understand the sensitivity of hazard and risk to these uncertainties. Where uncertainties in source processes are found to significantly feed through to risk, this becomes an important justification for geological and geotechnical work to reduce these, but it is important that the mere presence of uncertainty is not a justification for inaction.
- The workshop discussions highlighted the importance of consistent messaging, which was regarded as being very helpful in enabling operators in Piopiotahi / Milford Sound to communicate information to customers and staff. The recently released Risk Communications Strategy was viewed as an opportunity to help provide consistent core messages to operators while also allowing updates as knowledge improves. A continuing emphasis on consistent communications is recommended as the underpinning work progresses.

7.0 Summary and Discussion

In recent years, it has been identified that Piopiotahi / Milford Sound is likely to experience rockslide-induced tsunami, particularly after large earthquakes. This realisation was initiated by the discovery of large rockslide deposits on the floor of the Sound. As Piopiotahi / Milford Sound is a very popular tourist destination, this is understood to pose a (potentially significantly large) risk to both tourists and workers.

The situation in Milford has overseas equivalents that we can learn from, as fiords are a feature of formerly glaciated mountainous coastal regions around the world. As a step toward better understanding and management of the risks, this report examines the historical experience of rockslide-induced tsunami globally, the state of research into modelling and understanding of the potential hazards and risks posed, and approaches to mitigation of the risks.

Existing hazard and risk assessment at Milford has been performed using empirical approaches that draw primarily upon the properties of past tsunami caused by landslides in broadly similar environments in other countries, as well as the scaling-up of experimental studies of tsunami generation in wave tanks. However, there is potential for much more specific numerical modelling that takes into account the precise environment in Milford, particularly in terms of the topography of the slopes and bathymetry of the Sound. We summarise how such approaches have been used elsewhere, with a view to discussing their future use for Piopiotahi / Milford Sound.

Once the risk can be more accurately evaluated, should it still prove to be above the appropriate thresholds, we will be in a much better position to identify appropriate measures to mitigate it. In this study, we discuss some of the criteria for establishing what is an acceptable level of risk, bearing in mind that this may be both risk to an individual and societal risk, and put this in the context of New Zealand's hazard management frameworks.

Risk management in New Zealand is framed by internationally recognised disaster-risk-management principles and frameworks and is implemented at varying levels through a layered system of statutory planning, governance, financial, engineering, nature-based and social approaches. Central to this system are strategies of risk avoidance, mitigation, transfer, acceptance and communication, which collectively aim to mitigate loss from hazard events and prevent future disasters. Case studies from Matatā and Cape Kidnappers illustrate the practical challenges of managing high-consequence, low-frequency hazards, demonstrating the limits of engineering solutions and the importance of land-use planning, access management, informed consent and clear communication when residual risk remains high.

Previous New Zealand reports and articles have suggested that managing earthquake-induced landslide–tsunami risk requires a combination of short-term measures (such as alerting, warning, evacuation planning and risk communication) and long-term strategies (including access management, land-use controls and potential retreat from intolerable risk) applied across the '4Rs' of risk reduction, readiness, response and recovery. While there may be little prospect for reducing the level of the underlying hazard, there are nonetheless many ways in which the risk can be mitigated, either by reducing exposure by assisting people to leave the most hazardous locations before a wave arrives, reducing the amount of time spent in hazardous locations or reducing the danger to people by strengthening the built environment in ways that make a tsunami more survivable.

Experiences from Norway, Alaska and Greenland highlight how a combination of monitoring, early-warning systems, communication and governance can help to mitigate landslide–tsunami risk. In Norway, authorities monitor known at-risk slopes, maintain established multi-channel warning systems and invest in public education, although tourists remain less aware of evacuation processes. Alaska similarly focuses on monitoring key unstable slopes, such as Barry's Arm, and provides regular public updates to support awareness. Greenland demonstrates the value of low-tech, community-embedded approaches, such as local lookouts, awareness training and exercises and clear communication of monitoring data.

Across all case-study countries mentioned in Section 3.1, strong relationships, transparent decision-making and effective communication are crucial. It must be recognised that these places differ from Piopiotahi / Milford Sound in key characteristics. Some key differences include the known location of unstable slopes and therefore direct monitoring and warning, seismicity levels and resident populations. However, their shared challenges of high tourist numbers and transient populations and experiences of large earthquakes (Alaska and Chile) offer valuable lessons for management of risk at Piopiotahi / Milford Sound.

Whatever the approach taken, appropriate risk-management options need to be informed by an updated and accurate understanding of the risk. The co-creation of risk knowledge between stakeholders can help fill in knowledge gaps and create a shared understanding of the socio-material costs associated with management options (Johannessen et al. 2025). Framing risk-management options within an explicit risk-tolerability framework can provide a structured basis for future discussion and decision-making, ensuring that any management approach is proportionate, transparent and aligned with societal expectations for life safety in this internationally significant tourism setting.

8.0 Acknowledgements

We thank David Burbidge and Christina Magill for internal review of this report. We gratefully acknowledge the work of the Canterbury University team (Jesse Dykstra, Olivia Harris, Matthew Darling, Tom Robinson, Thomas Wilson and Tim Davies, among others), and that of Murray McSaveney, Tim Davies and the Great South team for raising awareness of societal risk issues at Piopiotahi / Milford Sound. Identification of papers and reports, and compilation of the glossary, was assisted by ChatGPT, Microsoft Copilot and Google search tools. ChatGPT was also used to help prepare some of the illustrations. We are grateful to Lara East for helping to locate difficult-to-access papers and reports, and to Kate Robb for document formatting and reference checking. We are also thankful to the operators, agencies and business owners who joined us at the workshops, as well as Tracey Fraser, who organised the workshops.

9.0 References

Abadie S, Morichon D, Grilli S, Glockner S. 2008. VOF/Navier-Stokes numerical modeling of surface waves generated by subaerial landslides. *La Houille Blanche*. 94(1):21–26. https://doi.org/10.1051/lhb:2008001

Afsari Bajestani S, Serrao-Neumann S, Hanna C, Fu X. 2024. Dealing with uncertainty in flood risk management and land use planning decisions: insights from Aotearoa New Zealand. *Climate Risk Management*. 46:100666. https://doi.org/10.1016/j.crm.2024.100666

[AGS] Australian Geomechanics Society. 2007. Practice note guidelines for landslide risk management. *Australian Geomechanics*. 42(1):63–114.

Anderson CC, Moure M, Demski C, Renaud FG. 2024. Risk tolerance as a complementary concept to risk perception of natural hazards: a conceptual review and application. *Risk Analysis*. 44(2):304–321. https://doi.org/10.1111/risa.14161

Arcos MEM, LeVeque RJ. 2015. Validating velocities in the GeoClaw tsunami model using observations near Hawaii from the 2011 Tohoku tsunami. *Pure and Applied Geophysics*. 172(3):849–867. https://doi.org/10.1007/s00024-014-0980-y

Aspaas A, Lacroix P, Sena C, Kristensen L, Langet, Renard F. 2024. Creep bursts on the Åknes landslide, Norway: detection, characterization and possible mechanisms. *Journal of Geophysical Research: Earth Surface*. 129(12):e2024JF007733. https://doi.org/10.1029/2024JF007733

Ataie-Ashtiani B, Shobeyri G. 2008. Numerical simulation of landslide impulsive waves by incompressible smoothed particle hydrodynamics. *International Journal for Numerical Methods in Fluids*. 56(2):209–232. https://doi.org/10.1002/fld.1526

Aven T. 2013. On the meaning and use of the risk appetite concept. *Risk Analysis*. 33(3):462–468. https://doi.org/10.1111/j.1539-6924.2012.01887.x

Aznar-Crespo P, Aledo A, Melgarejo-Moreno J. 2020. Social vulnerability to natural hazards in tourist destinations of developed regions. *Science of the total Environment*. 709:135870. https://doi.org/10.1016/j.scitotenv.2019.135870

Ball RJ, Hudson-Doyle EE, Nuth M, Hopkins WJ, Brunsdon D, Brown CO. 2022. Behavioural science applied to risk-based decision processes: a case study for earthquake prone buildings in New Zealand. *Civil Engineering and Environmental Systems*. 39(2):144–164. https://doi.org/10.1080/10286608.2022.2089980

Barnes PM. 2009. Postglacial (after 20 ka) dextral slip rate of the offshore Alpine fault, New Zealand. *Geology*. 37(1):3–6. https://doi.org/10.1130/G24764A.1

Barnes PM, Bostock HC, Neil HL, Strachan LJ, Gosling M. 2013. A 2300-year paleoearthquake record of the southern Alpine Fault and Fiordland subduction zone, New Zealand, based on stacked turbidites. *Bulletin of the Seismological Society of America*. 103(4):2424–2446. https://doi.org/10.1785/0120120314

Barnhart K, Jones R, George D, Coe J, Staley D. 2021. Preliminary assessment of the wave generating potential from landslides at Barry Arm, Prince William Sound, Alaska. Reston (VA): U.S. Geological Survey. 28 p. Open-File Report 2021-1071. https://doi.org/10.3133/ofr20211071

Barth NC, Boulton C, Carpenter BM, Batt GE, Toy VG. 2013. Slip localization on the southern Alpine Fault, New Zealand. *Tectonics*. 32(3):620–640. https://doi.org/10.1002/tect.20041

Barth NC, Kulhanek DK, Beu AG, Murray-Wallace CV, Hayward BW, Mildenhall DC, Lee DE. 2014. New c. 270 kyr strike-slip and uplift rates for the southern Alpine Fault and implications for the New Zealand plate boundary. *Journal of Structural Geology*. 64:39–52. https://doi.org/10.1016/j.jsg.2013.08.009

Berryman KR, Cochran UA, Clark KJ, Biasi GP, Langridge RM, Villamor P. 2012. Major earthquakes occur regularly on an isolated plate boundary fault. *Science*. 336(6089):1690–1693. https://doi.org/10.1126/science.1218959

Biasi GP, Langridge RM, Berryman KR, Clark KJ, Cochran UA. 2015. Maximum-likelihood recurrence parameters and conditional probability of a ground-rupturing earthquake on the Southern Alpine Fault, South Island, New Zealand. *Bulletin of the Seismological Society of America*. 105(1):94–106. https://doi.org/10.1785/0120130259

Bickers A. 2012. Review of Awatarariki Catchment Debris Control Project. Tauranga (NZ): Jayal Entreprises Ltd. 117 p. Prepared for Whakatāne District Council. https://www.whakatane.govt.nz/files/documents/about-council/council-projects/awatarariki-debris-detention-structure/Final%20Report%20-%20Review%20of%20Awatarariki%20Catchment%20Debris%20Control%20-June%202012.pdf

Boffa Miskell Ltd. 2018. Planning provisions for debris flow risk management on the Awatarariki Fanhead, Matatā: Section 32 evaluation report. [Place unknown] (NZ): Boffa Miskell Ltd. 47 p. + appendices. Prepared for Whakatāne District Council. https://www.boprc.govt.nz/media/714811/section-32-evaluation-report-planning-provisions-for-debris-flow-on-the-awatarariki-fanhead-matata-31-january-2018.pdf

Braathen A, Blikra LH, Berg SS, Karlsen F. 2004. Rock-slope failures in Norway: type, geometry, deformation mechanisms and stability. *Norwegian Journal of Geology*. 84:67–88.

Bradley BA, Bae SE, Polak V, Lee RL, Thomson EM, Tarbali K. 2017. Ground motion simulations of great earthquakes on the Alpine Fault: effect of hypocentre location and comparison with empirical modelling. *New Zealand Journal of Geology and Geophysics*. 60(3):188–198. https://doi.org/10.1080/00288306.2017.1297313

Bretherton E, Morgenstern R, Litchfield N. 2023. Managing active fault surface rupture risk through land use planning: barriers and opportunities. *Policy Quarterly*. 19(4):56–64. https://doi.org/10.26686/pq.v19i4.8568

Brodie JW. 1964. The Fiordland Shelf and Milford Sound. In: Skerman TM, editor. *Studies of a southern fiord*. Wellington (NZ): Department of Scientific and Industrial Research. (New Zealand Oceanographic Institute; memoir 17). p. 15–23.

Brown C, Abeling S, Horsfall S, Ferner H, Cowan H. 2022. Societal expectations for seismic performance of buildings. [Place unknown] (NZ): The Resilient Buildings Project; [accessed 2026 Feb]. https://www.resorgs.org.nz/wp-content/uploads/2022/04/RBP_SocietalExpectationsReport_2022.pdf

Brown C, Horn C, Horsfall S, Kilvington M. 2023. Natural hazard and climate change risk community engagement:
a framework to aid engagement design. [Place unknown] (NZ): Let's Talk About Risk; [accessed 2026 Feb]. https://www.resorgs.org.nz/our-projects/risk-and-resilience-decision-making/lets-talk-about-risk/

Bullard GK, Mulligan RP, Carreira A, Take WA. 2019. Experimental analysis of tsunamis generated by the impact of landslides with high mobility. *Coastal Engineering*. 152:103538. https://doi.org/10.1016/j.coastaleng.2019.103538

Cannata M, Marzocchi R, Molinari ME. 2012. Modeling of landslide-generated tsunamis with GRASS. *Transactions in GIS*. 16(2):191–214. https://doi.org/10.1111/j.1467-9671.2012.01315.x

Charlton DH, Clive MA, Cox SC, Lawson RV, Leonard GS, Jolly GE. 2025. Landslide-induced tsunami risk communication advice for visitors and workers in Milford Sound / Piopiotahi. Lower Hutt (NZ): GNS Science. 77 p. Consultancy Report 2025/14. Prepared for Milford Sound Stakeholder Group.

Cho Y-S. 1995. Numerical simulations of tsunami propagation and run-up [PhD thesis]. Ithaca (NY): Cornell University. 264 p.

Clague JJ, Bobrowsky PT, Hutchinson I. 2000. A review of geological records of large tsunami at Vancouver Island, British Columbia, and implications for hazard. *Quaternary Science Reviews.* 19(9):849–863. https://doi.org/10.1016/S0277-3791(99)00101-8

Clark KJ, Johnson PN, Turnbull IM, Litchfield NJ. 2011. The 2009 M_W 7.8 earthquake on the Puysegur subduction zone produced minimal geological effects around Dusky Sound, New Zealand. *New Zealand Journal of Geology and Geophysics*. 54(2):237–247. https://doi.org/10.1080/00288306.2010.543690

Clark KJ, Cochran UA, Berryman KR, Biasi G, Langridge R, Villamor P, Bartholomew T, Litchfield N, Pantosti D, Marco S, et al. 2013. Deriving a long paleoseismic record from a shallow-water Holocene basin next to the Alpine fault, New Zealand. *GSA Bulletin*. 125(5–6):811–832. https://doi.org/10.1130/B30693.1

Cochran UA, Clark KJ, Howarth JD, Biasi GP, Langridge RM, Villamor P, Berryman KR, Vandergoes MJ. 2017. A plate boundary earthquake record from a wetland adjacent to the Alpine Fault in New Zealand refines hazard estimates. *Earth and Planetary Science Letters*. 464:175–188. http://dx.doi.org/10.1016/j.epsl.2017.02.026

Corsa BD, Jacquemart M, Willis MJ, Tiampo KF. 2022. Characterization of large tsunamigenic landslides and their effects using digital surface models: a case study from Taan Fiord, Alaska. *Remote Sensing of Environment*. 270:112881. https://doi.org/10.1016/j.rse.2021.112881

Coster P. 2024 Jun 11. What does ALARP mean? London (GB): Worksafe UK; [updated 2026 Jun 8; accessed 2026 Jun 17]. https://www.worksafe.uk.com/risk-assessment/what-does-alarp-mean/

Cox C. 2024a. Carbon loss from earthquake induced landslides in Fiordland. *Pūhau Ana Te Rā: Tailwinds*. 2(2):1–17. https://doi.org/10.11157/patr.v2i2.48

Cox CA. 2024b. Landslides in Fiordland, New Zealand, and implications for carbon accounting [BSc Hons thesis]. Dunedin (NZ): University of Otago. 83 p.

Cox CA, Cox SC, Massey CI, Gorman AR. In prep (a). Earthquake-induced landslides and background rates of slope failure in Fiordland, New Zealand. To be submitted to *Landslides*.

Cox CA, Massey CI, Cox SC, Gorman AR. In prep (b). A regional-scale earthquake-induced landslide susceptibility model for Fiordland, New Zealand. To be submitted to *Natural Hazards*.

Craig A, Chinn D. 2021. Milford Opportunities Project: hazards and visitor risk review report. [Wellington] (NZ): Stantec NZ Limited. Prepared for the Milford Opportunities Project; [accessed 2026 Feb]. https://www.doc.govt.nz/globalassets/documents/our-work/milford-opportunities-project/stage-2/mop-hazards-and-visitor-risk-review-report-2021.pdf

Crosta GB, Imposimato S, Roddeman D. 2016. Landslide spreading, impulse water waves and modelling of the Vajont Rockslide. *Rock Mechanics and Rock Engineering*. 49(6):2413–2436. https://doi.org/10.1007/s00603-015-0769-z

Cruden DM, Varnes DJ. 1996. Landslide types and processes. In: Turner AK, Schuster RL, editors. *Landslides: investigation and mitigation*. Washington (DC): Transportation Research Board. p. 36–75. (Special Report; 247).

Dahl-Jensen T, Larsen LM, Pedersen SAS, Pedersen J, Jepsen HF, Pedersen G, Nielsen T, Pedersen AK, Von Platen-Hallermund F, Weng W. 2004. Landslide and tsunami 21 November 2000 in Paatuut, west Greenland. *Natural Hazards*. 31(1):277–287. https://doi.org/10.1023/B:NHAZ.0000020264.70048.95

Danzi L, Orchiston C, Higham J, Baggio R. 2025. Tourism disaster management: a social network analysis of nature-based destinations in Aotearoa New Zealand. *Journal of Travel Research*. 64(8):1901–1928. https://doi.org/10.1177/00472875241268623

Darling MJ, Robinson TR, Adams B, Wilson TM, Orchiston C. 2025. Minutes matter for life safety and risk exposure in Milford Sound, New Zealand. *Scientific Reports*. 15(1):36459. https://doi.org/10.1038/s41598-025-22101-3

Davies TR, McSaveney MJ. 2009. The role of rock fragmentation in the motion of large landslides. *Engineering Geology*. 109(1):67–79. https://doi.org/10.1016/j.enggeo.2008.11.004

Davies T, Dykstra J. 2025. Societal risk-to-life from natural hazards: assessments, acceptability and actions at Whakaari/White Island and Piopiotahi/Milford Sound, Aotearoa/New Zealand. *International Journal of Disaster Risk Reduction*. 119:105325. https://doi.org/10.1016/j.ijdrr.2025.105325

Dawe I. 2007. Updated hazard and risk analysis for the Wellington Region CDEM Group Plan. Wellington (NZ): Wellington Region Emergency Management Group; [accessed 2026 Jun]. https://ref.coastalrestorationtrust.org.nz/site/assets/files/8622/hazard-and-risk-analysis.pdf

De Pascale GP, Langridge RM. 2012. New on-fault evidence for a great earthquake in A.D. 1717, central Alpine Fault, New Zealand. *Geology*. 40(9):791–794. https://doi.org/10.1130/G33363.1

de Vilder SJ, Kelly SD, Buxton RB, Allan S, Glassey PJ. 2024. Landslide planning guidance: reducing landslide risk through land-use planning. Lower Hutt (NZ): GNS Science. 77 p. (GNS Science miscellaneous series; 144). https://doi.org/10.21420/R2X8-FJ49

Di Risio M, Sammarco P. 2008. Analytical modeling of landslide-generated waves. *Journal of Waterway, Port, Coastal, and Ocean Engineering*. 134(1):53–60. https://doi.org/10.1061/(ASCE)0733-950X(2008)134:1(53)

Di Risio M, De Girolamo P, Beltrami GM. 2011. Forecasting landslide generated tsunamis: a review. In: Mörner N-A, editor. *The tsunami threat – research and technology*. Rijeka (HR): InTech; [accessed 2026 Feb]. https://cdn.intechopen.com/pdfs/13079/InTech-Forecasting_landslide_generated_tsunamis_a_review.pdf

Dick RM. 2021. What lies beneath: investigating the distribution and dynamics of landslides in lakes, and fjords of New Zealand [PhD thesis]. Newcastle upon Tyne (GB): Newcastle University. 347 p. https://theses.ncl.ac.uk/jspui/handle/10443/5643

Dirga N. 2025 Aug 7. New Zealand's hottest destinations will start charging foreign tourists fees – here's why. *Radio New Zealand*; [accessed 2026 Jun]. https://www.rnz.co.nz/news/political/569262/new-zealand-s-hottest-destinations-will-start-charging-foreign-tourists-fees-here-s-why

[DOC] Department of Conservation. 2020. Cape Kidnappers: visitor experience management plan. [Place unknown] (NZ): DOC; [accessed 2026 Jun]. https://www.doc.govt.nz/globalassets/documents/about-doc/conservation-management/cape-kidnappers-visitor-experience-management-plan.pdf

[DOC] Department of Conservation. 2024. DOC risk thresholds for natural hazard risk management. Wellington (NZ): DOC; [accessed 2026 Feb]. https://www.doc.govt.nz/globalassets/documents/about-doc/role/managing-conservation/natural-hazards/doc-natural-hazard-risk-threshold-chart.pdf

Dohmen K, Blum P, Braun A, Fernandez-Steeger TM. 2025a. Landslide-triggered tsunamis – a review. *Natural Hazards*. 121(19):22341–22373. https://doi.org/10.1007/s11069-025-07551-2

Dohmen K, Braun A, Fernandez-Steeger T, Manuel T. 2025b. A catalog of landslide-triggered tsunamis [dataset]. Free Hanseatic City of Bremen (DE): Pangaea – Data Publisher for Earth & Environmental Science; [accessed 2026 Feb]. https://doi.org/10.1594/PANGAEA.979839

Domain Environmental Ltd. 2012. Matata debris flow management – the way forward. Auckland (NZ): Domain Environmental Ltd. Prepared for Whakatāne District Council; [accessed 2026 Feb]. https://www.whakatane.govt.nz/files/documents/about-council/council-projects/awatarariki-debris-detention-structure/Documents%20January%202013/Domain-Environmental-Ltd-Report-December-2012.pdf

Downes G, Cochran U, Wallace L, Reyners M, Berryman K, Walters R, Callaghan F, Barnes P, Bell R. 2005. EQC Project 03/490 – understanding local source tsunami: 1820s Southland tsunami. Lower Hutt (NZ): Institute of Geological & Nuclear Sciences. Client Report 2005/153. Prepared for the EQC Research Foundation; [accessed 2026 Feb]. https://www.naturalhazards.govt.nz/assets/Publications-Resources/3723-Understanding-local-source-tsunami-1820s-Southland-tsunami.pdf

Downes G, Barberopoulou A, Cochran U, Clark K, Scheele F. 2017. The New Zealand Tsunami Database: historical and modern records. *Seismological Research Letters*. 88(2A):342–353. https://doi.org/10.1785/0220160135

[DPMC] Department of the Prime Minister and Cabinet. 2025. New Zealand's national risks. Wellington (NZ): DPMC; [accessed 2026 Jun]. https://www.dpmc.govt.nz/our-programmes/risk-and-resilience/national-risk-and-resilience-framework/new-zealands-national-risks

Dykstra JL. 2012. The post-LGM evolution of Milford Sound, Fiordland, New Zealand: timing of ice retreat, the role of mass wasting & implications for hazards [PhD thesis]. Christchurch (NZ): University of Canterbury. 314 p. https://doi.org/10.26021/6036

Eian R. 2024 Nov 5. "Seeing how Norway works with unstable mountain slopes is invaluable". Trondheim (NO): Geological Survey of Norway; [updated 2024 Dec 11; accessed 2026 Jun]. https://www.ngu.no/en/nyheter/seeing-how-norway-works-unstable-mountain-slopes-invaluable

[EMS] Emergency Management Southland. 2025. Piopiotahi Milford Sound: a coordinated approach to understanding, communicating and managing natural hazard risk. Invercargill (NZ): EMS; [accessed 2026 Feb]. https://www.doc.govt.nz/contentassets/80a169ab5b904ecaaad1f980b2c4d471/milford-sound-hazard-explainer.pdf

[EMS] Emergency Management Southland. 2026. Emergency Management Southland: Group Plan 2026–2031. Invercargill (NZ): EMS; [accessed 2026 Jul]. https://www.cdsouthland.nz/media/c1ldabba/em-southland-group-plan-2026-2031-final-june-2026-interactive-pages.pdf

Enet F, Grilli ST. 2007. Experimental study of tsunami generation by three-dimensional rigid underwater landslides. *Journal of Waterway, Port, Coastal, and Ocean Engineering*. 133(6):442–454. https://doi.org/10.1061/(ASCE)0733-950X(2007)133:6(442)

[ERM] ERM-Hong Kong Ltd. 1998. Landslides and boulder falls from natural terrain: interim risk guidelines. Hong Kong (CN): Geotechnical Engineering Office. Report 75. 183 p.

Esposti Ongaro T, de' Michieli Vitturi M, Cerminara M, Fornaciai A, Nannipieri L, Favalli M, Calusi B, Macías J, Castro MJ, Ortega S, et al. 2021. Modeling tsunamis generated by submarine landslides at Stromboli Volcano (Aeolian Islands, Italy): a numerical benchmark study. *Frontiers in Earth Science*. 9. https://doi.org/10.3389/feart.2021.628652

Fine IV, Rabinovich AB, Thomson RE, Kulikov EA. 2003. Numerical modeling of tsunami generation by submarine and subaerial landslides. In: Yalçiner AC, Pelinovsky EN, Okal E, Synolakis CE, editors. *Submarine landslides and tsunamis*. Dordrecht (NL): Springer. p. 69–88. (NATO science series; 21). https://doi.org/10.1007/978-94-010-0205-9_9

Forsyth PJ, Turnbull IM, Beanland S, Thomson R. 2006. Surface effects and geological observations following the 1988 Te Anau and 1989 Doubtful Sound earthquakes, Fiordland, New Zealand. Lower Hutt (NZ): GNS Science. 29 p. (GNS Science report; 2006/29).

Fritz HM, Hager WH, Minor HE. 2003. Landslide generated impulse waves. *Experiments in Fluids*. 35(6):505–519. https://doi.org/10.1007/s00348-003-0659-0

Fritz HM, Hager WH, Minor HE. 2004. Near field characteristics of landslide generated impulse waves. *Journal of Waterway, Port, Coastal, and Ocean Engineering*. 130(6):287–302. https://doi.org/10.1061/(ASCE)0733-950X(2004)130:6(287)

Fritz HM, Giachetti T, Anderson S, Gauthier D. 2018. Field survey of the 17 June 2017 landslide generated tsunami in Karrat Fjord, Greenland [abstract]. In: *EGU General Assembly 2018*; 2018 Apr 8–13; Vienna, Austria. Munich (DE): European Geosciences Union. EGU2018-18345.

Fry B, Bannister S, Beavan J, Bland L, Bradley B, Cox S, Cousins J, Gale N, Hancox G, Holden C, et al. 2010. The M_W 7.6 Dusky Sound earthquake of 2009: preliminary report. *Bulletin of the New Zealand Society for Earthquake Engineering*. 43(1):24–40. https://doi.org/10.5459/bnzsee.43.1.24-40

Fuchs H, Boes R. 2010. Berechnung felsrutschinduzierter Impulswellen im Vierwaldstättersee [Calculation of rockslide-induced momentum waves in Lake Lucerne]. *Wasser Energie Luft*. 102(3):215–221. https://doi.org/10.3929/ethz-b-000256996. German.

Geertsema M, Menounos B, Bullard G, Carrivick JL, Clague JJ, Dai C, Donati D, Ekstrom G, Jackson JM, Lynett P, et al. 2022. The 28 November 2020 landslide, tsunami, and outburst flood – a hazard cascade associated with rapid deglaciation at Elliot Creek, British Columbia, Canada. *Geophysical Research Letters*. 49(6):e2021GL096716. https://doi.org/10.1029/2021GL096716

George DL, Iverson RM, Cannon CM. 2017. New methodology for computing tsunami generation by subaerial landslides: application to the 2015 Tyndall Glacier landslide, Alaska. *Geophysical Research Letters*. 44(14):7276–7284. https://doi.org/10.1002/2017GL074341

Gerstenberger MC, Bora S, Bradley BA, DiCaprio C, Kaiser A, Manea EF, Nicol A, Rollins C, Stirling MW, Thingbaijam KKS, et al. 2024. The 2022 Aotearoa New Zealand National Seismic Hazard Model: process, overview, and results. *Bulletin of the Seismological Society of America*. 114(1):7–36. https://doi.org/10.1785/0120230182

Gisler GR. 2008. Tsunami simulations. *Annual Review of Fluid Mechanics*. 40(40):71–90. https://doi.org/10.1146/annurev.fluid.40.111406.102208

Goeldner-Gianella L, Grancher D, Robertsen Ø, Anselme B, Brunstein D, Lavigne F. 2017. Perception of the risk of tsunami in a context of high-level risk assessment and management: the case of the fjord Lyngen in Norway. *Geoenvironmental Disasters*. 4(1):7. https://doi.org/10.1186/s40677-017-0068-y

Grilli ST, Watts P. 1999. Modeling of waves generated by a moving submerged body. Applications to underwater landslides. *Engineering Analysis with Boundary Elements.* 23(8):645–656. https://doi.org/10.1016/S0955-7997(99)00021-1

Grilli ST, Tappin DR, Carey S, Watt SFL, Ward SN, Grilli AR, Engwell SL, Zhang C, Kirby JT, Schambach L, et al. 2019. Modelling of the tsunami from the December 22, 2018 lateral collapse of Anak Krakatau volcano in the Sunda Straits, Indonesia. *Scientific Reports*. 9(1):11946. https://doi.org/10.1038/s41598-019-48327-6

Grindley J, Pepper A, Woodmansey P, Webby G. 2007. Cleddau village development natural hazards risk assessment. [Place unknown]: Opus International Consultants Ltd. Prepared for the Department of Conservation.

Guzzetti F, Ardizzone F, Cardinali M, Rossi M, Valigi D. 2009. Landslide volumes and landslide mobilization rates in Umbria, central Italy. *Earth and Planetary Science Letters*. 279(3):222–229. https://doi.org/10.1016/j.epsl.2009.01.005

Gylfadóttir SS, Kim J, Helgason JK, Brynjólfsson S, Höskuldsson Á, Jóhannesson T, Harbitz CB, Løvholt F. 2017. The 2014 Lake Askja rockslide-induced tsunami: optimization of numerical tsunami model using observed data. *Journal of Geophysical Research: Oceans*. 122(5):4110–4122. https://doi.org/10.1002/2016JC012496

Han L, Wang P, Yu T. 2022. Wave types and energy conversion of impulse waves generated by landslides into mountain reservoirs. *Scientific Reports*. 12:4035. https://doi.org/10.1038/s41598-022-07993-9

Hancox GT, Perrin ND. 2009. Green Lake Landslide and other giant and very large postglacial landslides in Fiordland, New Zealand. *Quaternary Science Reviews*. 28(11):1020–1036. https://doi.org/10.1016/j.quascirev.2008.08.017

Hancox GT, Perrin ND, Dellow GD. 2002. Recent studies of historical earthquake-induced landsliding, ground damage, and MM intensity in New Zealand. *Bulletin of the New Zealand Society for Earthquake Engineering*. 35(2):59–95. http://doi.org/10.5459/bnzsee.35.2.59-95

Hancox GT, Cox SC, Turnbull IM, Crozier MJ. 2003. Reconnaissance studies of landslides and other ground damage caused by the M_W 7.2 Fiordland earthquake of 22 August 2003. Lower Hutt (NZ): Institute of Geological & Nuclear Sciences. 32 p. (Institute of Geological & Nuclear Sciences science report; 2003/30).

Hancox GT, Cox SC, Turnbull IM, Crozier MJ. 2004 Landslides and other ground damage caused by the M_W 7.2 Fiordland earthquake of 22 August 2003. In: Farquhar G, Kelsey P, Marsh J, Fellows D, editors. *To the eNZ of the earth: proceedings of the 9th Australia New Zealand Conference on Geomechanics*; 2004 Feb 8–11; Auckland, New Zealand. London (GB): International Society for Soil Mechanics and Geotechnical Engineering. p. 747–753.

Hancox GT, Cox SC, Jongens R. 2010. The nature and significance of landslides caused by the M_W 7.6 earthquake of 15 July, 2009 in Fiordland, New Zealand. In: Williams AL, Pinches GM, Chin CY, McMorran TJ, Massey CI, editors. *Geologically active: proceedings of the 11th IAEG Congress*; 2010 Sep 5–10; Auckland, New Zealand. Boca Raton (FL): CRC Press. p. 219–228.

Hanna C, White I, Glavovic B. 2017. Managed retreat in New Zealand: revealing the terminology, approaches, and direction of local planning instruments. Hamilton (NZ): University of Waikato. 27 p. Prepared for National Science Challenge: Resilience to Natures Challenges.

Harbitz CB, Glimsdal S, Løvholt F, Kveldsvik V, Pedersen GK, Jensen A. 2014. Rockslide tsunamis in complex fjords: from an unstable rock slope at Åkerneset to tsunami risk in western Norway. *Coastal Engineering*. 88:101–122. https://doi.org/10.1016/j.coastaleng.2014.02.003

Harris OL. 2023. Agent-based modelling of evacuation scenarios for a landslide-generated tsunami in Milford Sound [MSc thesis]. Christchurch (NZ): University of Canterbury. 124 p. https://doi.org/10.26021/14950

Harris OL, Robinson TR, Wilson TM. 2024. Agent-based modelling of evacuation scenarios for a landslide-generated tsunami in Milford Sound, New Zealand. *International Journal of Disaster Risk Reduction*. 113:104847. https://doi.org/10.1016/j.ijdrr.2024.104847

Hauraki District Council; Waikato Regional Council; Waikato District Council. 2023. Wharekawa Coast 2120: community plan. Paeroa (NZ): Hauraki District Council; [accessed 2026 Feb]. https://www.hauraki-dc.govt.nz/council/plans-strategies/wharekawa-coast-2120-community-plan

Heinrich P, Piatanesi A, Hébert H. 2001. Numerical modelling of tsunami generation and propagation from submarine slumps: the 1998 Papua New Guinea event. *Geophysical Journal International*. 145(1):97–111. https://doi.org/10.1111/j.1365-246X.2001.00336.x

Heller V, Ruffini G. 2023. A critical review about generic subaerial landslide-tsunami experiments and options for a needed step change. *Earth-Science Reviews*. 242:104459. https://doi.org/10.1016/j.earscirev.2023.104459

Heller V, Hager WH, Minor H-E. 2008. Scale effects in subaerial landslide generated impulse waves. *Experiments in Fluids*. 44(5):691–703. https://doi.org/10.1007/s00348-007-0427-7

Heller V, Hager WH, Minor HE. 2009. Landslide generated impulse waves in reservoirs: basics and computation. Zurich (CH): ETH Zurich; [accessed 2026 Feb]. https://ethz.ch/content/dam/ethz/special-interest/baug/vaw/vaw-dam/documents/das-institut/mitteilungen/2000-2009/211.pdf

Henrich L, McClure J, Doyle EEH. 2018. Perceptions of risk characteristics of earthquakes compared to other hazards and their impact on risk tolerance. *Disasters*. 42(4):761–781. https://doi.org/10.1111/disa.12284

Hergarten S. 2024. Scaling between volume and runout of rock avalanches explained by a modified Voellmy rheology. *Earth Surface Dynamics*. 12(1):219–229. https://doi.org/10.5194/esurf-12-219-2024

Hermanns RL, Blikra LH, Naumann M, Nilsen B, Panthi KK, Stromeyer D, Longva O. 2006. Examples of multiple rock-slope collapses from Köfels (Ötz valley, Austria) and western Norway. *Engineering Geology*. 83(1):94–108. https://doi.org/10.1016/j.enggeo.2005.06.026

Horspool NA, Kaiser AE, Goded T, Charlton DH, Moratalla JM, Chadwick MP, Groom J, Houltham J, Abbott ER, Andrews JR, et al. 2023. GNS Shaking Layers Tool: guidelines for end users. Lower Hutt (NZ): GNS Science. 64 p. (GNS Science report; 2023/13). https://doi.org/10.21420/VZKK-TP35

Howarth JD, Cochran UA, Langridge RM, Clark K, Fitzsimons SJ, Berryman K, Villamor P, Strong DT. 2018. Past large earthquakes on the Alpine Fault: paleoseismological progress and future directions. *New Zealand Journal of Geology and Geophysics*. 61(3):309–328. https://doi.org/10.1080/00288306.2018.1464658

Howarth JD, Barth NC, Fitzsimons SJ, Richards-Dinger K, Clark KJ, Biasi GP, Cochran UA, Langridge RM, Berryman KR, Sutherland R. 2021. Spatiotemporal clustering of great earthquakes on a transform fault controlled by geometry. *Nature Geoscience*. 14(5):314–320. https://doi.org/10.1038/s41561-021-00721-4

[HSE] Health & Safety Executive. 2001. Reducing risks, protecting people: HSE's decision-making process. Sudbury (GB): HSE. 74 p.

Hu Y, Yu Z, Zhou J. 2020. Numerical simulation of landslide-generated waves during the 11 October 2018 Baige landslide at the Jinsha River. *Landslides*. 17(10):2317–2328. https://doi.org/10.1007/s10346-020-01382-x

Huang B, Yin Y, Liu G, Wang S, Chen X, Huo Z. 2012. Analysis of waves generated by Gongjiafang landslide in Wu Gorge, three Gorges reservoir, on November 23, 2008. *Landslides*. 9(3):395–405. https://doi.org/10.1007/s10346-012-0331-y

Huang B, Yin Y, Chen X, Liu G, Wang S, Jiang Z. 2014. Experimental modeling of tsunamis generated by subaerial landslides: two case studies of the Three Gorges Reservoir, China. *Environmental Earth Sciences*. 71(9):3813–3825. https://doi.org/10.1007/s12665-013-2765-5

Huang Z, Law KT, Liu H, Jiang T. 2009. The chaotic characteristics of landslide evolution: a case study of Xintan Landslide. *Environmental Geology*. 56(8):1585–1591. https://doi.org/10.1007/s00254-008-1256-6

Hughes KE. 2025. Reconstructing lacustrine tsunami hazard in high-seismicity regions of New Zealand's South Island [PhD thesis]. Wellington (NZ): Te Herenga Waka—Victoria University of Wellington. https://doi.org/10.26686/wgtn.29494436

Hughes L, Mead S, Power W, Wang X, Miller C. 2025. Assessing the tsunami hazard from sub-aerial landslides on Whakaari / White Island. In: Eccles J, Rowe M, Campbell K, editors. *Geoscience Society of New Zealand Annual Conference 2025: Abstracts Volume*; 2025 Nov 24–27; Auckland, New Zealand. Wellington (NZ): Geoscience Society of New Zealand. (Geoscience Society of New Zealand miscellaneous publication; 172A).

Hughes SA. 1993. Physical models and laboratory techniques in coastal engineering. London (GB): World Scientific. 588 p. (Advanced series on ocean engineering; 7). https://doi.org/10.1142/2154

Hungr O, Evans SG, Hazzard J. 1999. Magnitude and frequency of rock falls and rock slides along the main transportation corridors of southwestern British Columbia. *Canadian Geotechnical Journal*. 36(2):224–238. https://doi.org/10.1139/t98-106

Iverson RM. 2000. Landslide triggering by rain infiltration. *Water Resources Research*. 36(7):1897–1910. https://doi.org/10.1029/2000WR900090

Jaboyedoff M, Carrea D, Derron M-H, Oppikofer T, Penna IM, Rudaz B. 2020. A review of methods used to estimate initial landslide failure surface depths and volumes. *Engineering Geology*. 267:105478. https://doi.org/10.1016/j.enggeo.2020.105478

Johannessen S, Marie Hov Andreassen S, Kolstø Haavik T, Taarup J, Ivar Kruke B. 2025. Co-creation of risk in evacuation settings: a risk governance approach to natural hazards risks. *Safety Science*. 185:106780. https://doi.org/10.1016/j.ssci.2025.106780

Jørstad FA. 1968. Waves generated by landslides in Norwegian fjords and lakes. Oslo (NO): Norwegian Geotechnical Institute. p. 13–32. (Norwegian Geotechnical Institute publication; 79).

Keefer DK. 1984. Landslides caused by earthquakes. *Geological Society of America Bulletin*. 95(4):406–421. https://doi.org/10.1130/0016-7606(1984)95%3C406:LCBE%3E2.0.CO;2

Keys HJR, Green PM. 2008. Ruapehu Lahar New Zealand 18 March 2007: lessons for hazard assessment and risk mitigation 1995–2007. *Journal of Disaster Research*. 3(4):284–286. https://doi.org/10.20965/jdr.2008.p0284

Kilvington M, Saunders WSA. 2015. "I can live with this": the Bay of Plenty Regional Council public engagement on acceptable risk. Lower Hutt (NZ): GNS Science. 71 p. (GNS Science miscellaneous series; 86).

Kilvington M, Brown C, Horn C, Ross-Donald C. 2025. Natural hazard and climate change risk tolerance conversations: guidance to aid design. [Place unknown] (NZ): Let's Talk About Risk; [accessed 2026 Feb]. https://www.resorgs.org.nz/wp-content/uploads/LTAR_risk_tolerance_conversations_guidance.pdf

Kirby JT, Grilli ST, Horrillo J, Liu PLF, Nicolsky D, Abadie S, Ataie-Ashtiani B, Castro MJ, Clous L, Escalante C, et al. 2022. Validation and inter-comparison of models for landslide tsunami generation. *Ocean Modelling*. 170:101943. https://doi.org/10.1016/j.ocemod.2021.101943

Knudson KP, Hendy IL, Neil HL. 2011. Re-examining Southern Hemisphere westerly wind behaviour: insights from a late Holocene precipitation reconstruction using New Zealand fjord sediments. *Quaternary Science Reviews*. 30(21–22):3124–3138. https://doi.org/10.1016/j.quascirev.2011.07.017

Korup O. 2005. Distribution of landslides in southwest New Zealand. *Landslides*. 2(1):43–51. https://doi.org/10.1007/s10346-004-0042-0

Kristensen L, Anda E, Noël F, Skrede I, Pless G. 2025. Do we monitor the most critical slopes? Recent Norwegian cases and response [abstract]. In: *Rock Slope and Gravity Conference: forecasting and modelling large rock slop failures in a changing mountain environment*; 2025 Nov 26–28; Lausanne, Switzerland. Lausanne (CH): University of Lausanne. p. 71.

Lane EM, Mountjoy JJ, Power WL, Popinet S. 2016. Initialising landslide-generated tsunamis for probabilistic tsunami hazard assessment in Cook Strait. *The International Journal of Ocean and Climate Systems*. 7(1):4–13. https://doi.org/10.1177/1759313115623162

Larsen IJ, Montgomery DR, Korup O. 2010. Landslide erosion controlled by hillslope material. *Nature Geoscience*. 3(4):247–251. https://doi.org/10.1038/ngeo776

Lastras G, Amblas D, Calafat AM, Canals M, Frigola J, Hermanns RL, Lafuerza S, Longva O, Micallef A, Sepúlveda SA, et al. 2013. Landslides cause tsunami waves: insights from Aysén fjord, Chile. *Eos, Transactions American Geophysical Union*. 94(34):297–298. https://doi.org/10.1002/2013EO340002

Leonard M. 2004. T-phase perception: the August 2003, M_W 7.1, New Zealand earthquake felt in Sydney 1,800 km away. *Seismological Research Letters*. 75(4):475–480. https://doi.org/10.1785/gssrl.75.4.475

[LGNZ] Local Government New Zealand. 2014. Managing natural hazard risk in New Zealand – towards more resilient communities: a think piece for local and central government and others with a role in managing natural hazards. [Place unknown] (NZ): LGNZ; [accessed 2026 Jun]. https://www.wcrc.govt.nz/repository/libraries/id:2459ikxj617q9ser65rr/hierarchy/Documents/Publications/Regional%20Plans/Regional%20Policy%20Statement/Review%20Resources/Managing%20natural%20hazard%20risk%20in%20New%20Zealand%2C%20LGNZ%20%282014%29.pdf

Liu PLF, Cho Y-S, Briggs MJ, Kanoglu U, Synolakis CE. 1995. Runup of solitary waves on a circular island. *Journal of Fluid Mechanics*. 302:259–285. https://doi.org/10.1017/S0022112095004095

Løvholt F, Pedersen G, Gisler G. 2008. Oceanic propagation of a potential tsunami from the La Palma Island. *Journal of Geophysical Research: Oceans*. 113(C9):C09026. https://doi.org/10.1029/2007JC004603

Løvholt F, Glimsdal S, Harbitz CB. 2020. On the landslide tsunami uncertainty and hazard. *Landslides*. 17(10):2301–2315. https://doi.org/10.1007/s10346-020-01429-z

Lüthi MP, Vieli A. 2016. Multi-method observation and analysis of a tsunami caused by glacier calving. *The Cryosphere*. 10(3):995–1002. https://doi.org/10.5194/tc-10-995-2016

Mabin M, Tipler C. 2008. Milford village tsunami hazard: a review. [Place unknown]: URS New Zealand Ltd. Prepared for the Department of Conservation.

Malamud BD, Turcotte DL, Guzzetti F, Reichenbach P. 2004. Landslide inventories and their statistical properties. *Earth Surface Processes and Landforms*. 29(6):687–711. https://doi.org/10.1002/esp.1064

Marc O, Hovius N, Meunier P, Gorum T, Uchida T. 2016. A seismologically consistent expression for the total area and volume of earthquake-triggered landsliding. *Journal of Geophysical Research: Earth Surface*. 121(4):640–663. https://doi.org/10.1002/2015JF003732

Marlborough District Council. 2023. Marlborough Sounds future access study: engagement documents. Blenheim (NZ): Marlborough District Council; [accessed Feb 2026]. https://www.marlborough.govt.nz/services/roads-and-transport/marlborough-sounds-future-access-study/2023-public-consultation-msfas/engagement-documents

Massey C, Townsend D, Rathje E, Allstadt KE, Lukovic B, Kaneko Y, Bradley B, Wartman J, Jibson RW, Petley DN, et al. 2018. Landslides triggered by the 14 November 2016 M_w 7.8 Kaikōura earthquake, New Zealand. *Bulletin of the Seismological Society of America*. 108(3B):1630–1648. https://doi.org/10.1785/0120170305

Massey CI, Townsend DT, Lukovic B, Morgenstern R, Jones K, Rosser B, de Vilder S. 2020a. Landslides triggered by the M_W7.8 14 November 2016 Kaikōura earthquake: an update. *Landslides*. 17(10):2401–2408. https://doi.org/10.1007/s10346-020-01439-x

Massey CI, Lukovic B, de Vilder S, Archibald GC. 2020b. Landslide risk analysis for Clifton Beach, Cape Kidnappers, Hawke's Bay. Lower Hutt (NZ): GNS Science. 101 p. Consultancy Report 2020/28. Prepared for Hastings District Council and the Department of Conservation. https://www.doc.govt.nz/globalassets/documents/about-doc/conservation-management/cape-kidnappers-gns-qra-report.pdf

Matti S, Cullen M, Reichardt U, Vigfúsdóttir A. 2023. Planned relocation due to landslide-triggered tsunami risk in recently deglaciated areas. *International Journal of Disaster Risk Reduction*. 86:103536. https://doi.org/10.1016/j.ijdrr.2023.103536

[MCDEM] Ministry of Civil Defence & Emergency Management. 2019. National Disaster Resilience Strategy. Wellington (NZ): MCDEM; [accessed 2026 Feb]. https://www.civildefence.govt.nz/assets/Uploads/documents/publications/ndrs/National-Disaster-Resilience-Strategy-10-April-2019.pdf

McSaveney MJ, Beetham RD, Leonard GS. 2005. The 18 May 2005 debris flow disaster at Matata: causes and mitigation suggestions. Lower Hutt (NZ): Institute of Geological & Nuclear Sciences. 51 p. Client Report 2005/71. Prepared for Whakatāne District Council.

Mere AM, Barth NC, Schwartz JJ, Kylander-Clark A. 2024. Slip history, tectonic evolution, and fault zone structure along the southern Alpine Fault, New Zealand. *Geochemistry, Geophysics, Geosystems*. 25(11):e2024GC011839. https://doi.org/10.1029/2024GC011839

Meyrat G, McArdell B, Müller CR, Munch J, Bartelt P. 2023. Voellmy-type mixture rheologies for dilatant, two-layer debris flow models. *Landslides*. 20(11):2405–2420. https://doi.org/10.1007/s10346-023-02092-w

Miller DJ. 1960. The Alaska earthquake of July 10, 1958: giant wave in Lituya Bay. *Bulletin of the Seismological Society of America*. 50(2):253–266. https://doi.org/10.1785/BSSA0500020253

Ministry for the Environment. 2025. National Policy Statement for Natural Hazards 2025. Wellington (NZ): Ministry for the Environment; [accessed 2026 Feb]. https://environment.govt.nz/publications/national-policy-statement-for-natural-hazards/

Mountjoy JJ, Wang X, Woelz S, Fitzsimons S, Howarth JD, Orpin AR, Power WL. 2019. Tsunami hazard from lacustrine mass wasting in Lake Tekapo, New Zealand. In: Lintern DG, Mosher DC, Moscardelli LG, Bobrowsky PT, Campbell C, Chaytor JD, Clague JJ, Georgiopoulou A, Lajeunesse P, Normandeau A, et al., editors. *Subaqueous mass movements and their consequences: assessing geohazards, environmental implications and economic significance of subaqueous landslides*. London (GB): Geological Society of London. p. 413–426. (Geological Society of London special publication; 477). https://doi.org/10.1144/SP477.21

[NGI] Norwegian Geotechnical Institute. 2023. Investigation on risk acceptance floods and landslides: sub-investigation 1. Oslo (NO): NGI. Report Doc No. 20230421-01-R. Prepared for the Ministry of Petroleum and Energy.

[NHC] Natural Hazards Commission Toka Tū Ake. 2023. Natural hazard risk tolerance literature review. Wellington (NZ): NHC; [accessed 2026 Feb]. https://www.naturalhazards.govt.nz/resilience-and-research/research/search-all-research-reports/natural-hazard-risk-tolerance-literature-review/

[NHC] Natural Hazards Commission Toka Tū Ake. 2025. Risk tolerance methodology. Wellington (NZ): NHC; [accessed 2026 Feb]. https://www.naturalhazards.govt.nz/assets/Publications-Resources/Risk-Tolerance-Methodology-2025.pdf

Noda E. 1970. Water waves generated by landslides. *Journal of the Waterways, Harbors and Coastal Engineering Division*. 96(4):835–855. https://doi.org/10.1061/AWHCAR.0000045

Norwegian Building Authority. 2017. Forskrift om tekniske krav tilbyggverk [Regulations on technical requirements for construction works]. Oslo (NO): Norwegian Building Authority. Byggteknisk Forskrift TEK17. Norwegian; [accessed 2026 Jun]. https://www.dibk.no/globalassets/byggeregler/regulation-on-technical-requirements-for-construction-works--technical-regulations.pdf

Oppikofer T, Hermanns RL, Roberts NJ, Böhme M. 2019. SPLASH: semi-empirical prediction of landslide-generated displacement wave run-up heights. In: Lintern DG, Mosher DC, Moscardelli LG, Bobrowsky PT, Campbell C, Chaytor J, Clague J, Georgiopoulou A, Lajeunesse P, Normandeau A, et al., editors. *Subaqueous mass movements and their consequences: assessing geohazards, environmental implications and economic significance of subaqueous landslides*. London (GB): Geological Society of London. p. 353–366. (Geological Society of London special publications; 477). https://doi.org/10.1144/SP477.1

Orchiston C, Mitchell J, Wilson T, Langridge R, Davies T, Bradley B, Johnston D, Davies A, Becker J, McKay A. 2018. Project AF8: developing a coordinated, multi-agency response plan for a future great Alpine Fault earthquake. *New Zealand Journal of Geology and Geophysics*. 61(3):389–402. https://doi.org/10.1080/00288306.2018.1455716

Orchiston C, Cochran U, Vause A. 2025. A review of tsunami hazard for southern Aotearoa New Zealand with implications for future research. *New Zealand Journal of Geology and Geophysics*. 68(4):568–590. https://doi.org/10.1080/00288306.2024.2419369

Otero J, Almanzar J. 2024. Assessment of Milford Sound geology, seabed bathymetry and hazards. Version 2. Invercargill (NZ): Great South. 43 p.

Paetzel M, Dale T. 2010. Climate proxies for recent fjord sediments in the inner Sognefjord region, western Norway. In: Howe JA, Austin WEN, Forwick M, Paetzel M, editors. *Fjord systems and archives*. London (GB): Geological Society of London. p. 271–288. (Geological Society of London special publications; 344). https://doi.org/10.1144/SP344.19

Panizzo A, De Girolamo P, Di Risio M, Maistri A, Petaccia A. 2005a. Great landslide events in Italian artificial reservoirs. *Natural Hazards and Earth System Sciences*. 5(5):733–740. https://doi.org/10.5194/nhess-5-733-2005

Panizzo A, De Girolamo P, Petaccia A. 2005b. Forecasting impulse waves generated by subaerial landslides. *Journal of Geophysical Research: Oceans*. 110(C12):C12025. https://doi.org/10.1029/2004JC002778

Paris A, Okal EA, Guérin C, Heinrich P, Schindelé F, Hébert H. 2019. Numerical modeling of the June 17, 2017 landslide and tsunami events in Karrat Fjord, West Greenland. *Pure and Applied Geophysics*. 176(7):3035–3057. https://doi.org/10.1007/s00024-019-02123-5

Pedersen G, Gjevik B. 1983. Run-up of solitary waves. *Journal of Fluid Mechanics*. 135:283–299. https://doi.org/10.1017/S0022112083003080

Pickrill RA. 1993. Sediment yields in Fiordland. *Journal of Hydrology (New Zealand)*. 31(1):39–55.

Pitblado R, Bardy M, Nalpanis P, Crossthwaite P, Molazemi K, Bekaert M, Raghunathan V. 2012. International comparison on the application of societal risk criteria. *Process Safety Progress*. 31(4):363–368. https://doi.org/10.1002/prs.11525

Power W, Downes G, Mcsaveney M, Beavan J, Hancox G. 2005. The Fiordland earthquake and tsunami, New Zealand, 21 August 2003. In: Satake K, editor. *Tsunamis: case studies and recent developments*. Dordrecht (NL): Springer. p. 31–42. https://doi.org/10.1007/1-4020-3331-1_2

Power WL, Burbidge DR, Gusman AR. 2023. Tsunami hazard curves and deaggregation plots for 20 km coastal sections, derived from the 2021 National Tsunami Hazard Model. Lower Hutt (NZ): GNS Science. 545 p. (GNS Science report; 2022/61). https://doi.org/10.21420/XPA4-VD47

Reyners M, McGinty P, Cox S, Turnbull I, O'Neill T, Gledhill K, Hancox G, Beavan J, Matheson D, McVerry G, et al. 2003. The Mw 7.2 Fiordland earthquake of August 21, 2003: background and preliminary results. *Bulletin of the New Zealand Society for Earthquake Engineering*. 36(4):233–248. https://doi.org/10.5459/bnzsee.36.4.233-248

[RNZ] Radio New Zealand. 2025 Jun 4. Milford Sound plans: 'We've got to get on with it'. *Radio New Zealand*; [accessed 2026 Feb]. https://www.rnz.co.nz/news/national/563096/milford-sound-plans-we-ve-got-to-get-on-with-it

Roberts SG, Oishi Y, Li M. 2013. High resolution tsunami inundation simulations. In: *20th International Congress on Modelling and Simulation*; 2013 Dec 1–6; Adelaide, Australia. Canberra (AU): Modelling and Simulation Society of Australia and New Zealand Inc. p. 310–316.

Robinson TR, Davies TRH, Wilson TM, Orchiston C. 2016. Coseismic landsliding estimates for an Alpine Fault earthquake and the consequences for erosion of the Southern Alps, New Zealand. *Geomorphology*. 263:71–86. https://doi.org/10.1016/j.geomorph.2016.03.033

Rosen Y. 2025 Sep 12. Joint effort assess landslide and tsunami risks in Alaska's Prince William Sound. *Alaska Public Media*; [accessed 2026 Jun]. https://alaskapublic.org/news/environment/2025-09-12/joint-effort-assesses-landslide-and-tsunami-risks-in-alaskas-prince-william-sound

Sassa K, Dang K, Yanagisawa H, He B. 2016. A new landslide-induced tsunami simulation model and its application to the 1792 Unzen-Mayuyama landslide-and-tsunami disaster. *Landslides*. 13(6):1405–1419. https://doi.org/10.1007/s10346-016-0691-9

Saunders WSA, Kilvington M. 2016. Innovative land use planning for natural hazard risk reduction: a consequence-driven approach from New Zealand. *International Journal of Disaster Risk Reduction*. 18:244–255. https://doi.org/10.1016/j.ijdrr.2016.07.002

Scheele L, Yugsi Molina F, Oppikofer T, Hermanns RL, Kveldsvik V, Glimsdal S. 2013. ICG P10 2006: tsunami modeling and prediction: modeling of the Aysén Fjord rock slide tsunami. London (GB): ICG. p. 19. ICG Report 3013-10-1, NGI Report 20061073-02-R.

Sepúlveda SA, Serey A. 2009. Tsunamigenic earthquake-triggered rock slope failures during the April 21, 2007 Aisén earthquake, southern Chile (45.5°S). *Andean Geology*. 36(1):131–136.

Sepúlveda SA, Serey A, Lara M, Pavez A, Rebolledo S. 2010. Landslides induced by the April 2007 Aysén Fjord earthquake, Chilean Patagonia. *Landslides*. 7(4):483–492. https://doi.org/10.1007/s10346-010-0203-2

Shore M. 2020. Clifton Beach landslide hazard assessment. Hastings (NZ): Stantec. 72 p. + appendices. Prepared for Hastings District Council and the Department of Conservation. https://www.doc.govt.nz/globalassets/documents/about-doc/conservation-management/cape-kidnappers-stantec-hazard-assessment-report.pdf

Shugar DH, Barnhart KR, Berdahl M, Caplan-Auerbach J, Ekström G, Fathian A, Geertsema M, Hicks SP, Higman B, Jensen EK, et al. 2026. A 481-meter-high landslide-tsunami in a cruise ship–frequented Alaska fjord. *Science*. 392(6803):eaec3187. https://doi.org/10.1126/science.aec3187

Siegrist M, Árvai J. 2020. Risk perception: reflections on 40 years of research. *Risk Analysis*. 40(S1):2191–2206. https://doi.org/10.1111/risa.13599

Sim KB, Lee ML, Wong SY. 2022. A review of landslide acceptable risk and tolerable risk. *Geoenvironmental Disasters*. 9(1):3. https://doi.org/10.1186/s40677-022-00205-6

Singh J, Sepúlveda SA. 2025. Assessing the landslide failure surface depth and volume: a new spline interpolation method. *Engineering Geology*. 357:108319. https://doi.org/10.1016/j.enggeo.2025.108319

Slingerland RL, Voight B. 1979. Occurrences, properties, and predictive models of landslide-generated water waves. In: Voight B, editor. *Rockslides and avalanches, 2: engineering sites*. Amsterdam (NL): Elsevier. p. 317–394. (Developments in geotechnical engineering; 14). https://doi.org/10.1016/B978-0-444-41508-0.50017-X

Slovic P. 1987. Perception of risk. *Science*. 236(4799):280–285. https://doi.org/10.1126/science.3563507

Sorensen RM. 1993. Basic wave mechanics: for coastal and ocean engineers. New York (NY): John Wiley and Sons Inc. 284 p.

Spee K. 2008. Community recovery after the 2005 Matata disaster: long-term psychological and social impacts. Lower Hutt (NZ): GNS Science. 36 p. (GNS Science report; 2008/12).

Strom A, Li L, Lan H. 2019. Rock avalanche mobility: optimal characterization and the effects of confinement. *Landslides*. 16(8):1437–1452. https://doi.org/10.1007/s10346-019-01181-z

Strouth A, McDougall S. 2021. Societal risk evaluation for landslides: historical synthesis and proposed tools. *Landslides*. 18(3):1071–1085. https://doi.org/10.1007/s10346-020-01547-8

Strouth A, McDougall S. 2022. Individual risk evaluation for landslides: key details. *Landslides*. 19(4):977–991. https://doi.org/10.1007/s10346-021-01838-8

Strzelecki MC, Jaskólski MW. 2020. Arctic tsunamis threaten coastal landscapes and communities – survey of Karrat Isfjord 2017 tsunami effects in Nuugaatsiaq, western Greenland. *Natural Hazards and Earth System Sciences*. 20(9):2521–2534. https://doi.org/10.5194/nhess-20-2521-2020

Sutton S, Greer L. 2020. Cape Kidnappers landslide risk management options analysis. Wellington (NZ): Department of Conservation. DOC-6294050; [accessed 2026 Feb]. https://www.doc.govt.nz/globalassets/documents/about-doc/conservation-management/cape-kidnappers-options-paper.pdf

Svennevig K, Hicks SP, Forbriger T, Lecocq T, Widmer-Schnidrig R, Mangeney A, Hibert C, Korsgaard NJ, Lucas A, Satriano C, et al. 2024. A rockslide-generated tsunami in a Greenland fjord rang Earth for 9 days. *Science*. 385(6714):1196–1205. https://doi.org/10.1126/science.adm9247

Szekely A, Lipari F, Antonioni A, Paolucci M, Sánchez A, Tummolini L, Andrighetto G. 2021. Evidence from a long-term experiment that collective risks change social norms and promote cooperation. *Nature Communications*. 12(1):5452. https://doi.org/10.1038/s41467-021-25734-w

Taig T. 2022. Guidelines for DOC on dealing with natural hazard risk. Marston (GB): TTAC Limited. Prepared for GNS Science; [accessed 2026 Feb]. https://dxcprod.doc.govt.nz/globalassets/documents/about-doc/role/managing-conservation/natural-hazards/doc-risk-guidelines.pdf

Taig T, McSaveney MJ. 2015. Milford Sound risk from landslide-generated tsunami. Lower Hutt (NZ): GNS Science. 57 p. Consultancy Report 2014/224. Prepared for Environment Southland.

Tanyaş H, Allstadt KE, van Westen CJ. 2018. An updated method for estimating landslide-event magnitude. *Earth Surface Processes and Landforms*. 43(9):1836–1847. https://doi.org/10.1002/esp.4359

Tappenden KM. 2014. The district of North Vancouver's landslide management strategy: role of public involvement for determining tolerable risk and increasing community resilience. *Natural Hazards*. 72(2):481–501. https://doi.org/10.1007/s11069-013-1016-0

Tappin DR, Watts P, Grilli ST. 2008. The Papua New Guinea tsunami of 17 July 1998: anatomy of a catastrophic event. *Natural Hazards and Earth System Sciences*. 8(2):243–266. https://doi.org/10.5194/nhess-8-243-2008

Tinti S, Pagnoni G, Zaniboni F. 2006. The landslides and tsunamis of the 30th of December 2002 in Stromboli analysed through numerical simulations. *Bulletin of Volcanology*. 68(5):462–479. https://doi.org/10.1007/s00445-005-0022-9

Toka Tū Ake EQC. 2023a. Natural hazard risk tolerance literature review. Wellington (NZ): Toka Tū Ake EQC; [accessed 2026 Feb]. https://www.naturalhazards.govt.nz/assets/Publications-Resources/Risk-Tolerance-Literature-Review.pdf

Toka Tū Ake EQC. 2023b. Risk tolerance methodology. Wellington (NZ): Toka Tū Ake EQC; [accessed 2026 Feb]. https://www.naturalhazards.govt.nz/assets/Research/Risk-Tolerance-Methodology_published-version.pdf

Tonkin & Taylor. 2013. Quantitative landslide and debris flow hazard assessment: Matatā escarpment. [Place unknown] (NZ): Tonkin & Taylor. 95 + appendices. Prepared for Whakatāne District Council. https://www.boprc.govt.nz/media/752320/quantitative-hazard-assessment-matata-escarpment-tt-ref-29115-whakatane-district-council-november-2013-for-web.pdf

Turnbull IM, Beanland S. 1988. Earthquake effects, Lake Te Anau. Located at: Earth Sciences New Zealand, Dunedin, NZ; New Zealand Geological Survey Immediate Report EDS 88/6. 9 p.

Turnbull IM, Allibone AH, Jongens R, compilers. 2010. Geology of the Fiordland area [map]. Lower Hutt (NZ): GNS Science. 97 p. + 1 map, scale 1:250,000. (Institute of Geological & Nuclear Sciences 1:250,000 geological map; 17).

[UNDRR] United Nations Office for Disaster Risk Reduction. 2015. Sendai Framework for Disaster Risk Reduction 2015–2030. Switzerland (CH): UNISDR. 35 p.

[UNDRR] United Nations Office for Disaster Risk Reduction. 2017. Sendai Framework terminology on disaster risk reduction – definition: disaster risk. Geneva (CH): UNDRR; [accessed 2026 Feb 3]. https://www.undrr.org/terminology/disaster-risk

Uribe F, Fuentes M, Campos J. 2025. Modeling of the 2007 Aysén tsunami generated by the Punta Cola and North Mentirosa Island landslides. *Coasts*. 5(2):19. https://doi.org/10.3390/coasts5020019

[USGS] United States Geological Survey. 2021 Oct 5. Barry Arm Alaska, tsunami hazard maybe not so severe. Reston (VA): USGS; [accessed 2026 Jun]. https://www.usgs.gov/programs/landslide-hazards/science/barry-arm-alaska-tsunami-hazard-maybe-not-so-severe

Uslu B, Power W, Greenslade D, Eblé M, Titov V. 2011. The July 15, 2009 Fiordland, New Zealand tsunami: real-time assessment. *Pure and Applied Geophysics*. 168(11):1963–1972. https://doi.org/10.1007/s00024-011-0281-7

Vinnell LJ, Milfont TL, McClure J. 2019. Do social norms affect support for earthquake-strengthening legislation? Comparing the effects of descriptive and injunctive norms. *Environment and Behavior*. 51(4):376–400. https://doi.org/10.1177/0013916517752435

Vriens E, Andrighetto G, Tummolini L. 2024. Risk, sanctions and norm change: the formation and decay of social distancing norms. *Philosophical Transactions of the Royal Society B: Biological Sciences*. 379(1897). https://doi.org/10.1098/rstb.2023.0035

Walder JS, Watts P, Sorensen OE, Janssen K. 2003. Tsunamis generated by subaerial mass flows. *Journal of Geophysical Research: Solid Earth*. 108(B5):2236. https://doi.org/10.1029/2001JB000707

Waldmann N, Vasskog K, Simpson G, Chapron E, Støren EWN, Hansen L, Loizeau J-L, Nesje A, Ariztegui D. 2021. Anatomy of a catastrophe: reconstructing the 1936 rock fall and tsunami event in Lake Lovatnet, Western Norway. *Frontiers in Earth Science*. 9. https://doi.org/10.3389/feart.2021.671378

Wang X, Power W. 2011. COMCOT: a tsunami generation, propagation and run-up model. Lower Hutt (NZ): GNS Science. 121 p. (GNS Science report; 2011/43).

Wang X, Power WL, Massey CI, Ries W, Andres N. 2013. Modelling water wave impact in Lake Taupo by Waihi landslides [abstract]. In: Reid CM, Wandres A, editors. *Geosciences 2013: Annual Conference of the Geoscience Society of New Zealand: abstracts*; 2013 Nov 24–27; Christchurch, New Zealand. Wellington (NZ): Geoscience Society of New Zealand. p. 101. (Geoscience Society of New Zealand miscellaneous publication; 136A).

Wang Y, Xu G. 2009. Back-analysis of water waves generated by the Xintan landslide. In: Wang F, Li T, editors. *Landslide disaster mitigation in Three Gorges Reservoir, China*. Berlin (DE): Springer. p. 433–445. https://doi.org/10.1007/978-3-642-00132-1_19

Ward SN, Day S. 2010. The 1958 Lituya Bay landslide and tsunami – a tsunami ball approach. *Journal of Earthquake and Tsunami*. 4(4):285–319. https://doi.org/10.1142/S1793431110000893

Watts P. 1998. Wavemaker curves for tsunami generated by underwater landslides. *Journal of Waterway, Port, Coastal, and Ocean Engineering*. 124(3):127–137. https://doi.org/10.1061/(ASCE)0733-950X(1998)124:3(127)

Watts P, Grilli ST, Tappin DR, Fryer GJ. 2005. Tsunami generation by submarine mass failure. II: predictive equations and case studies. *Journal of Waterway, Port, Coastal, and Ocean Engineering*. 131(6):298–310. https://doi.org/10.1061/(ASCE)0733-950X(2005)131:6(298)

Whakatāne District Council. 2015. A process towards a settlement framework to mitigate debris flow risk – Awatarariki fanhead, Matata. Whakatāne (NZ): Whakatāne District Council; [accessed 2026 Jun]. https://www.whakatane.govt.nz/files/documents/about-council/council-projects/debris-flow-and-landslide-hazards/policy_committee_2_july_2015.pdf

Williams AM, Baláž V. 2013. Tourism, risk tolerance and competences: travel organization and tourism hazards. *Tourism Management*. 35:209–221. https://doi.org/10.1016/j.tourman.2012.07.006

Wilson KJ, Litchfield NJ, Turnbull IM. 2009. Coastal deformation and tsunami deposit observations following the July 15, 2009, M_W 7.8 Dusky Sound earthquake. Lower Hutt (NZ): GNS Science. 61 p. (GNS Science report; 2009/46).

Winter MG, Bromhead EN. 2012. Landslide risk: some issues that determine societal acceptance. *Natural Hazards*. 62(2):169–187. https://doi.org/10.1007/s11069-011-9987-1

[WMO] World Meteorological Organization. 2022. Early warnings for all: the UN Global early warning initiative for the implementation of climate adaptation – Executive Action Plan 2023–2027. Geneva (CH): World Meteorological Organization. 56 p.

WSP. 2024. Milford Opportunities Project natural hazard assessment. Part B: basic risk assessment. Alexandra (NZ): WSP; [accessed 2026 Feb]. https://www.doc.govt.nz/globalassets/documents/our-work/milford-opportunities-project/technical-reports/mop-natural-hazard-part-b-risk-assessment.pdf

Xiao L, Wang J, Ward SN, Chen L. 2018. Numerical modeling of the June 24, 2015, Hongyanzi landslide generated impulse waves in Three Gorges Reservoir, China. *Landslides*. 15(12):2385–2398. https://doi.org/10.1007/s10346-018-1057-2

Yavari-Ramshe S, Ataie-Ashtiani B. 2016. Numerical modeling of subaerial and submarine landslide-generated tsunami waves – recent advances and future challenges. *Landslides*. 13(6):1325–1368. https://doi.org/10.1007/s10346-016-0734-2

Yin Y-p, Huang B, Chen X, Liu G, Wang S. 2015. Numerical analysis on wave generated by the Qianjiangping landslide in Three Gorges Reservoir, China. *Landslides*. 12(2):355–364. https://doi.org/10.1007/s10346-015-0564-7

APPENDICES

This page left intentionally blank.

APPENDIX 1 Glossary of Terms and Acronyms

Advected	Carried or transported by a flowing fluid, such as water or air.
Annual exceedance probability	The probability of a tsunami, flood or inundation event of a certain size or greater occurring in any year. The term is mostly used here to describe the chance of an event reaching or exceeding a certain depth in any given year.
Average recurrence interval	Also known as ‘annual return period’. The average time interval between events of a specified magnitude (or larger) when averaged over many occurrences; the number of years predicted to pass before an event of a given magnitude occurs. Annual recurrence interval (ARI) (or ‘return period’) can be misinterpreted on the assumption that, because one large event has just occurred, the time period will then pass before another such event. The term ‘annual exceedance probability’ is commonly preferred for weather-related hazards, as this conveys the continuous probability that large events could occur at any time.
Backsplash	The rebound or return surge of water that moves back towards an impact area after the initial wave has surged outwards, often causing secondary waves or additional shoreline flooding.
Bagnold rheology	A flow model for granular materials (like sand or gravel) where resistance to movement increases rapidly as speed increases due to grain collisions.
Basal processes (landslides)	The physical processes occurring at the base of a landslide that control how it slides, such as friction, grinding, water pressure or lubrication.
Bi-linear rheology	A flow model where a granular material (like sand, gravel or broken rock) behaves with one type of resistance at low speeds and a different, typically stronger, resistance at higher speeds, reflecting a change in how the grains interact during movement.
Bingham rheology	A type of flow behaviour where a material behaves like a solid until a certain stress is applied, then flows like a thick fluid (for example, toothpaste or mud).
Celerity	The speed at which a wave travels through water.
Change detection (digital elevation model differencing)	A method of comparing two elevation models taken at different times to measure how much the ground surface has changed.
Climate	In a narrow sense, ‘climate’ is usually defined as the average weather or, more rigorously, as the statistical description in terms of the mean and variability of relevant quantities over a period of time, ranging from months to thousands of years.

COMCOT	Cornell Multi-Grid Coupled Tsunami: A program is a tsunami modelling package developed by Cornell University. It is designed to study the entire life-span of a tsunami, including generation, propagation, run-up and inundation. COMCOT utilises a modified leap-frog finite difference scheme to solve shallow-water equations in both spherical and Cartesian coordinates. It can simulate various tsunami-generating mechanisms, such as faulting and landslides, and is capable of handling both linear and nonlinear scenarios.
COVRI	Coefficient of Variation of a Risk Index: A measure of relative variability, calculated as the standard deviation divided by the mean of the variable. It shows how much values vary relative to their average. A higher COVRI means that data are more spread out or uncertain compared with the mean value, while a lower COVRI means that values are more consistent and tightly clustered.
Coulomb friction	A simple model of friction where resistance to sliding depends on how hard two surfaces are pressed together.
Cumulative frequency	The total number of events larger than a given size occurring over a certain time period.
Delta	A landform created where a river flows into a fiord, lake or the sea and slows down, causing sediment to settle and build outward into the water, often forming a fan- or triangular-shaped area.
Department of Conservation	The New Zealand Government agency responsible for protecting and conserving the nation’s natural and historic heritage.
Department of the Prime Minister and Cabinet	New Zealand’s central public-service department providing impartial, high-quality advice and support to the Prime Minister, Cabinet and Governor-General. It acts as the ‘constitutional and institutional glue’ of the executive government, supporting decision-making, national security and key policy priorities.
Dynamic weakening	A process where friction drops rapidly during fast movement, allowing a landslide to travel farther than expected.
Earthquake-induced landslides	Landslides triggered by earthquake shaking, usually sudden and fast.
Empirical	Based on, concerned with or verifiable by observation or experience (rather than theory or pure logic).
Empirical scaling relationship	A relationship based on observed data that links two quantities, such as landslide size and frequency.
Epistemic	Relating to knowledge or to the degree of its validation.
Epistemic uncertainty	Uncertainty caused by incomplete knowledge or limited data.

Event trees	A diagram or series of steps that lay out possible future scenarios step by step, showing different paths that an event could take and how likely each path is.
Exceedance	The chance that a certain value (such as wave height or ground shaking) will be equalled or exceeded within a given time period.
Exfoliation	The process where outer layers of rock peel or flake off due to stress release, temperature change or weathering.
Exposure	The presence of people and livelihood; ecosystems, environmental functions, services and resources; infrastructure; or economic, social or cultural assets in places and settings that could be adversely affected by natural hazards and climate change.
Extreme sea level	Comes from a combination of mean sea level, any long-term mean sea-level anomaly, astronomical tide, storm surge and wave set-up.
F-N criteria	A way of evaluating societal risk by plotting how often (F = frequency) events occur against how many people are affected (N = number of fatalities) to judge whether the level of risk is acceptable or tolerable.
Failure rate	The speed at which a landslide mass breaks away and is delivered into motion, describing how quickly material collapses from the slope.
Foreset bed	Inclined layers of sediment deposited on the front (downhill side) of a growing delta, sand dune or underwater slope. Commonly unstable and subject to downslope movement (slumping).
Fragmentation-driven processes (landslides)	The physical changes that occur as rock breaks apart during movement, where the creation of smaller fragments alters friction, energy loss and how far the landslide can travel.
Froude number	A measure comparing how fast something is moving through water to how fast waves naturally travel in that depth of water.
GIS	Geographic Information System: Computer software used to store, map and analyse spatial or geographic data. A framework for gathering, managing and analysing data rooted in the science of geography.
GRASS	An open-source GIS used for geospatial data management, analysis, image processing and spatial modelling. It supports both raster and vector data, offering over 500 modules for processing, and is widely used by environmental scientists and government agencies.
Hypsometry	The measurement and analysis of elevation and the distribution of land area at different heights.
InSAR	Interferometric Synthetic Aperture Radar: A satellite method that measures very small ground movements over time.
Lidar	Provides high-resolution topography datasets.

Liquefaction	A change in material state that occurs when a saturated or partially saturated soil substantially loses strength and stiffness in response to an applied stress, such as shaking during an earthquake or other sudden change in stress condition. Material that is ordinarily a solid behaves like a liquid.
Lobate	Having a rounded, tongue-like or lobe-shaped outline.
Mega-tsunami	A tsunami of exceptional size, particularly in terms of run-up height, where this is commonly used to describe tsunami with run-ups exceeding 100 m.
Ministry of Business, Innovation and Employment	A public service department in New Zealand responsible for delivering policy, services, advice and regulation to support business growth. Its purpose is to promote and support a thriving and sustainable economy, contributing to the well-being of New Zealanders. It manages various initiatives, including science, health and safety in the workplace and employment relations.
Ministry for the Environment	The New Zealand Government's primary advisor on environmental policy, climate change and natural-resource management.
Mean sea level	Average (mean) level of the sea relative to a vertical datum over a defined epoch, usually of several years to decades.
Mobility (landslide)	How easily and how far a landslide can travel once it starts moving.
Morphology	The shape, form and structure of a landform or deposit such as a landslide.
Multi-phase flow model	A model that treats moving material as a mixture of solids, water and sometimes air.
Natural Hazards Commission Toka Tū Ake	Formerly the Earthquake Commission (EQC). A New Zealand Government entity that provides natural-disaster insurance for residential property owners and invests in hazard research. It acts as a primary insurer for home damage from earthquakes, volcanic eruptions and landslides and covers land damage from storms and floods to reduce financial impact on citizens.
Navier-Stokes equations	Fundamental mathematical equations that describe how fluids move under the influence of pressure, friction and gravity. By combining conservation of momentum with conservation of mass (if the fluid is incompressible), these describe how the velocity of a fluid changes over space and time due to forces acting on it. They are used to simulate wave generation, propagation, turbulence near impact and interaction between water air and land.
Newtonian rheology	A type of flow behaviour where resistance to movement resistance depends directly on how fast the material is sheared (like water or thin oil), increasing steadily and proportionally with velocity.
Peak ground acceleration	The maximum ground acceleration recorded at a specific location during an earthquake. It measures the intensity of shaking at a site rather than the total energy released by the earthquake and is typically expressed in units of *g* (acceleration due to gravity; 1 g ≈ 9.81 m s^{-2}) or Gal (1 Gal = 1 cm s^{-2}).

Peak wave amplitude	The maximum height of a tsunami wave above the normal (ambient) sea level at the time of the tsunami.
Percentile	A measure used in statistics indicating the value below which a given percentage of observations in a group of observations or projections fall. The 50th percentile is the median. Used to measure the spread of numerous sea-level-rise projection simulations from various models and inputs for a particular representative concentration pathway.
Planimetric mapping	Mapping features as viewed from directly above, without accounting for steep slopes.
Porosity	The percentage of empty space (pores) within soil or rock.
Probabilistic tsunami-hazard analysis	A method that estimates the likelihood of different tsunami heights (or inundation flow depths) occurring at a location.
Prograded	Extended outward over time as sediment accumulated, causing a shoreline, delta or sediment body to build further into a lake or sea.
Rainfall-induced landslides	Landslides triggered by intense or heavy rainfall; commonly sudden and fast shallow slope movements where loss of cohesion is triggered by intense rainfall that weakens shallow soils and bedrock interfaces but may involve triggering of creeping slow landslides.
Rheology	The way that material flows and deforms during movement.
Risk appetite	The amount of risk that a person organisation or society is willing to take in order to achieve its objectives.
Risk tolerance	The specific level of risk that a person organisation or society is willing to accept or can withstand in pursuit of its objectives.
Runout	The horizontal distance that a landslide travels from its source.
Run-up elevation	The maximum vertical height that a tsunami wave reaches on land above background sea or lake level; this is usually measured at the inland limit of inundation relative to the ambient sea level at the time of the tsunami but can be measured relative to a vertical datum.
Seiche	A standing wave that oscillates back and forth in an enclosed or partially enclosed body of water, such as a lake, harbour or bay, acting much like water sloshing in a bathtub. Caused by strong winds, rapid atmospheric pressure changes or earthquakes, these waves can cause rapid water-level changes, leading to flooding on one end and dry conditions on the other, sometimes lasting for hours or days.
Shallow-water phase velocity	The natural speed at which long waves travel in water of a certain depth.
Sloping Local Base Level method	A method used to estimate landslide volume by reconstructing the likely pre-failure slope surface.

SPLASH equation	A semi-empirical formula used to estimate tsunami run-up height from landslide volume and distance.
Sub-aerial landslide	A landslide that starts on land and enters a body of water.
Submarine landslide	A landslide that occurs entirely underwater.
Tsunami	A series of long-duration water waves caused by the large-scale, sudden displacement of water, most commonly triggered by underwater earthquakes, volcanic eruptions or landslides. In a tsunami, the whole column of water, from seabed to surface, is moved by the wave.
Unconsolidated	A deposit consisting of loose grains not held together by cement. River-terrace deposits are a typical example of an unconsolidated aquifer.
Undrained loading	A situation where soil or rock is suddenly compressed or stressed so quickly that water trapped inside it cannot escape, causing internal pressure to rise and temporarily reduce its strength.
UNDRR	United Nations Office for Disaster Risk Reduction: A focal point within the United Nations system for disaster risk reduction, working to prevent and reduce disaster risk, strengthen resilience and coordinate global efforts. It serves as the custodian of the Sendai Framework (2015–2030), supporting countries in its implementation, monitoring and verification.
Velocity-dependent friction	Friction that changes depending on how fast the material is moving.
Voellmy rheology	A flow model combining simple friction with an additional resistance that increases with speed.
V_S shear wave velocity	A fundamental geotechnical and geophysical parameter measuring the speed at which shear (S) waves travel through soil or rock, typically ranging from 100 to 300 ms^{-1} in soft soil to over 1500 ms^{-1} in bedrock. V_{s30} is the shear wave speed in the shallowest 30 m of ground. It directly indicates material stiffness and is crucial for seismic site classification, ground response analysis and predicting liquefaction potential.
Vulnerability	The predisposition to be adversely affected. Vulnerability encompasses a variety of concepts and elements, including exposure, sensitivity or susceptibility to harm or damage, as well as a lack of capacity to cope and adapt (adaptive capacity).
Wave height	As used by the coastal engineering community, this is the vertical height of a tsunami wave measured from its trough (lowest point) to its crest (highest point) while it is still in the water. Some modelling papers will instead use the ‘zero to peak wave height’ measured from the background water level to the crest of the wave – to avoid ambiguity, we refer to this as the ‘peak wave amplitude’ instead.
Weber number	A number used in modelling that compares gravity forces with surface tension forces in fluids.

APPENDIX 2 Uncertainties in the Hazard and Risk Chain

	Contributing Factor	Factors to Consider	Uncertainties
Hazard Chain	Earthquake sources	Combined probability: • Alpine Fault • Plate boundary • Intra-plate fault.	Is it possible to incorporate earthquake magnitudes, directivity, energy release, recurrence, time lapsed (since last event)?
	Ground motion	Length and strength of shaking; peak ground acceleration versus cyclicity.	Is topographic amplification of ground motion and directionality significant enough that it needs to be considered?
	Fault displacement	Will the sea floor or fiord be displaced?	• Is the displacement sufficient to be tsunamigenic? • Is there potential for seiching effects?
	Tsunami source	Combined probability: • Landslide-induced tsunami • Delta or slope collapse • Offshore fault(s) • Offshore landslide • Seiche.	Which slopes are landslide prone, can the delta liquefy and collapse, reach of offshore tsunami, potential for seiche.
	Landslide susceptibility – temporal	• What are the relative earthquake-induced, rainfall-induced or spontaneous hazard probabilities. • Are past landslide magnitude-frequency relationships indicative of present hazard?	• Has slope stress and landslide susceptibility evolved since ice withdrawal? • Were pre-historic landslide deposits from single or multiple events? • Should 'worst case' be used, or new earthquake-induced landslide dynamics models from the 2003 and 2009 earthquakes?
	Landslide susceptibility – spatial	• Which slopes are prone? • What potential triggers? • Any evidence for incipient movement?	How much debris will fall into the water, at what velocity, in what shape?
	Tsunami – landslide	• What is probability? • Where are potential sources; what arrival times and wave sizes are credible?	• Wave height and volume? • How much attenuation/amplification? • What landslide location, volume, speed is needed for wave >X m height? • Multiple landslides at once?
	Tsunami – delta front or submerged slope	Is there a credible hazard from a large collapse of the river delta or fiord slopes?	• Can the delta sediments liquefy? • What volume submarine landslide is credible? • What volumes are needed to create waves of >Xm height?
	Tsunami – offshore	Is there a credible hazard from the plate boundary / fault offset or offshore landslides?	What is hazard at mouth of the Sound? How much attenuation will occur through fiords (e.g. Stirling Basin) to Milford village.
	Waves	What are credible wave sizes, arrival times and run-ups?	New combined bathymetry and lidar topography are available. Run-up models and inundation depths generated numerically (using Manning's coefficient).

	Contributing Factor	Factors to Consider	Uncertainties
Risk	Exposure – spatial	Location of people on boats, onshore, in buildings, at terminal, on road.	• Are there any available data (e.g. boats, buses, car, foot traffic, imagery)? • Density functions can be mapped using WiFi/cellphone – but does it merge onshore and offshore?
	Exposure – temporal	There is population variability and movements at daily/weekly/ seasonal/decadal time scales.	Some frequency data from 2017 to 2019. Dynamic population exposure data (Darling et al. 2025) suggests that peak numbers may be under-estimated (4–5x?). Societal risk is changing all the time.
	Exposure – group types	• Visitors (overnight. daytime, boat trip, >3 hours, various travel modes). • Workers (live locally, visit daily).	• Do any data exist? • What groups can be assessed? • Is age (mobility/speed) important? • Can highest risk group be identified (how much does this vary between individual and societal risk)?
	Vulnerability	Protection in boats/vessels?	• Are people much less vulnerable in certain areas or protected (e.g. boats, buses)? • Are age profiles known?
	Human behaviour	Awareness, perception, trust and response.	• How aware are people of the hazard? • Do people feel informed to take action? • If so, would they take that action?
	Evacuation scenarios	• Waiting versus not waiting. • Walking versus running.	Agent based modelling completed. • Total time to evacuate? • How many can safely evacuate? • By what method and to where? • Congestion? • Capacity?
	Mitigation and controls (see below)	What options: • Messaging: to where, how fast? • Communication options.	• Signage? • Blocks (e.g. fence)? • Can bottlenecks be reduced?
	Individual life risk	Annual fatality risk individuals.	• Need to be added to (and compared with) risk during travel to/from Milford? • Or from earthquake-induced rockfall? • Or other activities (Taig 2022). • Is its contribution significant?
	Societal risk	Mass fatality risk (what are the various metrics – F-N pairs).	What is 'acceptable' risk tolerance? There are large spatial-temporal cycles. Operators can provide recent daily, monthly and yearly visitor numbers – and future projections.

	Contributing Factor	Factors to Consider	Uncertainties
Controls	Evacuation routes	Present versus new/improved?	Are there any options?
	Safe points/evacuation structures	What are the maximum flow depths and how do these vary spatially?	Are there any plausible options?
	Warning system	• Anything more than 'Long or strong get gone'? • Arrival time? • How triggered?	• Will the earthquake be the only warning? • How likely is a large landslide that is *not* the result of long or strong shaking?
	Education and signage	'Long or strong, get gone'?	Better to adopt the 'worst case scenario' and be wrong than take no action.
	Protective equipment	There are many unknowns as to what spatial reach, inundation depths and velocities might occur. This makes it very difficult to know what would be effective and justify investment.	• Is there any evidence that protective equipment might be effective? • Are there good examples (e.g. from Japan) that suggest it might be warranted?
	Overseas examples	Stromboli, Norway, Palu (Suluwesi), Alaska.	Applicability to Piopiotahi / Milford Sound landslide-induced tsunami.

APPENDIX 3 Alpine Fault Segmentation for Hazard Calculations

A ∼4 kyr record shows temporal switching between multi-section (M_W>8) and single-section (M_W∼7–7.9) Alpine Fault earthquakes and that about one-half of ruptures have terminated at or near the Central–Southern section boundary (Howarth et al. 2018, 2021). The hypothesis that minor geometric complexities can act as conditional barriers to rupture of major faults was tested by Howarth et al. (2021) using both paleoseismic observations and modelling. Using multi-cycle earthquake simulations, they suggested that this observed earthquake behaviour is primarily controlled by fault geometry, suggesting that along-strike changes in fault geometry from the Central section to the Southwest section of the fault does control earthquake rupture length. Mode switching occurs at the Central and Southwest section boundary, resulting in temporal clustering of major (M_W7–7.9) and great (M_W>8) earthquakes on the Alpine Fault. Despite the substantial influence on earthquake behaviour, Howarth et al. (2021) suggested that the scale of the geometric changes at the Central and Southwest section boundary seemed insufficient to constitute a segment boundary in conventional fault-source modelling for seismic hazard. More recent integration of geologic/geomorphic mapping and the identification and correlation of fault-offset basement units (Mere et al. 2024) suggests that the Southwest section of the Alpine Fault is less structurally mature than other parts of the fault to the northeast, consistent with the notion that a segment boundary exists between two distinct and somewhat mis-aligned structures.

The record of ruptures of the Southwest section of the Alpine Fault comes from Hokuri Creek and John O'Groats River near the mouth of Piopiotahi / Milford Sound. A record of 22 earthquakes was unearthed from Hokuri Creek and combined with Haast (two events) to define an 8000-year mean recurrence of 329 ± 68 years for the 24 events (Berryman et al. 2012). It was the first work that highlighted the remarkable regularity of the fault's earthquake cycle compared with other transform plate-boundary faults around the world. However, it lacked a record of the more recent earthquakes. Further work from a John O'Groats wetland, immediately adjacent to the mouth of Piopiotahi / Milford Sound, added information on a further seven events spanning the last ~2000 years (Cochran et al. 2017). Estimates of earthquake frequency were then refined using 27 events since ∼6000 BC to provide a mean recurrence interval of 291 ± 23 years for the rupture of the South Westland section of the Alpine Fault. Being shorter than the current inter-seismic period since the last earthquake (~1717 AD), it provided a 29% conditional probability for surface-rupture within 50 years (from 2017), which was a slight increase over similar estimates combining the Hokuri Creek–Haast records (Biasi et al. 2015).

The combined Hokuri–John O'Groats earthquake record (Cochran et al. 2017) is presently the best available representation of late Holocene activity on the South Westland part of the Alpine Fault. Here it appears to be dominantly strike-slip, with a small component of slip that causes net uplift to the northwest. Single-event displacement measurements at Hokuri Creek indicate that the northwestern side moved 7.5 ± 1 m dextral (right lateral motion) and 1 ± 0.5 m vertically in the last earthquake recorded at that site (Clark et al. 2013). The most recent earthquake at John O'Groats River, modelled to be between AD 1819–1646 from carbon dating (Howarth et al. 2018), correlates with the AD 1717 earthquake, so is suggested to have been a whole-fault rupture (and therefore magnitude c. M8.1) (DePascale and Langridge 2012).

When modelling rupture hazard and shaking probability, factors that need to be considered are: (1) the record of earthquakes on the Southwest section results in a slightly lower probability (p = 0.0058) of Alpine Fault rupture than those on the Central Section (p = 0.015), (2) Howarth et al. (2021) do not recommend that the Central and Southwest boundary has characteristics of a true segment in terms of seismic hazard analysis and (3) many of the same recent earthquakes correlate across the boundary. Noting that there are only a few models of Alpine Fault ground shaking, and no published susceptibility modelling linking the probability that this would be sufficient to dislodge landslides, our recommendation is that the higher probability (p = 0.015) from of an earthquake on the Central section is the one that needs to be considered at Milford. It may well rupture both sections and/or cause sufficient shaking to dislodge landslides. Uncertainty in the shaking is, in part, included within the uncertainty that the landslides will fall/not fall into the fiords.

APPENDIX 4 Summary of International Literature on Risk Tolerance or Mitigation for Landslides

Reference	Aim	Main Outcomes
Goeldner-Gianella et al. (2017)	Determine how well informed the local and (domestic) tourist population in fjord Lyngen in Norway are about risk and evacuation, as well as confidence in the information.	Local population has a clear understanding of hazard but tsunami remains unfamiliar for tourists. There is a lack of knowledge about the warning system, particularly for tourists. This is despite a widespread education campaign. People want this tsunami warning system to provide information on the time available for evacuation and where to go. Confidence in local authorities is varied, with higher confidence in hazard monitoring than risk and management.
Tappenden (2014)	Evaluation of public involvement in the District of North Vancouver's Landslide Management Strategy, including tolerance criteria, following a fatal landslide.	Provides a detailed case-study of a community-driven risk-tolerance process. Used expert education sessions, review of international criteria, public open houses and an online survey to get public input on risk tolerability.
Strouth and McDougall (2022)	Provides a critical review of individual risk evaluation, including tolerance thresholds (usually 10^{-4} to 10^{-6} annual probability of fatality) in landslide risk management, as well as the use of the ALARP ('as low as reasonably practicable') principle.	Risk values are often difficult to communicate due to their small probabilities (suggests the use of micromorts as an alternative). It provides an overview of common pitfalls in robustly quantifying risk, including how scenarios are defined, and mixing up incremental and exceedance probabilities. Individual risk criteria is often copied from other jurisdictions or hazard types without considering local context. Risk-tolerance criteria is often unachievable, particularly for existing developments, and may not be the same as for at-risk individuals (i.e. homeowners who may accept greater risk to stay in their homes).
Winter and Bromhead (2012)	Uses international examples (United Kingdom, Hong Kong, Jamaica, United States of America, Japan, Italy) to examine how societal risk tolerance changes with different social, economic and political contexts.	Introduces a ternary willingness diagram as a conceptual model for comparing different contexts, where 'willingness' refers to the willingness to accept risk, pay for risk reduction and alter the environment to enable risk reduction.
Matti et al. (2023)	Evaluation of governance structures, risk assessments, legal frameworks and community experiences with regard to planned re-locations due to increasing landslide-induced tsunami risk in Iceland and Greenland.	The two case studies emphasise the need for affected community involvement in decision making with regards to re-location, ensuring adequate compensation and clear planning timelines.
Johannessen et al. (2025)	Provides four case-studies on risk governance from Arctic and sub-Arctic communities in Norway and Greenland that are subject to avalanche, landslide or tsunami risk.	There are divergent risk perceptions between residents, experts and authorities. There are successful patterns of evacuation depend on 'co-creation of risk', including both the hazard and full consequences. With continuous communication during an extended and evolving risk situation where evacuation might be required, there is increased patience and reduced tension with decisions.

Reference	Aim	Main Outcomes
Strouth and McDougall (2021)	Provides a critical review of the application of the Hong Kong societal risk criteria (F-N approach) to a Western Canadian setting.	It has been a challenge to apply and meet the Hong-Kong-style F-N criteria, with the application of this risk-evaluation criteria resulting in unaffordable risk management and mitigation options. Suggests that the F-N criteria should be guidelines rather than strict thresholds
Sim et al. (2022)	Provides a review of landslide societal risk-tolerance criteria globally.	The review provides an overview of risk tolerance criteria used in Hong Kong, China, Australia, Canada, Norway and Malaysia, as well as New Zealand. This review highlights that many nations adopt risk criteria from elsewhere (notably Hong Kong and the Australia), and that there is a mismatch between published criteria and actual implementation.

APPENDIX 5 Risk Communications Strategy

The ‘Piopiotahi / Milford Sound Collective Hazard Risk Communications Strategy’ is attached to this report as Appendix 5.

earthsciences.nz